URBAN DEVELOPMENT DIRECTORATE (UDD)

Ministry of Housing and Public Works

Government of the People's Republic of Bangladesh

FINAL Report On HYDRO-GEOLOGICAL SURVEY UNDER MIRSHARAI UPAZILA DEVELOPMENT PLAN (MUDP)

Package No.: 5 (Five)

August, 2018

Submitted by

Center for Geoservices and Research

Flat# GCA (Gr. Floor), House # 409,
Road # 06, Mirpur DOHS, Dhaka-1216.

Contents

List of Figures

List of Tables

1. Introduction

Water is the most important constituent of life. Every human activity requires water. The Mirashrai Upazila of Chittagong district is likely to experience rapid industrialization and urbanization in the near future as the largest economic zone in Bangladesh is proposed to be developed in this Upazila. Both industrialization and urbanization have large impacts on water as these activities increases demands of water as well as poses threat to water contamination. To characterize the current water situation, to identify suitable locations for water resources development, and to identify risk of water contamination the Urban Development Directorate (UDD) have initiated a hydrogeological investigations throughout the Upazila. ‘Center for Geoservices and Research’ was employed by UDD to carry out the study in the Upazila.

The aim of hydrology and hydro-geological study for the study areas of Mirshari Region is to identify the surface water body and aquifer of the region including its seasonal variation. The study is also intended to identify the availability fresh ground water, which would be required for the additional people including tourists after implementation of the project, i.e. the foundation of the economic zone. This study comprises of Hydro-geological and geophysical investigations and ground water modeling, water quality mapping, surface water distribution and its management planning by using those data.

1.1. Location and Accessibility

Mirsharai Upazila (Chittagong District) is located between 22˚39′ and 22˚59′ north latitudes and between 91˚27′ and 91˚39′ east longitudes and has an area of 482.88 km^2 (BBS). It is bounded by the Feni River in the North, Sitakunda upazila in the south, Chittagong hill tracts in the east, and the Sandwip Chanel in the west. Mirsharai Thana was founded in 1901 and it was turned into an Upazila in 1983. Mirsharai Upazila consists of 2 Municipality, 16 Union and 113 Mouza with a total population of 398,716 (Three Lakh Ninety Eighty Thousand Seven Hundred Sixteen).

The Upazila is located at a distance of 192.2 km from Dhaka. It can be accessed by both train and bus from the capital city Dhaka. Both mode of transport takes about 4 and half hours to reach there. 4.5 hours long bus journey. It can also be accessed from the Chittagong Divisional headquarters which is located about 56 km to the south of the Upazila and takes 1.5 hour travel by either bus or train. The Bangladesh Road Transport Corporation introduced a direct bus service from Dhaka to Mirsharai via Comilla (Source: Bangalapedia, 2012)

Mirsharai, the combination of lake and hilly area contains attractive scenic beauty on the southeastern part of Bangladesh. The most important attraction of the upazila is that one can travel Mohamaya Chara Lake by speed boat and explore hilly area and can enjoy Khoyachora, Baghbani, Napitachora, Sonaichora, Mithachora and Boyalia waterfalls.

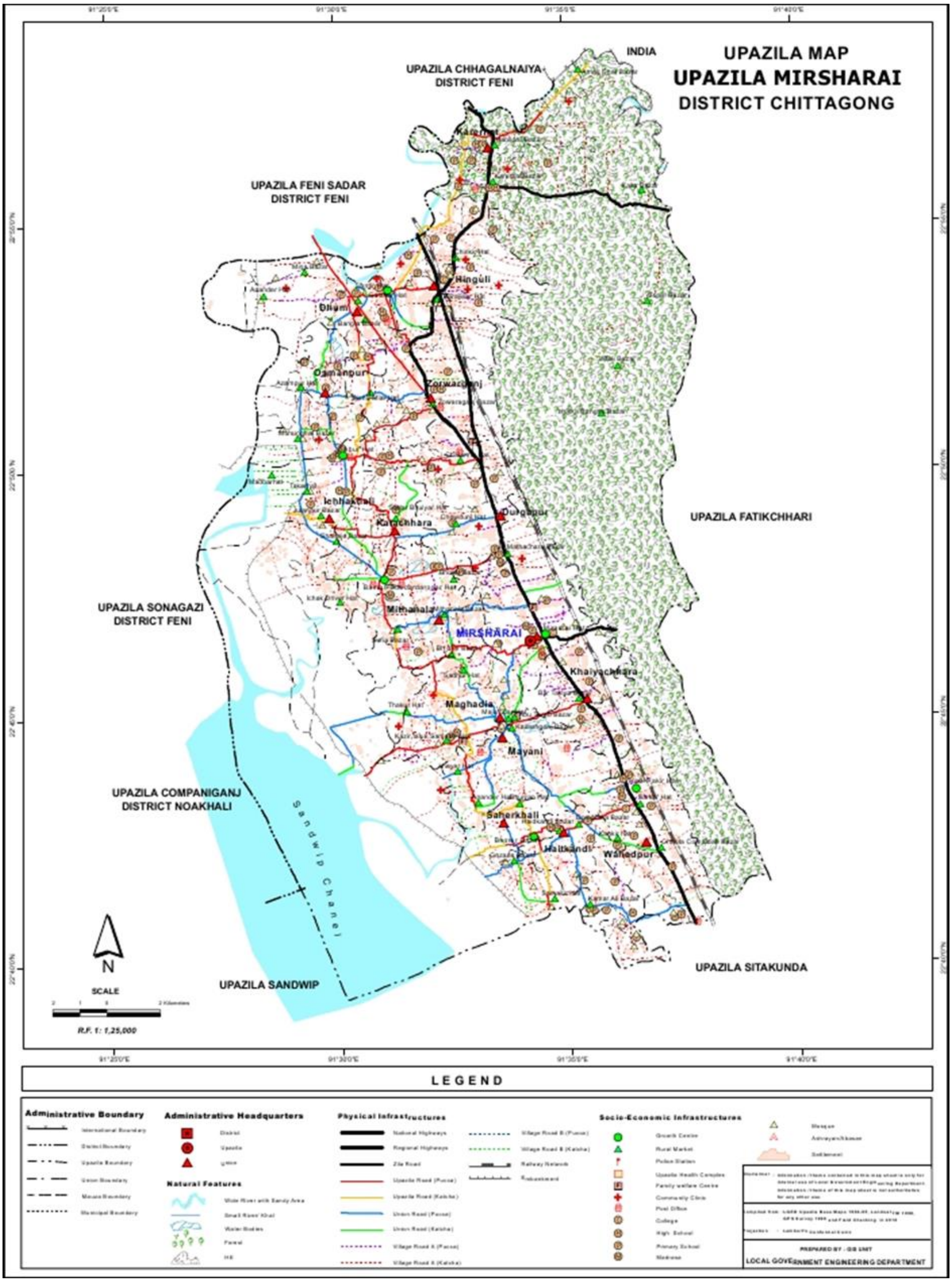

Figure 1: Map Showing Location and Accessibility (Source: LGED)

1.2. Topography and Relief

Topographically the Upazila contains both hilly areas and plain lands. Approximately, one half of the Upazila lies in the low lying hills of the Chittagong hill tracts in the east. The hilly region has high relief and is sparsely populated. The highest elevation in the hills is about a100 m and the lowest elevation in the hills is about 30 m. The western half of the area is plain lands with an average elevation of only about 5 m above mean sea level. This area is heavily populated. Numerous small streams crossed the hilly region and flows towards Sandwip Channel across the plain land (Figure 1).

2. Methodology

This study utilizes both field and laboratory procedures to assess the hydrological and hydrogeological conditions of the study area. Field study includes- a) drilling of boreholes at 5 locations for lithological sample collection for laboratory analysis as well as installation of monitoring wells, b) electrical resistivity survey, c) water quality survey including field measurement of important water quality parameters as well as sample collection for laboratory analysis, d) measurement of the depth to groundwater levels, and d) slug test to determine aquifer properties. Details of each of the above mentioned field activities are discussed in the subsequent sections.

2.1. Field Investigations

2.1.1. Drilling and Installation of Monitoring Wells

A total of 5 boreholes were drilled at different locations within the study area (Figure-2 and Table-1) for direct assessment of subsurface geological conditions with depth and space as well as to install wells to monitor groundwater level and water quality. Locations of the boreholes/monitoring wells were chosen carefully to ensure their distribution throughout the Upazila and to maximize the data coverage.

Table 1: Details of the boreholes and monitoring wells.

Borehole ID	Latitude	Longitude	Total Drilling Depth [m]	Screen Depth [m]
MW-01	22.88738	91.5546	219	165
MW-02	22.82665	91.48352	222	210
MW-03	22.78856	91.55094	204	195
MW-04	22.73395	91.50329	216	201
MW-05	22.70814	91.56847	159	156

Reverse circulation conventional drilling method was used in drilling the monitoring wells (Figure 3). Subsurface Geological variations with depth were recorded at each drilling locations during the time of the drilling by investigating the drilling cuttings at a regular interval of 3.0 m. The information was then recorded using a standard data recording format in Appendix-I. Additionally, the drilling cuttings were sampled at every 3.0 m and approximately 500 gm (Figure 3) of sample from each depth points were preserved in a polybag for transporting to a lab for grain size analysis.

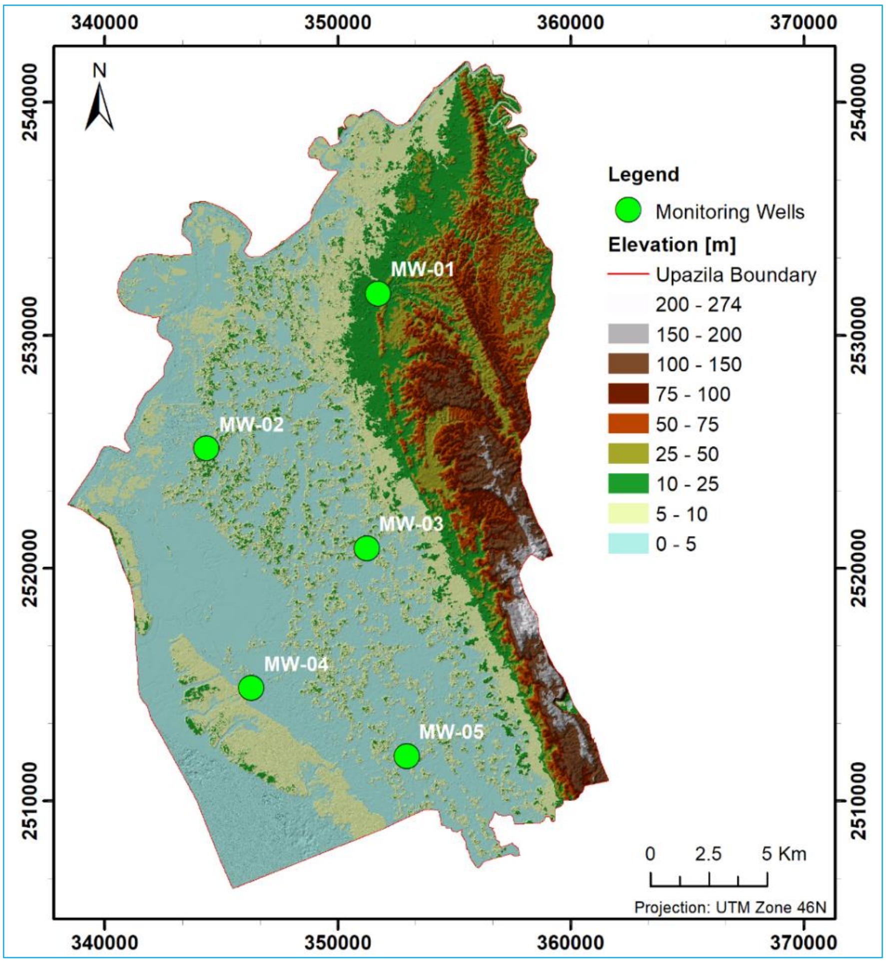

Figure 2: Digital Elevation Model of the study area (Source:UDD) along with the locations of the monitoring wells and drilling sites.

Monitoring well was installed at each borehole site. After careful investigation of the drillers log prepared during the drilling, a suitable aquifer zone was chosen at each site for well screen. At each location, 9.0 m long screen with 1.5 inches diameter were installed.

Figure 3: Monitoring well drilling and Wash samples.

The borehole depth interval between the top of the screen to the land surface was cased using 1.5 inches PVC pipe except in two locations. The exceptions were in areas where the water table was relatively deeper than other areas. In these locations 40.0 m long and 3 inches diameter housing was installed (Figure 4). After installation of a monitoring well it was washed properly following standard procedure. The standard lithological log is attached in Appendix-I.

Figure 4: Established Monitoring well with 3 Inches Housing Pipe.

2.1.2. Electrical Resistivity Survey

Vertical Electrical Sounding (VES) is by far the most used method for geo-electric surveying, because it is one of the cheapest geophysical method and it gives very good results in many area of interest.

The field measurements technique is adjustable for the different topographic conditions and the interpretation of the data can be done with specialized software, with a primary interpretation immediately after the measurements. The results of **VES** measurements can be interpreted qualitatively as well as quantitatively.

The principle of this method is to insert a electric current, of known intensity, through the ground with the help of two electrodes (power electrodes – AB) and measuring the electric potential difference with another two electrodes (measuring electrodes – MN) (Figure-5). The investigation depth is proportional with the distance between the power electrodes.

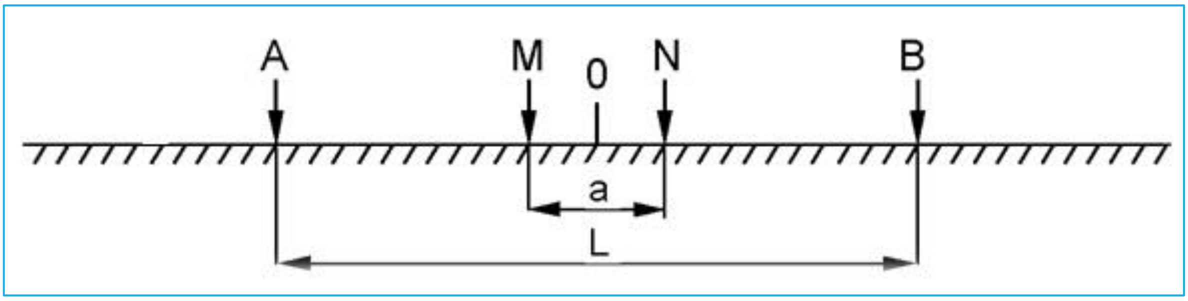

Figure 5: Schulumberger array of VES.

Since direct investigation of the surface geology by drilling boreholes is costly and usually done in widely distributed locations, the information gap in-between drill sites is usually fulfilled using various geophysical surveys. In this study vertical electrical sounding

(VES) method was used to deduce the subsurface lithological/hydrogeological variation with depth at a number of locations distributed all over the study area (Figure 6).

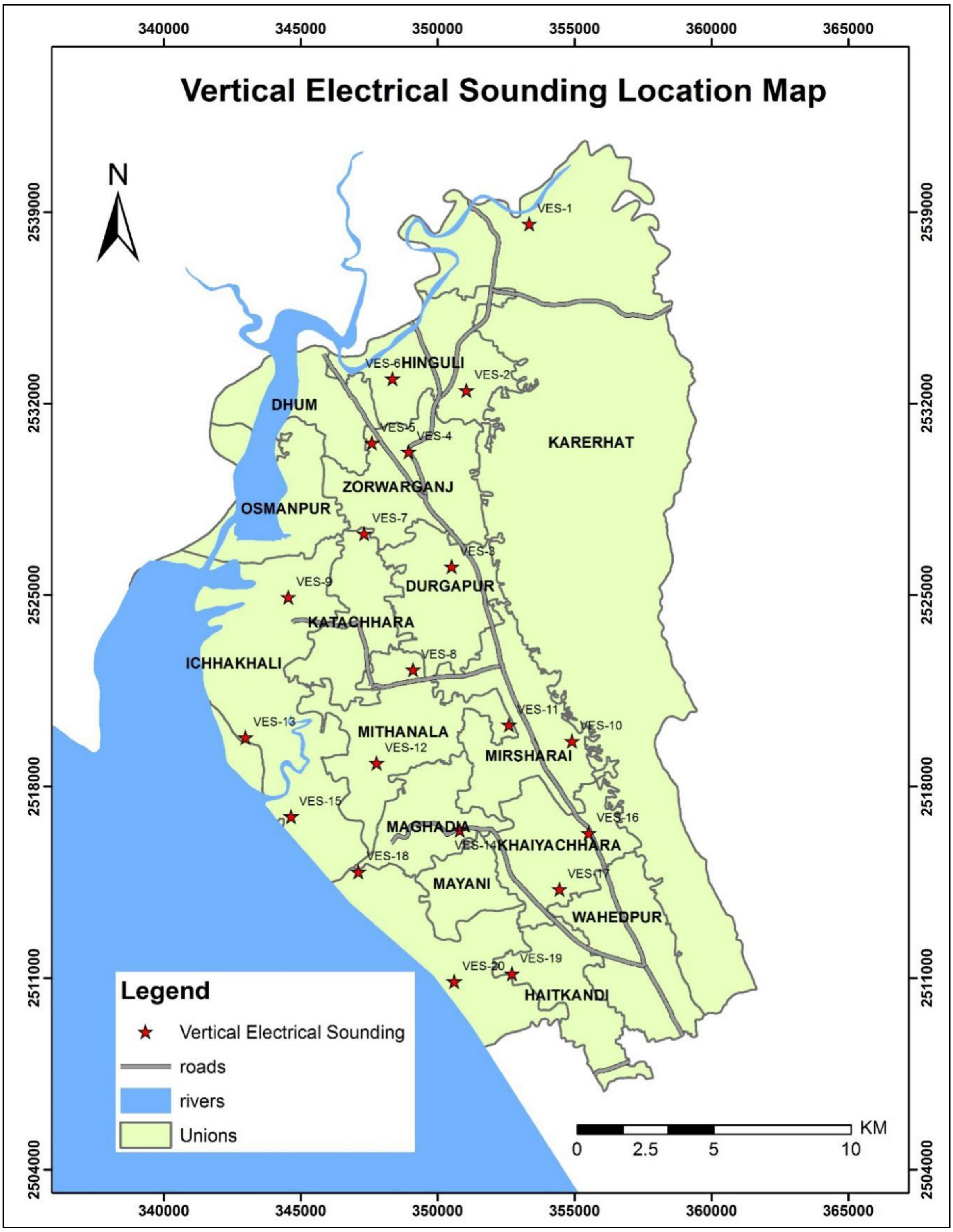

Figure 6: Vertical Electrical Sounding Locations in the project area.

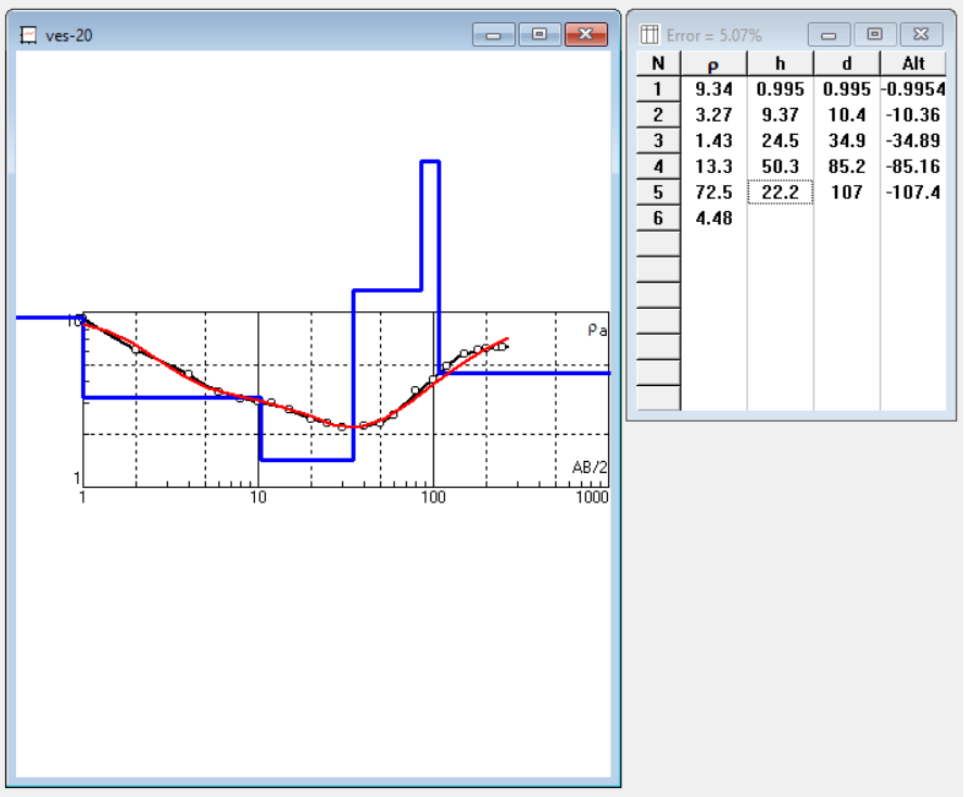

Error = 5.07%

N	ρ	h	d	Alt
1	9.34	0.995	0.995	-0.9954
2	3.27	9.37	10.4	-10.36
3	1.43	24.5	34.9	-34.89
4	13.3	50.3	85.2	-85.16
5	72.5	22.2	107	-107.4
6	4.48			

Figure 7: Sounding Curve VES 20 and the respective subsurface geo-electric model (Left), layer resistivity, thickness and depth to the right.

Rho [ohm-m]	**Thickness [m]**	**Depth [m]**	**Lithology**
9.34	1	1	Top soil
1.43-3.27	34	35	Brackish Sand
13.3	50	86	Clay
72.5	22	108	FW Sand

Table 2: Interpreted result for VES-20 obtained from geo-electric model

Raw data from field for VES, Sounding Curves and subsurface geo-electrical model as well as interpretation from geo-electrical model of rest of the VES are given in Appendix-II.

Figure 8: Resistivity Survey (VES) in Presence of UDD personnel and Local Pouroshova Commissioner.

2.1.3. Water Quality Survey and Sampling

A number of field parameters were measured in the field using field kits and handheld filed instrument at more than 76 locations including shallow and deep wells in the study area (Figure 9). At every location, at least two wells, one at depth shallower than 100 m and the other at depth deeper than 100.0 m were surveyed.

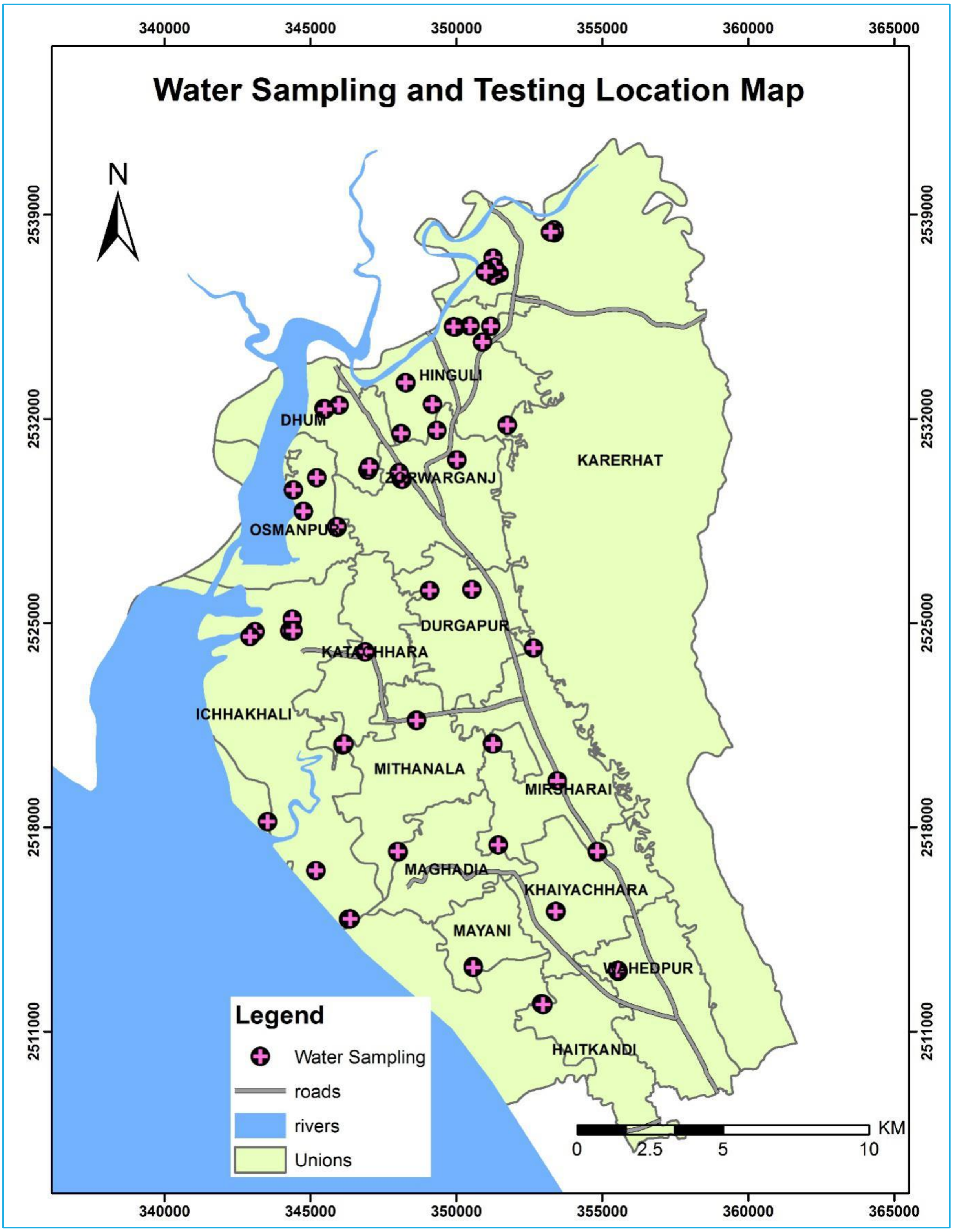

Figure 9: Water sampling and testing location map

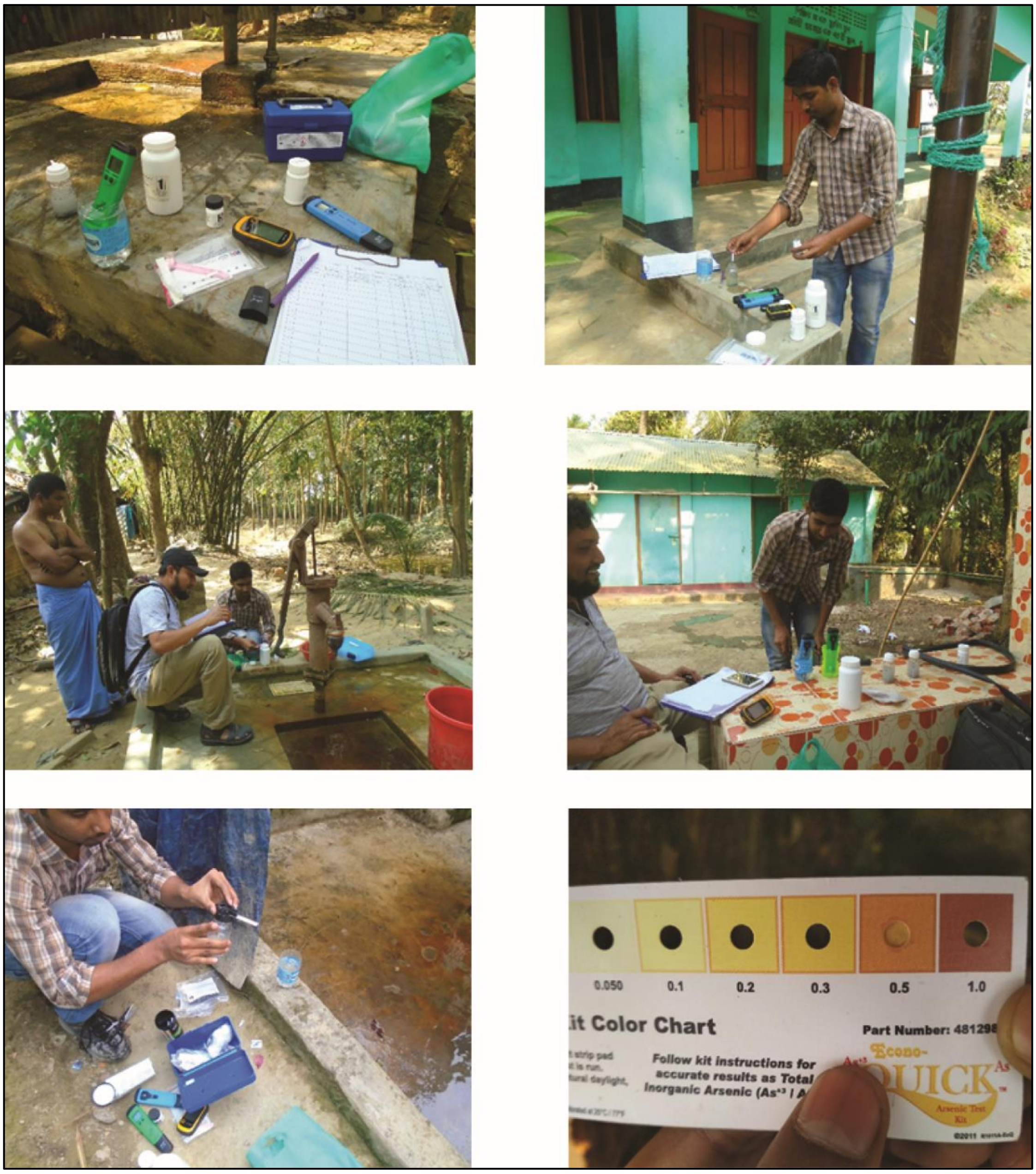

Figure 10: Water Sampling and Field Tests of Arsenic, EC, PH, EH, Temperature etc.

Water samples were also collected from these wells for detail chemical analysis in the laboratory. For each well, two samples each 125 ml and one acidified, was collected in plastic bottles. Each well was purged for at least 10 minutes before field measurements and sampling. The field parameters measured using handheld meters include- pH, Eh, EC, and Temperature. Arsenic was measured in the field using Econo-Quick™ Field kit. Details of the field data are given in Appendix-III.

2.1.4. *Groundwater Level Survey*

Depth to groundwater was measured in the filed using the Kaizen Imperial^{TM} level meter at each of the water sampling locations (Figure 9). Like the water sampling, water level was measured in both a shallow and a deep well at every location except when the pair was not available. The depth to water data collected from the field was later converted to groundwater level with the help of the DEM supplied by UDD.

Figure 11: Water Level data collection in various location in Field.

2.1.5. Slug Test

Slug test was carried out in 22 locations almost uniformly distributed within the Upazila (Figure 10). During the test procedure a slug (2.0 m long iron rod of 0.75 inches diameter) was rapidly lowered in the well (after removing well head) (Figure 11). The slug displaces water in the well equal to its volume and caused the water level in the well to rise almost instantaneously and decays to its original position with time. Time required for the water level to reach its original position provides estimates of hydraulic conductivity of the aquifer zone surrounding the screen. An automatic water level logger was kept in the well before the slug was lowered. The logger recorded the changes of water level in the well with time. (Figure 12 & 13). The interpretation of slug test is given in Appendix-IV.

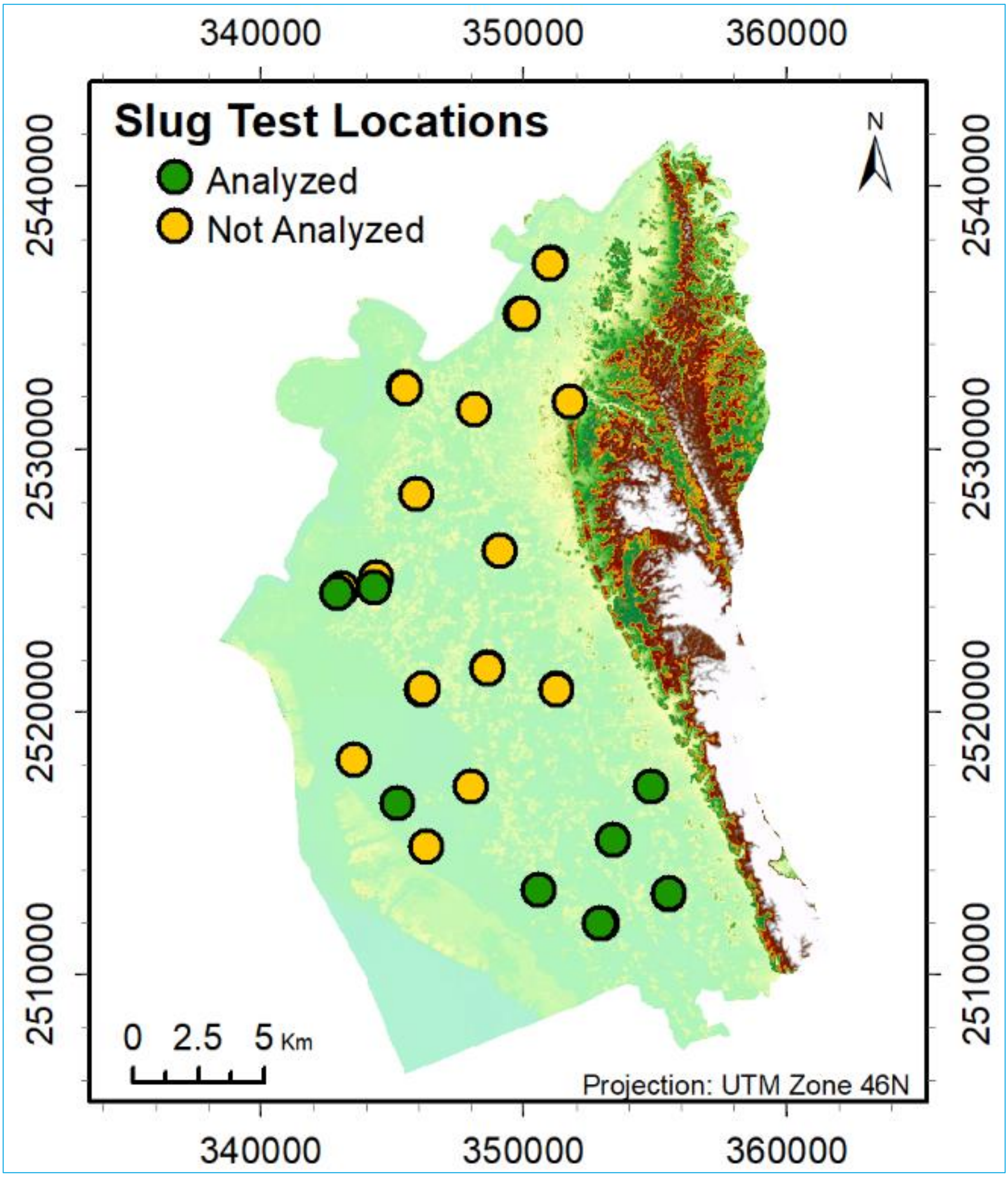

Figure 12: Map showing the locations where slug tests were carried out in the field. Most of the location has a pair of a deep and a shallow wells. Not all data have been analyzed yet, data points are highlighted for which hydraulic conductivity has be

Figure 13: Slug Test in field.

The Hvorslev equation (1) was used to analyze the slug test data for wells with overdamped response (Figure 14). A few wells showed underdamped response (Figure 15), slug test data for these wells were analyzed using Bouwer and Rice equation (2).

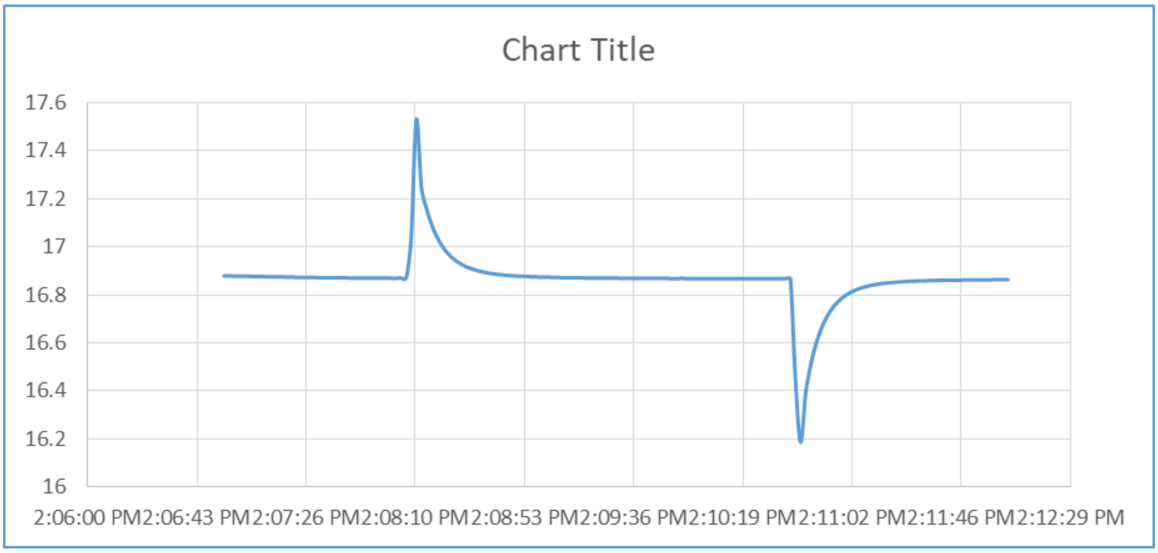

Figure 14: Overdamped Response.

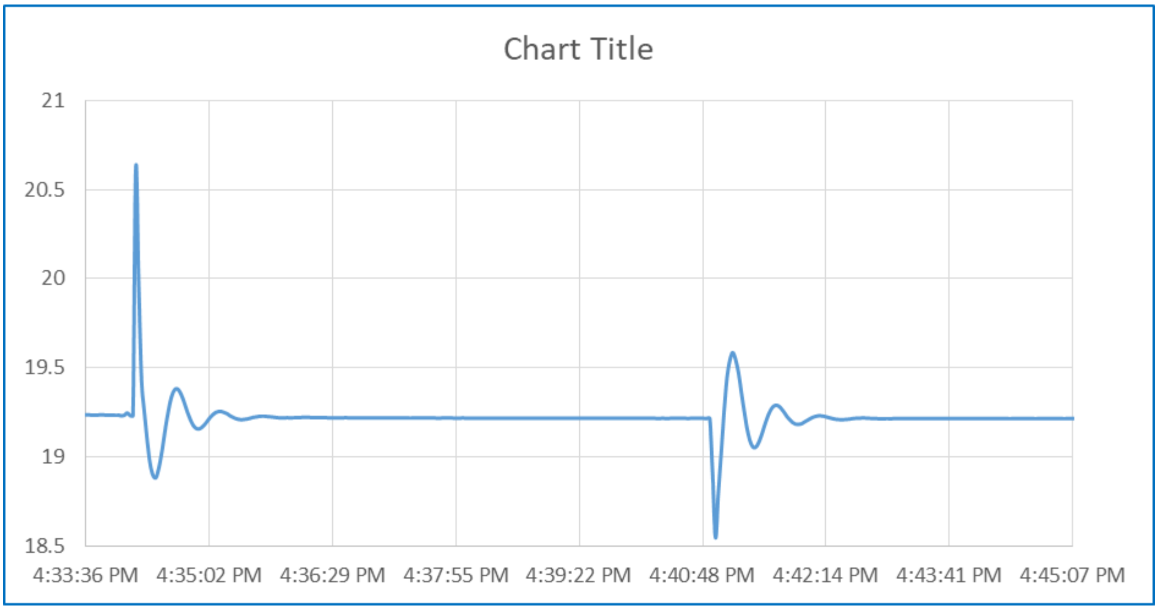

Figure 15: Underdamped Response.

Hvorslev Equation (1):

$$K = \frac{r_c^{\,2} \cdot \ln\left(\dfrac{L_e}{r_w}\right)}{2 \cdot L_e \cdot t_0}$$

where r_c is the radius of the well casing (m), L_e is the length of the well screen (m), r_w is the radius of the well screen (m), t_0 (s) is the basic time lag and the time value (t) is derived from a plot of field data. Generally, t_{37} (s) is used, which is the time when the water level rises or falls to 37% of the initial hydraulic head H_0 (m), the maximum difference respect the static level

Bouwer and Rice (1976) Equation (2):

$$K = \frac{r_c^{\,2} \cdot \ln\left(\frac{R_e}{r_w}\right)}{2L_e} \cdot \frac{1}{t} \cdot \ln\left(\frac{H_0}{H}\right)$$

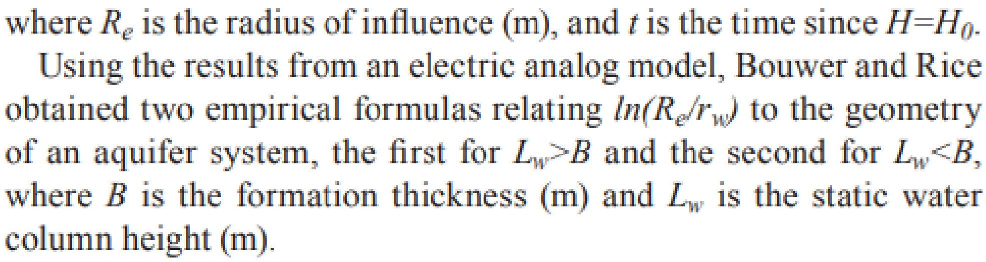

where R_e is the radius of influence (m), and t is the time since $H=H_0$.

Using the results from an electric analog model, Bouwer and Rice obtained two empirical formulas relating $ln(R_e/r_w)$ to the geometry of an aquifer system, the first for $L_w>B$ and the second for $L_w<B$, where B is the formation thickness (m) and L_w is the static water column height (m).

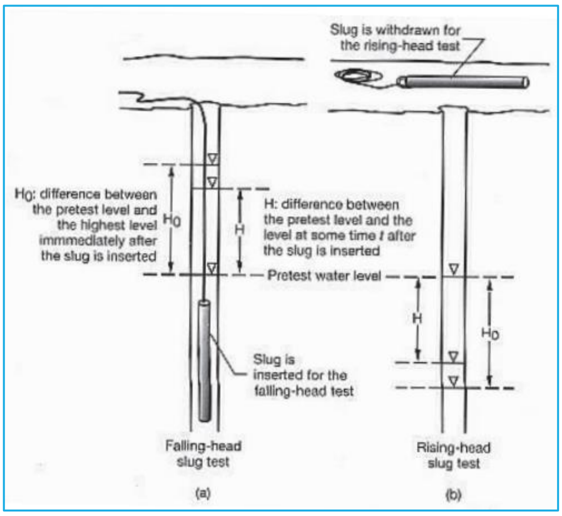

Figure 16: Slug Test Operative Method.

2.1.6. Identification of Surface Water body, Flash Flood zoning and mitigation approach

2.1.6.1. Catchment area and Prospective Artificial Reservoir

A 10 m resolution DEM supplied by the client was used to construct a drainage map of the Mirasharai Upazila. Using the drainage map and topography prospective surface water reservoirs were delineated. It should be noted that this part of the study was beyond the scope of the ToR. The quality of the final output prepared largely depends on the quality of the supplied DEM.

2.1.6.2. Flash Flood Zoning and Mitigation

Flash floods are one of the most common types of natural disasters that can be caused by many different naturally-occurring events such as thunderstorms, hurricanes, tidal waves and melting ice or snow. Among the negative effects great extent of damage that can be cause to man-made structures. The occurrence of this catastrophic phenomenon is directly related to population pressures which is the climate change and the environmental impact of human activity.

In Mirsharai, flood events occur mostly in small - to medium-sized catchments drained by ephemeral water courses. Usually, disasters, in these flash flood prone basins, are mainly caused by high- intensity rainfall falling over a short period of time. Several regions in Mirsharai suffer from frequent and extreme flood that is a phenomenon generally caused by intense rainstorms.

The drainage basins in Mirsharai are relatively small with moderate to steep slopes in hilly part and gentle slope in the plain land. These systems become particularly active during extreme rain events and this may be a source of significant damage to human infrastructure. Despite the importance of these floods, the hydrological analysis of catchments in Mirsharai has been especially difficult due to the lack of precipitation discharge gauges and soil property data. Generally, Flash floods in this area are linked to storming events, but there are additional factors that can intensify flooding such as the pattern of the drainage network, the morphology of the catchment and the human interventions.

It has been shown that a catchment’s morphometric variables control its hydrologic response. Understanding a basin’s response to extreme rainfall based on geomorphological indices can be valuable when studying flood hazard in catchments.

The objective of the study is to present the risk zoning for Flash flood events of the area, prefecture and to model surface runoff by creating a system based on GIS technology. Particularly, a unit hydrograph is constructed for the excess rainfall by estimating the stream flow response at the outlets of the existing sub-basins extracted from the UDD provided 10 m DEM prepared from high resolution (50 cm) stereo-pair satellite image.

The model is based on raster data structures. Grids such as elevation, land use, soil type, are used to describe spatially distributed soil parameters. Moreover, hydrologic features of each grid, like slope, flow accumulation, flow direction and flow length were calculated using standard function included in GIS.

Methodology and Data Set:

Data Set:

The topography of the land surface is one of the most fundamental geophysical measurements of the Earth, and it is a dominant controlling factor in virtually all physical processes that occur on the land surface. Consequently, topographic information was the most important data used at the current study. This information was provided by the Client (UDD) came with 10m DEM prepared from high resolution (50 cm) stereo-pair satellite image from Digital Globe (Figure-19). The particular geomorphological and morphological characteristics such as slope map, flow direc- tion, flow accumulation and flow length layers as well as hydrological basins and the drainage net- work were estimated for the study area. ArcGIS version 10.4.1 and especially spatial analysis exten- sion contributed to this procedure.

Another layer that was important for the study purpose was the land cover map. This map was derived from the Sentinel-2A satellite image dated 17 January 2018 with spatial resolution 10 m and spectral resolution 13 band (used Band 2, 3 and 8).

Finally, geological data of year 2001 from Geological Survey of Bangladesh (GSB), Soil Map data of year 1997 were also used for the study's purposes. They have been collected from Soil Research Development Institute (SRDI), Bangladesh.

All these derived maps were used for the construction of the runoff model for the flood event that was described previously. Consequently, the collection of the meteorological data, which have been provided from Bangladesh Meteorological Department (BMD) was an important part of the study. These data refer to Sitakund station which is the nearest station to the selected basin.

Method:

All the basic steps that were needed for the study are illustrated in Figure 18. The most important steps in order to simulate the real rainfall event were the calculation of the travel-time layer which indicates the time needed for the water to reach the outlet of the basin, as well as the extraction of the isochrones map which are lines of equal travel time to the outlet of basin. Subsequently, a routing model which combines all the above maps was created in GIS environment. The estimation of the direct runoff at the outlet of the catchment was produced by assuming that the extreme rainfall event was a phenomenon with a spatially homogeneous distribution.

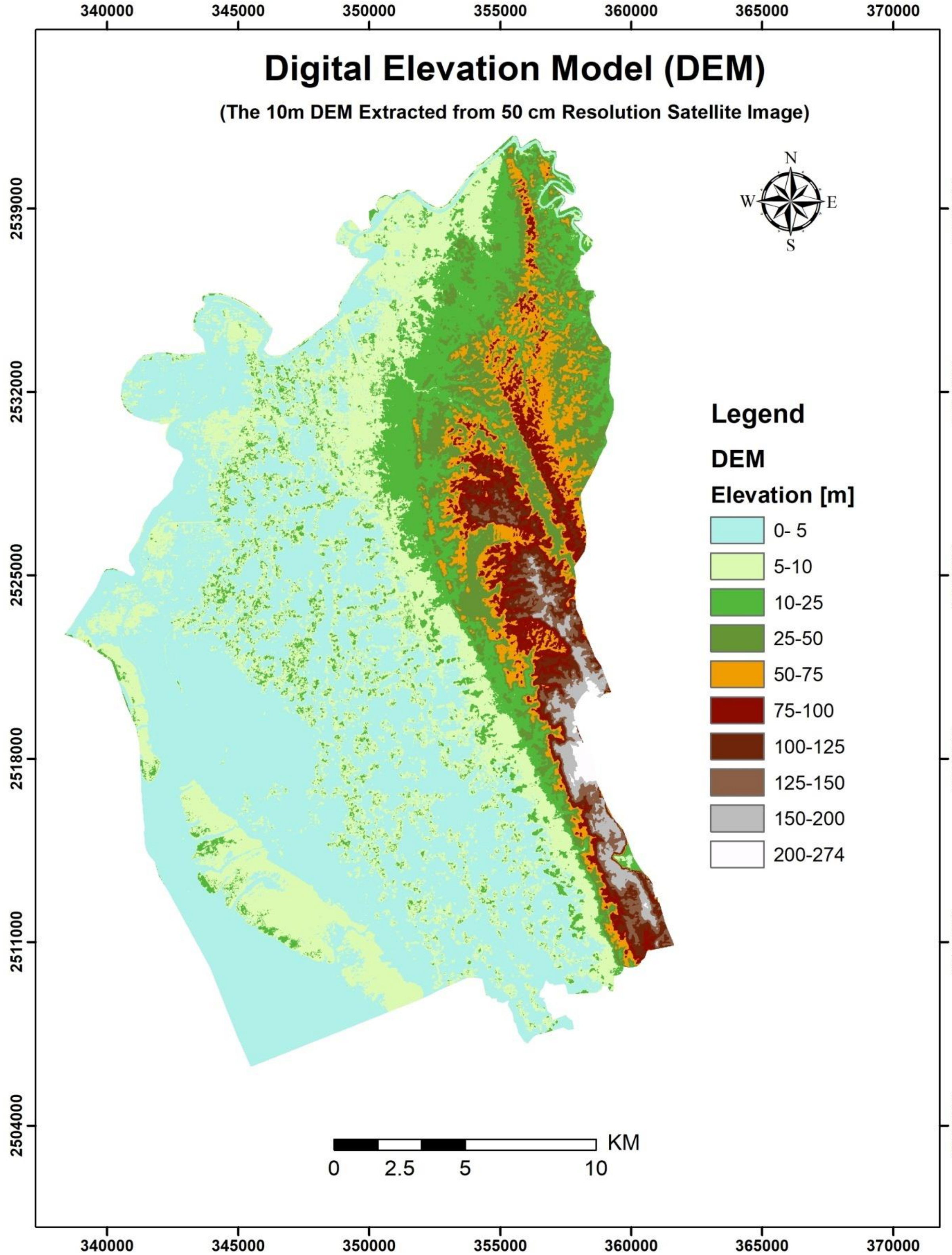

Figure 17: Digital Elevation Model (DEM)

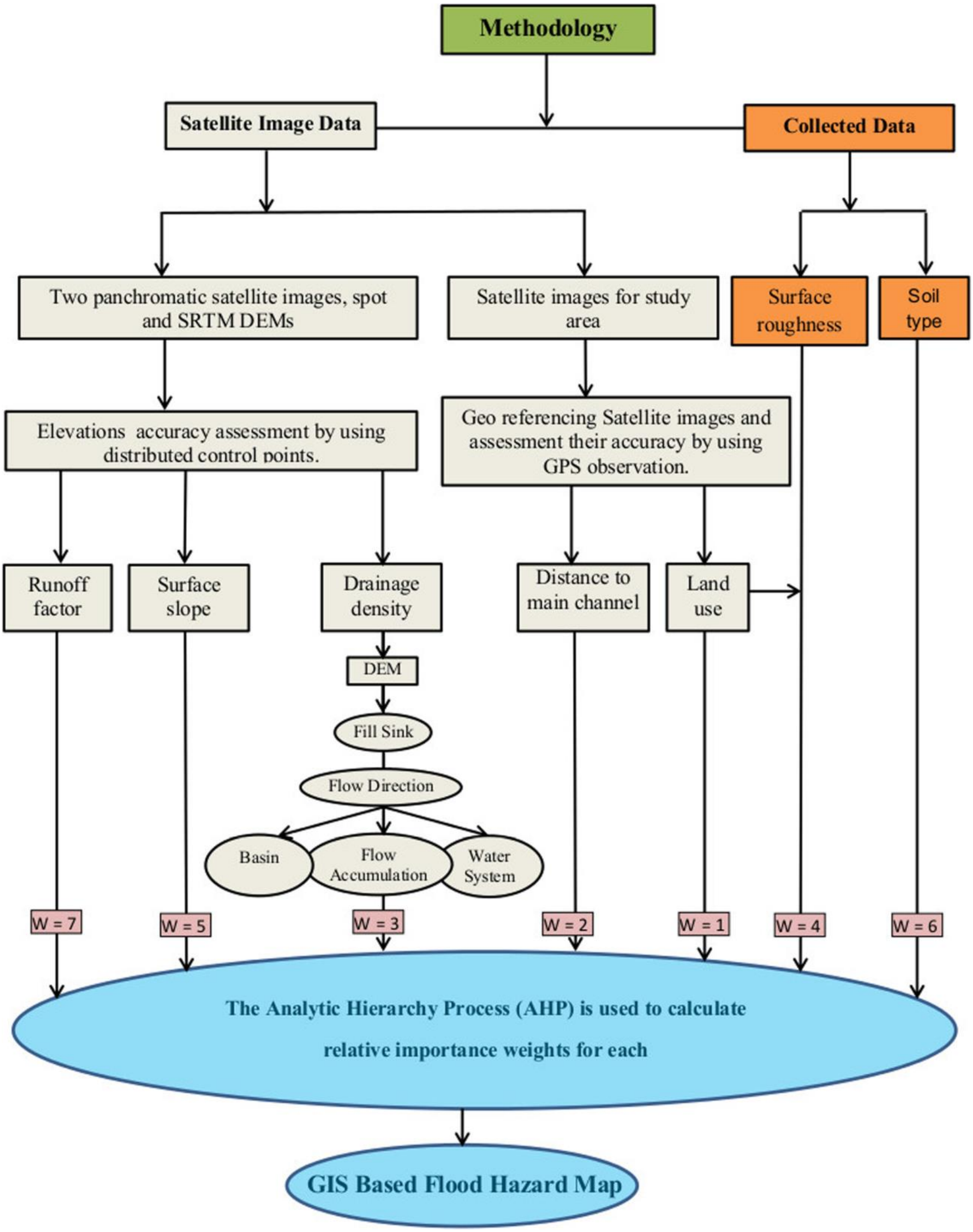

(w =the weight of each flood causative factor).

Figure 18: Methodology for flood hazard mapping (Modified after Ismail Elkhrachy, 2015)

If the rainfall intensity exceeds the evaporation rate and infiltration capacity of the soil, surface runoff occurs as a flash flood. It also occurs when rainfall falls on impervious surfaces, such as roadways and other paved areas. There are many factors affecting flood hazard identification and modeling, varying from one study area to another. For instance urban flood modeling is extremely complex due to interactions with various man-made structures such as buildings, roads, culverts, channels, tunnels, and underground structures. A composite flood hazard index based on seven causal factors is used during this work. These factors, which are listed here, have been elected based on different case studies with similar characteristics (Eimers et al., 2000; Yalcin and Akyurek, 2004; Pramojanee et al., 2001; El Morjani, 2011; Pedzisai, 2010 and Ho et al., 2010, Ismail Elkhrachy, 2015).

1. **Run off:** The likelihood of a flood increases as the amount of rain at a location increases. Higher pre- cipitation intensity can result in more runoff because the ground cannot absorb the water quickly enough.
2. **Soil Influences:** Soil type and texture are very important factors in determining the water holding and infiltration characteristics of an area and consequently affect flood sus- ceptibility. Some soil types can cause very rapid runoff even in dry conditions. As a general rule, runoff from intense rainfall is likely to be more rapid and greater with clay soils than with sand.
3. **Surface slope:** Land surface slope is one of the effective ele- ments in floods. The danger from flash flood increases as the surface slope increases. It is a reliable indicator for flood susceptibility. When river slope increases then the flow velocity in the river also will increase.
4. **Surface roughness:** Surface roughness in terms of hydrody- namic friction is an essential input for flash flood simula- tion (National Oceanic and Atmospheric Administration, 2010). From Manning’s which are empirical values. Reducing channel roughness results in faster stream flow velocities and less infiltration.
5. **Drainage density:** Drainage density is the length of all chan- nels within the basin divided by the area of the basin. If the drainage network is dense at any area, it will be a good indi- cator to high flow accumulation path and more likely to get flooded.
6. **Distance to main channel:** Areas located close to the main channel and flow accumulation path are more likely to get flooded.
7. **Land cover:** This describes the appearance of the landscape and is generally classified by the amount and type of vegetation, which is a reflection of its use, environment, cultivation and seasonal phenology. Land cover is other essential influences on runoff (Alexakis et al., 2014).

Channel depth and river bed characteristic is an important factor in hydrodynamic modeling. For example, when the discharge of a river increases, the channel may become completely full. Any discharge above this level will result in the river over- flowing its banks and causing a flood. But vertical resolution for used DEMs is not enough to get an accurate cross section information for delineated streams or Drainage Rivers. The sequences of operations are schematically shown in Figure-20 and can be summarized as following:

a. Georeferencing the satellite imagery and registering of the result to the UTM coordinate system zone 46 doing unsupervised classification for the study area, converting physical feature information to raster file.

b. Calculating surface slope from DEM. Slope means the maximum rate of change from every cell to its neighbors.

c. Calculating drainage density from draining network and basin information.

d. Extracting main channel from draining network (which has maximum stream order) followed by calculating perpendicular distance from zone centroid to main channel.

e. Preparing model file by Arc Hydro and HEC-GeoHMS tools and computing hydrologic parameters by HEC-HMS software.

f. Integrating all data in a GIS environment using the Analytical Hierarchical Process (AHP) method to calculate flood hazard map.

Figures show some of data layers used in the analysis. Each is depicted in a stretch color scale, where black represents the highest values and white the lowest values. ArcMap 10.4.1 was used to execute the above steps for both DEM and Sentinel-2A images to extract drainage flow net and LU/LC in the study area. The flow networks and basin boundaries were then vectored. The basin characteristics and the morphometric parameters were calculated from 10m DEM.

2.2. Laboratory Analysis

2.2.1. Grain Size Analysis

Lithologic samples collected from the monitoring wells were sorted and depending on the lithological variability samples from each aquifer unit was selected for grain size analysis.

Grain size analysis includes oven drying the samples and then sieving through various mesh sizes and calculation of weight percentage for different size fraction (Figure 19). Grain size data was later used in calculation of hydraulic conductivity of the aquifer unit using empirical formula.

In 1893, Hazen published his formula for estimating hydraulic conductivity:

$K = C_H \text{ x } D_{10}^2$

K = Hydraulic conductivity [m/s]

C_H = Empirical constant, in this study set to 0.01157 [-]

d_{10} = The particle size for which 10% of the material is finer [mm]

The Hydraulic Conductivity obtained from the grain size analysis of the samples from monitoring wells are attached in Appendix-V.

Figure 19: Grain size Analysis in Laboratory

2.2.2. Water Quality Analysis

Water samples collected from the field were brought to the laboratory for detail chemical analysis. Chemical analysis includes determination of the concentration of major ions and trace elements. All the samples were tested in the laboratory. The water quality data are given in Appendix-VI. List of chemical species and analytical methods are given in Table -3.

Serial no.	Chemical constituents	Methods and Instruments
1	Sodium (Na^+)	Atomic absorption spectrometer(GBC sens AAS)
2	Potassium (K^+)	Atomic absorption spectrometer(GBC sens AAS)
3	Calcium(Ca^{2+})	Atomic absorption spectrometer(GBC sens AAS)
4	Magnesium(Mg^{2+})	Atomic absorption spectrometer(GBC sens AAS)
5	Bicarbonate(HCO_3^-)	Titration method (standard H_2SO_4 for HCO_3^-)
6	Chloride(Cl^-)	Titration method (standard $AgNO_3$ for Cl^-)
7	Nitrate(NO_3^-)	UV visible spectro-photometer(wave length 410nm)
8	Iron (Fe)	Atomic absorption spectrometer(GBC sens AAS)
9	Manganese (Mn)	Atomic absorption spectrometer(GBC sens AAS)
10	Arsenic (As)	Atomic absorption spectrometer(GBC sens AAS)
11	Sulphate(SO_4^{2-})	UV visible spectro-photometer(wave length 410nm)

Table 3: List of chemical species and analytical methods

2.3. Groundwater Modeling

A three dimensional groundwater flow model has been developed using the USGS finite difference flow code MODFLOW. The model consists of 345 rows and 210 columns, each 100 m in length and width, respectively, resulting in a total number of 72450 cells per layer (Figure 20). There are a total of 6 layers in the model representing three aquifers, two aquitards, and a thin low permeability layers at the top. Thickness and depth of each layer varies from place to place as depicted from the 3D lithological modelling.

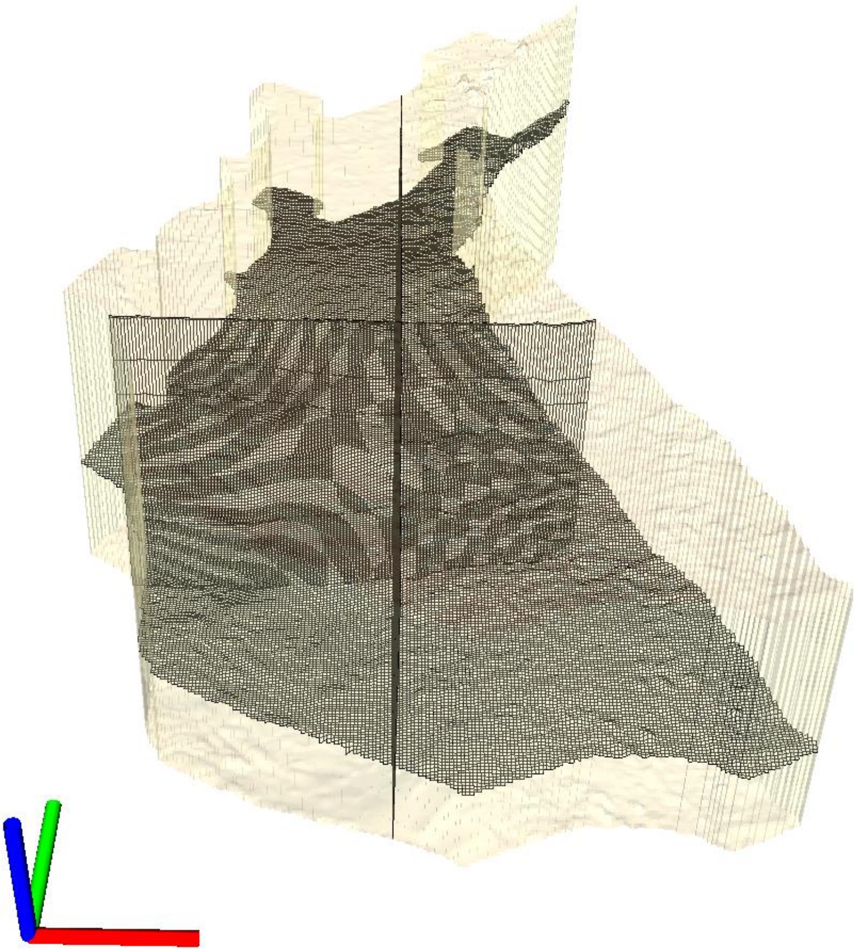

Figure 20: Groundwater Model Setup and discritization

The left boundary of the model is represented by constant head in response to the presence of the Feni River in the North West, and the Sandwip Channel in the West, South West. Head along the Feni River is approximated to be decreasing from north to south following the same gradient as the land surface elevation along the river. Head for the Sandwip channel is considered to be zero since this is located very close to the sea. The southern boundary of the model is represented by another constant head boundary; the head value along this boundary is based on the head measurement from the field. The eastern part of the study area is bounded by hills; therefore, it was represented by a no-flow boundary condition in the model. At the bottom of aquifer three there is a clay layer ubiquitously present in the study area, therefore, the bottom boundary of the model also represented by a no-flow boundary. The top boundary was approximated using a constant value of recharge along with a drain allowing the model to accept as much recharge as required and reject the access recharge water through the drains. This trick was applied in the modelling because field estimation of groundwater recharge is difficult and never gives a reliable estimate. The model was run in steady state condition.

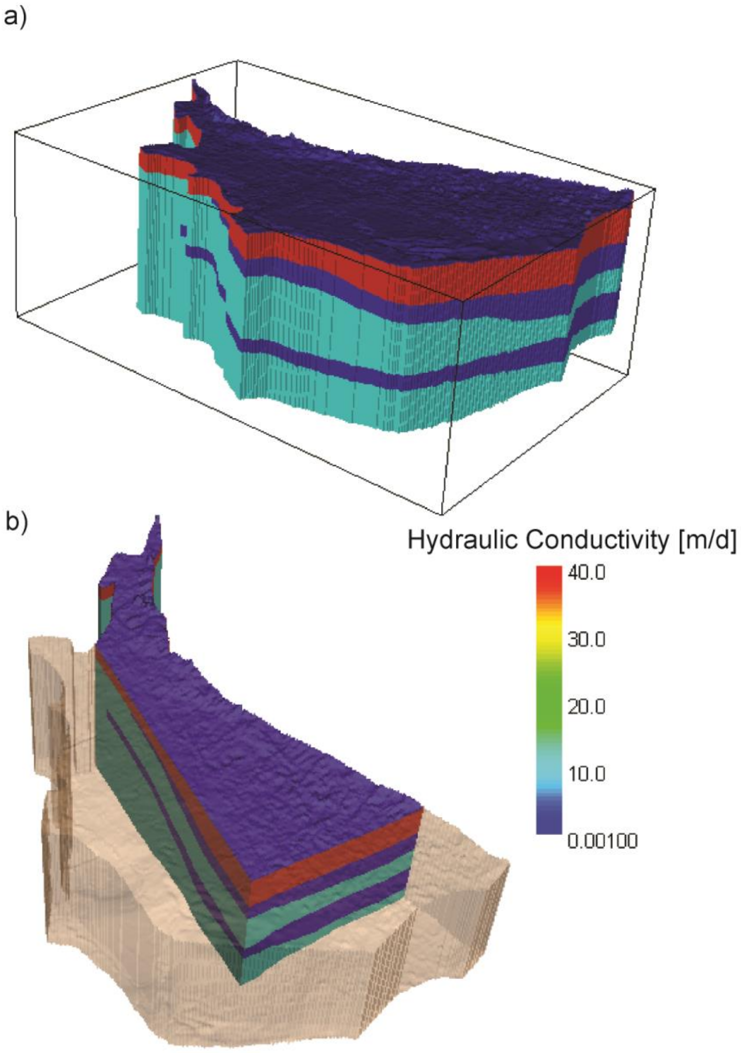

Figure 21: Model layers and their hydraulic conductivities

Hydraulic conductivity values that were estimated from slug test and grain size analysis for different aquifer layers were assigned in the model. It should be noted that the hydraulic conductivity is scale dependant, meaning its value depends on the scale of measurement. Usually, small scale measurements tend to underestimate it. Both slug test and grain size analysis provides estimate on a scale of cm to m, therefore, the estimated values are the lower estimate (Table: 4). The modelling began with the exact value of the field estimated average value of hydraulic conductivity for each layer and later these parameters were adjusted to obtain a match of the simulated head data to the observed head data. It should be noted that the observed head data is highly affected by the topography and elevation of the well head, due to poor data on topography the exact match between the simulated head and the observed head is not possible. Therefore, emphasis was given to match the overall trend in flow direction and the ranges of head values between the observation and model simulation.

2.3.1. Calculation of Pumping Rate

There are rarely any data quantify the exact amount of groundwater withdrawal anywhere in Bangladesh. However, there are ways to get some estimates of water demand/withdrawal based on population in an area. Michel and Voss (2009)[1] considered 50 litre of water consumption per person per day in rural settings in Bangladesh, while Khan et al. (2016)[2] found that the per capita water consumption in urban settings increases by a factor of about 4 times increment of pumping for various future scenario was calculated based on the total union population every five years.

2.3.2. Model Scenarios

Three different future scenarios has been tested using model. They are as follows-

2.3.2.1. Business as usual

Under this scenario a population growth rate of 0.77% per year has been considered. Using this population growth rate total union wise population at every 5 years interval was calculated for the next 20 years.

2.3.2.2. High population growth rate in rural and urban setting

If the proposed Economic Zone is established in the study region there is likely to be a high influx of population in near future. However, it is difficult to predict the temporal and spatial trend in the population growth rate in the study area. UDD expect that there will be a total of 5 million people in the study area after 20 years from now, which is a 10 fold increase of the current population is requiring a growth rate of about 13% per year. Of course, the population growth in various unions won’t be uniform; some union will have very high population growth while some other will have low to moderate growth. Also, the growth may not be uniform with time; some years might have flux of population while the other might not. In the study however, we have assumed uniform growth in space and time. This assumption may not be accurate but it will provide insights about the likely drawdown caused by future pumping.

Total annual pumping rate was calculated considering both rural and urban settings. For rural settings 50 liter/person/day was considered and for urban settings 200 liter/person/day was considered.

Only domestic pumping was considered in the modeling, future industrial and irrigation pumping was not considered as there are no data about those.

3. Result

3.1. Groundwater Resources

3.1.1. Aquifer Framework

Aquifer framework in the study are has been delineated based on the interpreted VES data, borehole logs from the five monitoring wells, and additional 4 borehole logs from the Department of Public Health Engineering (DPHE) located in the study area. At ecah location of borehole and VES, lithological data has been grouped into layers of aquifers and aquitards based on lithological characteristics and similarities. Available data indicate that there are three aquifers present in the study area separated by two aquitards. The depth and thickness of each aquifer varies considerably from place to place.

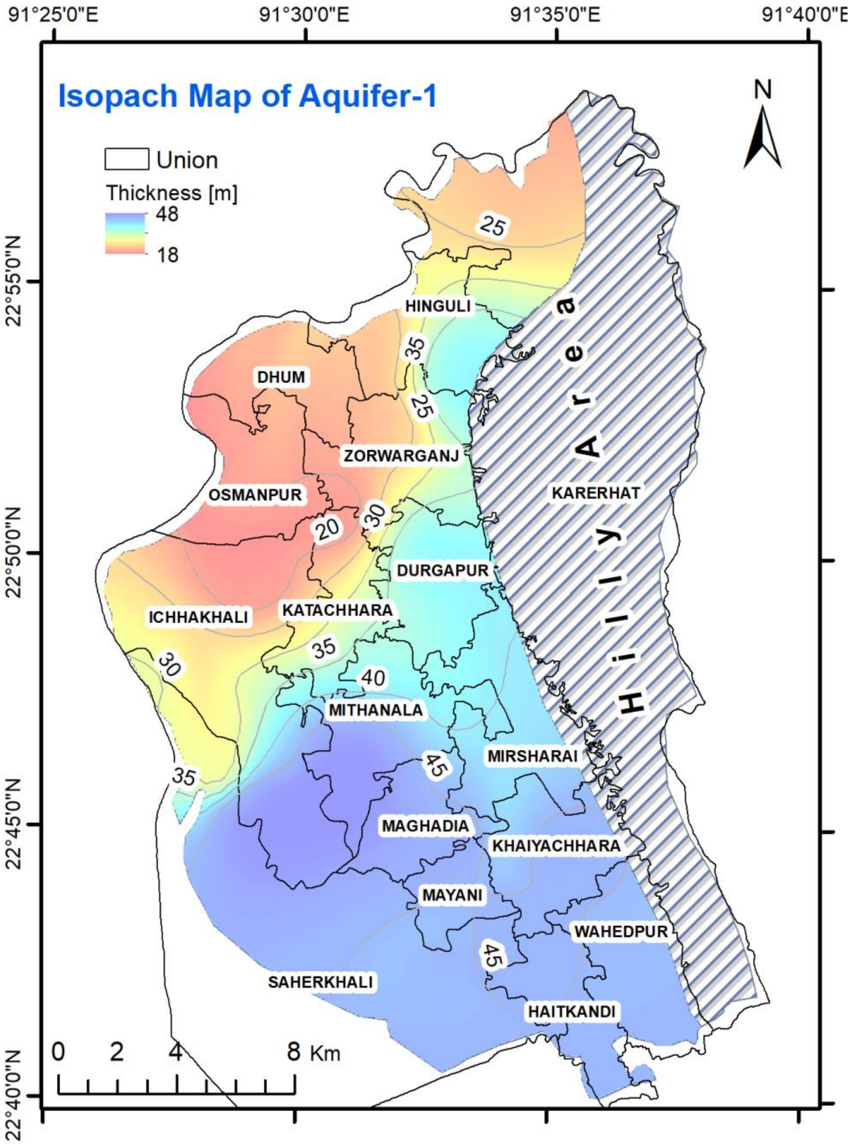

Figure 22: Isopach map of the shallow (1st) aquifer

The shallowest aquifer occurs at the surface and extends down to a depth of 20 to 45 m. The thickness of this aquifer is greatest towards the south and east towards the north and north west (Figure 22). Except the central part of the study area, the aquifer is exposed all over the study area below a very thin soil layer. In the central part of the study area the aquifer lies beneath a 5-7 m thick clay layer.

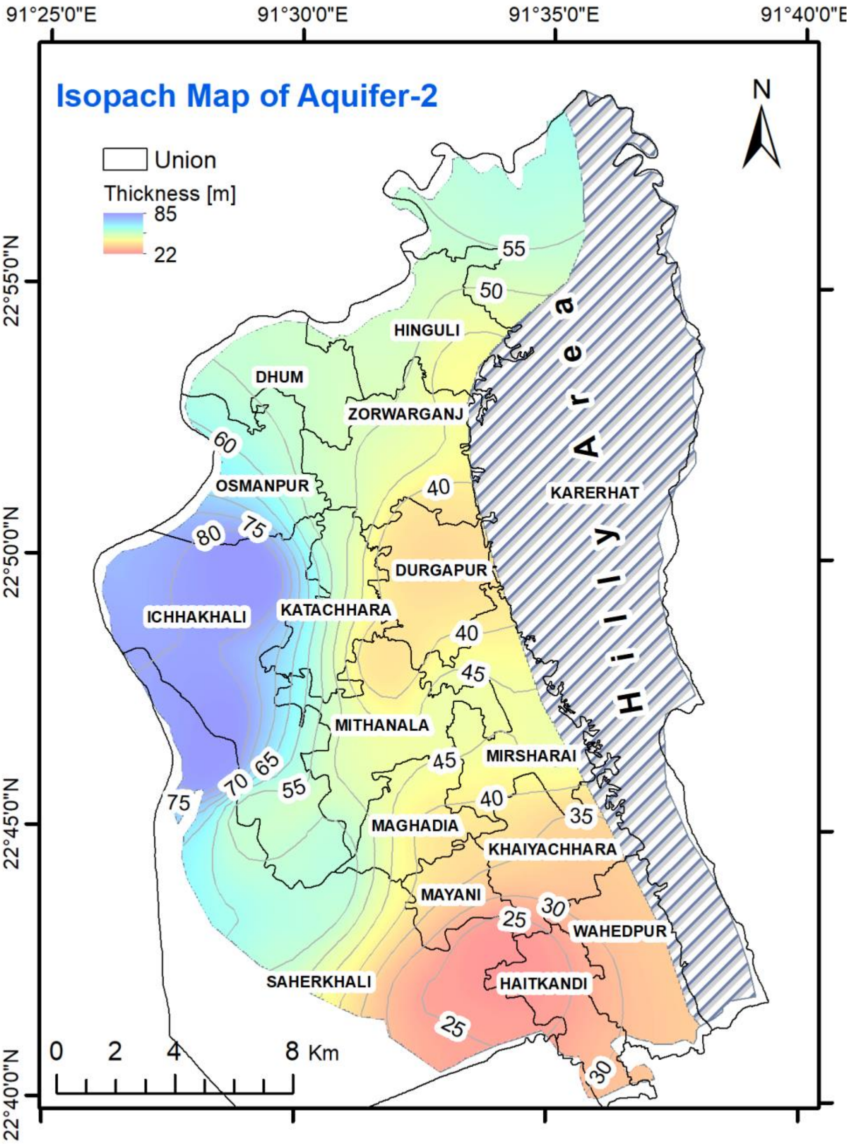

Figure 23: Isopach map of the second (intermediate) aquifer.

The second aquifer is 25 to 85 m thick and is separated from the first aquifer by an aquitard of variable thickness. The second aquifer is thickest in the west and thinnest in the south. In the north the aquitard is absent and both the first and second aquifers are connected. The aquitard separating the first and shallow aquifers are thickest in the south, about 50 m and absent in the north (Figure 23).

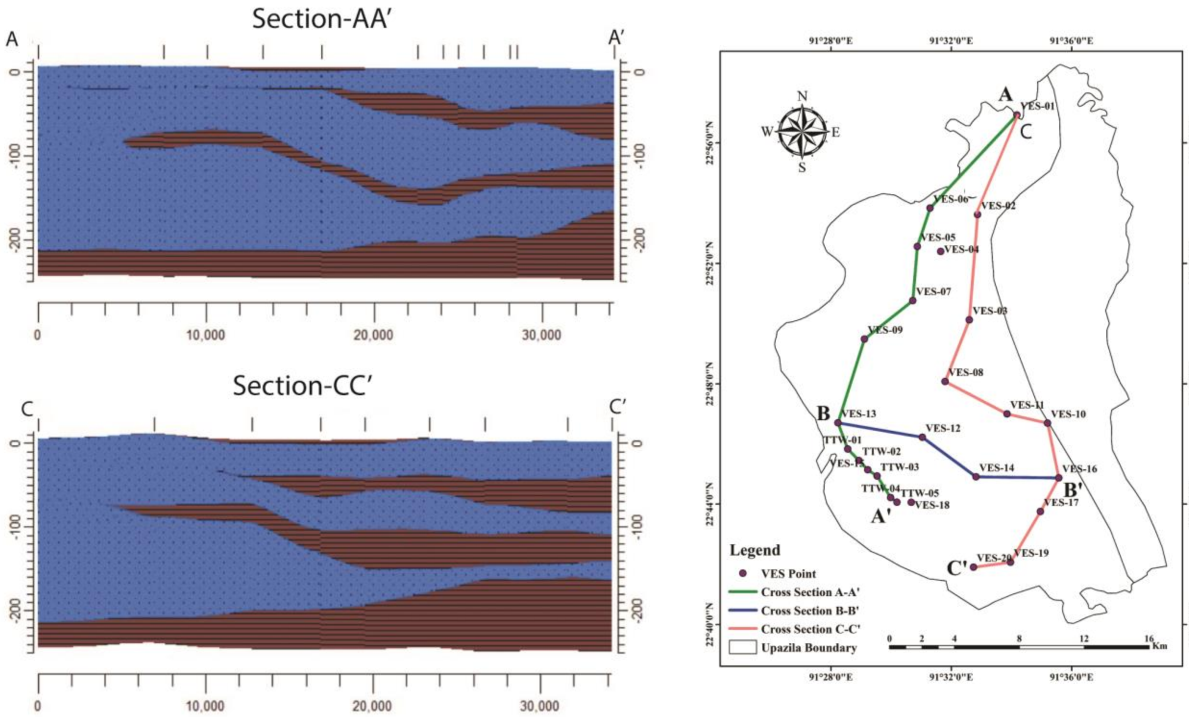

Figure 24: Cross section showing the vertical distribution of aquifer and aquitards in the study area

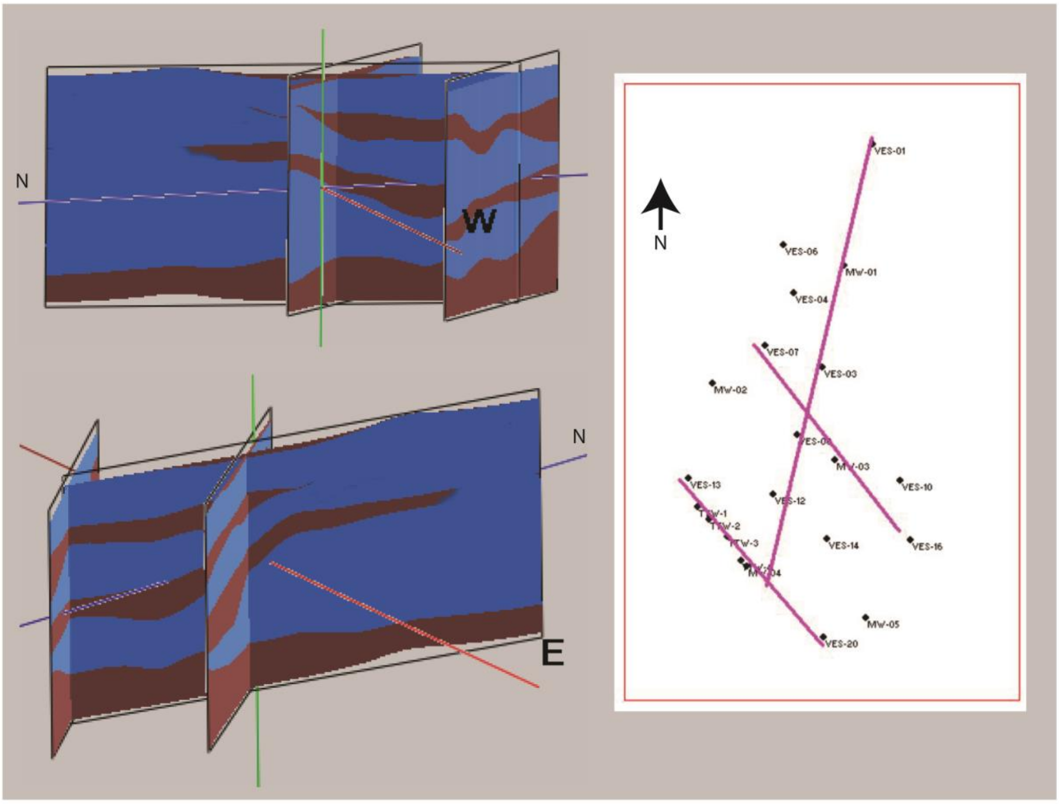

Figure 25: Fence diagram showing aquifer framework in the study area

The third or deep aquifer occurs around 100 m depth in the north and below 150m depth in the south. The aquifer is thinnest in the south and south east (20 m) and thickest in the north and North West (80 to 120m) (Figure 24). It is separated from the second aquifer by a 30-50 m thick aquitard in the south but connected with the second aquifer in the north (Figure 24 and 25). The thickness of the In fact, in the north the distinction between first, second, and third, aquifer is somewhat arbitrary as all these aquifers are connected to make only a single and very thick aquifer.

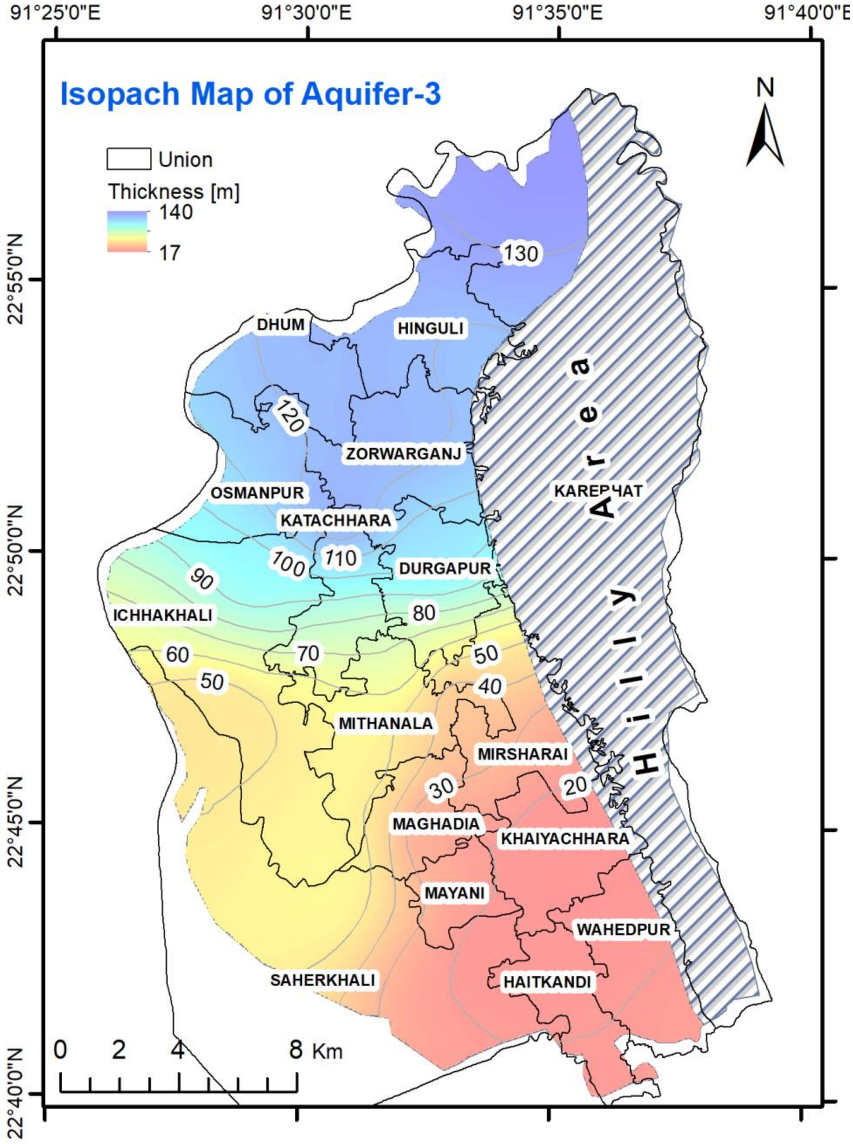

Figure 26: Isopach map of the deep aquifer

A three dimensional model of the aquifer architecture is produced using Rockworks software (Figure 27). This aquifer architecture provide the basic framework for the groundwater model. Layers shown in this model are included in the groundwater flow model. Hydraulic conductivity of each layer is estimated based on the interpretation of the slug test data and empirical equation derived estimate based on the grain size data. Hydraulic conductivity values for each layer are summarized in Table-4.

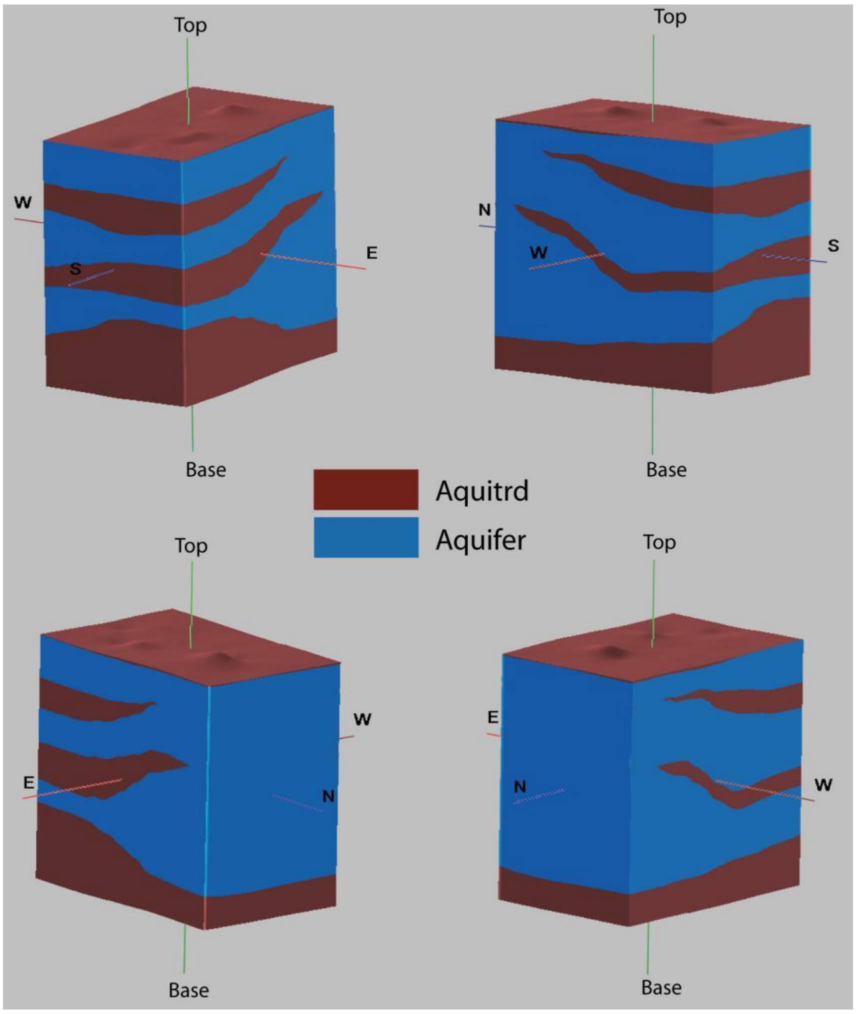

Figure 27: 3D model of aquifer architecture

Aquifer No.	Method							
	Slug Test				Grain Size Analysis			
	No. of Data	K [m/d]			No. of Data	K [m/d]		
		Average	Min.	Max.		Average	Min.	Max.
Aquifer-1	5	6.61	0.87	9.3	33	5.82	1.6	19
Aquifer-2	Nill	-	-	-	34	4.6	0.5	22
Aquifer-3	6	4.75	1	8.45	32	1.15	0.5	4.2

Table 4: Hydraulic properties derived from Grain Size analysis.

3.1.2. Groundwater Flow Direction

Groundwater flow direction was determined based on the field measurement of depth to groundwater level. The depth data was later converted to groundwater elevation based on the DSM supplied by UDD.

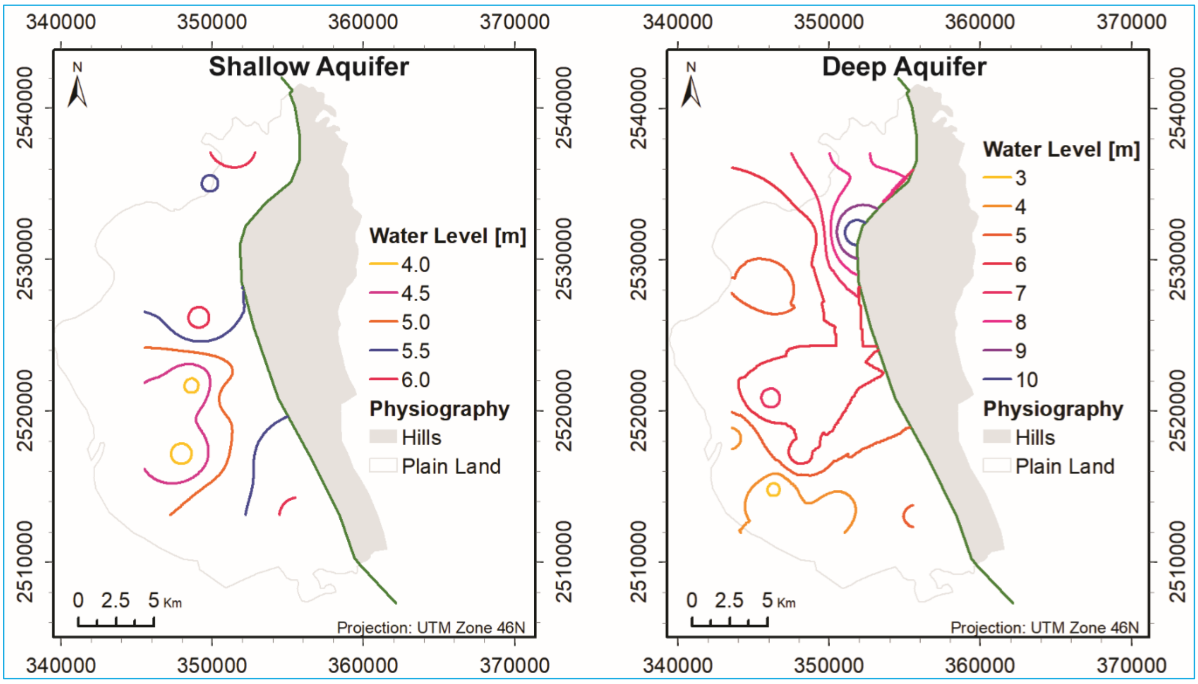

Figure 28: Groundwater level contour in the study area of the shallow aquifer and deep aquifer.

Figure-28 shows the groundwater level for both the shallow and deep aquifer. Groundwater level in the shallow aquifer varies between 4 m and 6 m. Though the data are very patchy, some regional trend in flow direction can be deduced from the figure. Generally, head is higher in the north and northeast and then that in the south and southwest. Groundwater flows from the north-northeast to south-southwest direction. The patchiness in the data is most likely due to inaccurate topography data together with uncertainties in the platform height of the wells. Groundwater level data for the deep aquifer is comparatively more coherent than the shallow data. There is a strong trend in groundwater level, groundwater flows from NNE to SSW direction.

It is worth noting that artesian flow has been observed in the field in the extreme north corner of the study area (Figure-24). Only the deep (>250 m deep) aquifer in that location flows automatically with an approximate head of 5 m above the land surface.

Figure 29: Artesian well the north-eastern part of the Project area.

3.1.3. Groundwater Quality

3.1.3.1. Major ions

Water chemistry data was analysed in the lab in the department of geology university of Dhaka using spectrophotometry. All the water samples were grouped in to shallow and deep aquifer samples and the analysed samples were plotted in piper diagram for both groups (Figure-30). Figure 30 shows that the water of the shallow aquifer ranges from $MgCO_3$-HCO_3 type to NaCl type. The MgCO3-HCO_3 water type is found in the north and usually indicates recently recharges water, while the NaCl type water is found in the south indicating seawater intrusion. In the central part of the study area water samples indicate mixing between these two end members.

In contrast to the shallow aquifer, water of the deep aquifer is mostly Ca-K-Mg-CO_3-HCO_3 indicating unaffected by seawater intrusion. However, the line extending from Na/K towards Mg indicates ion exchange within the aquifer, which is a common natural phenomena and indicating longer residence time of water.

a) Shallow/First aquifer

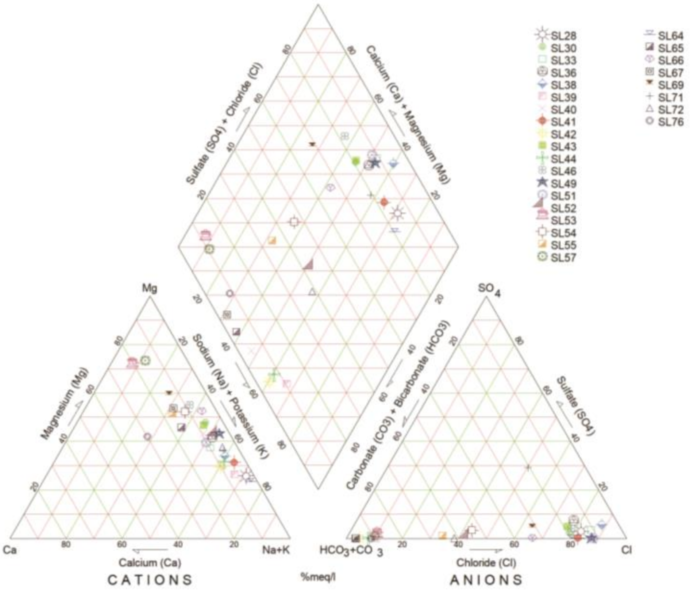

a) Deep/Third aquifer

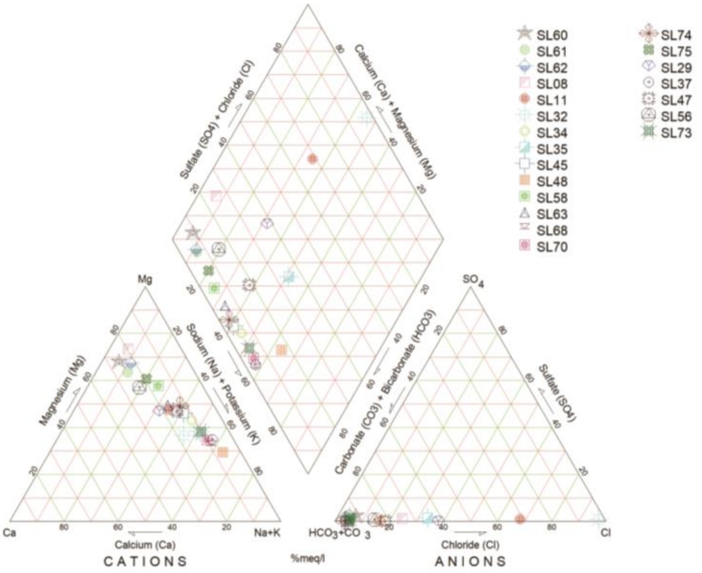

Figure 30: Piper diagram showing the major ion chemistry of a) shallow aquifer sample, and b) deep aquifer water samples.

3.1.3.2. Salinity/Electrical Conductivity

Electrical conductivity (EC) in groundwater is a measure of salinity and can indicate seawater intrusion or similar phenomenon. The EC in the shallow aquifer varies between 500 µS in the north to more than 8000 µS in the south and south west near the Sandwip Chanel. While, the groundwater in the deep aquifer is very fresh throughout the region with maximum EC value of 900 µS encountered in the extreme south. The EC value is exceptionally low (<200 µS) for both the shallow and deep aquifers in the northern tip of the study area.

The brackish water zone in the shallow aquifer is also picked clearly by the VES data (Figure 31). The lowest resistivity value is found between 20-50 m depth intervals in the resistivity pseudo profile, indicating the depth interval where the brackish water occurs. The low value below this depth is due to the influence of low resistivity at this depth and is not due to the presence of brackish water. Both the resistivity profile and EC contour indicate that only the shallow aquifer contains brackish water in the south, the second and third (deep) aquifer contain fresh water and can be used for drinking purpose.

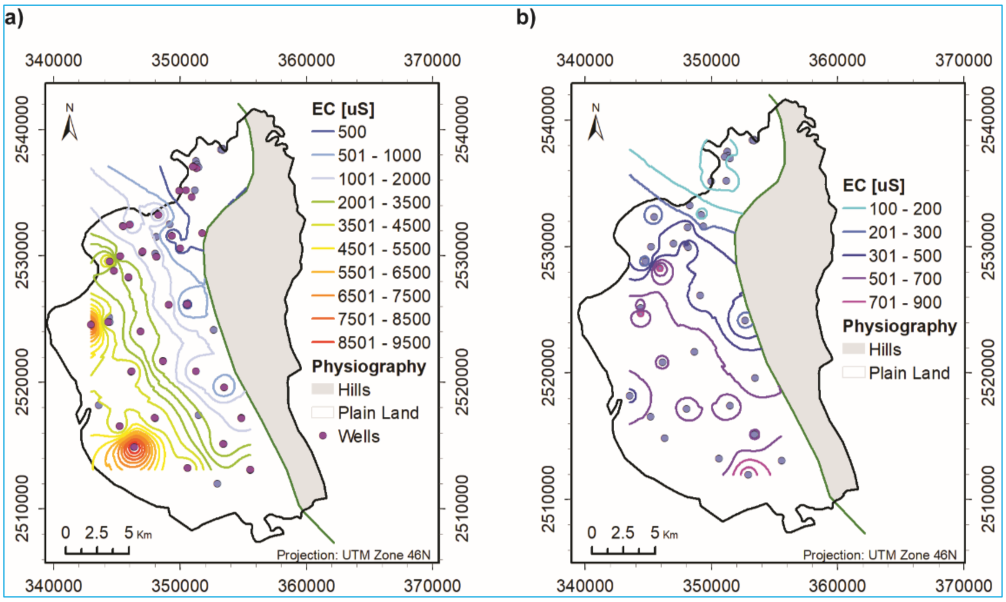

Figure 31: Map showing the spatial variability of electrical conductivity in the (a) shallow and (b) deep aquifer, respectively.

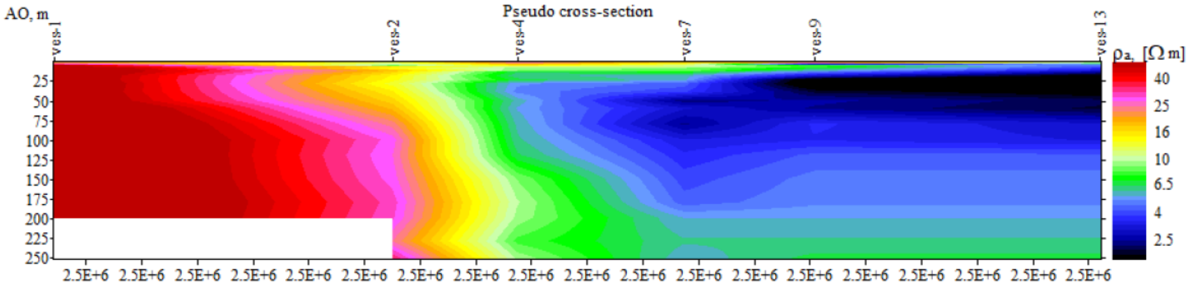

Figure 32: Resistivity pseudo section in north (VES-1) to south (VES-13) direction showing the extent of the brackish water in the shallow aquifer. For location of VES see Figure-6.

The EC contour at the shallow aquifer align perfectly with the orientation of the Sandwip channel, indicating that the channel is well connected with the shallow aquifer in this region resulting in the intrusion of saline water from the channel to the shallow aquifer.

3.1.3.3. Arsenic

Field kit measured arsenic concentrations in a number of wells distributed within the study area are shown in Figure-26. Field kit data suggest that the shallow aquifer is heavily contaminated with elevated arsenic concentration throughout the Upazila except in the extreme northern corner. However, the deep aquifer is largely low in arsenic concentration except one or two locations. In these locations it is highly likely that the sampled wells are actually shallower than reported, depth verification is required before making any conclusion on the arsenic contamination of the deep aquifer in the study area. Moreover, field kits only provide indication of the likelihood of contaminated wells. Without laboratory analysis confirmation about the arsenic status for the deep aquifer where only a few samples show marginally high concentration would not be accurate.

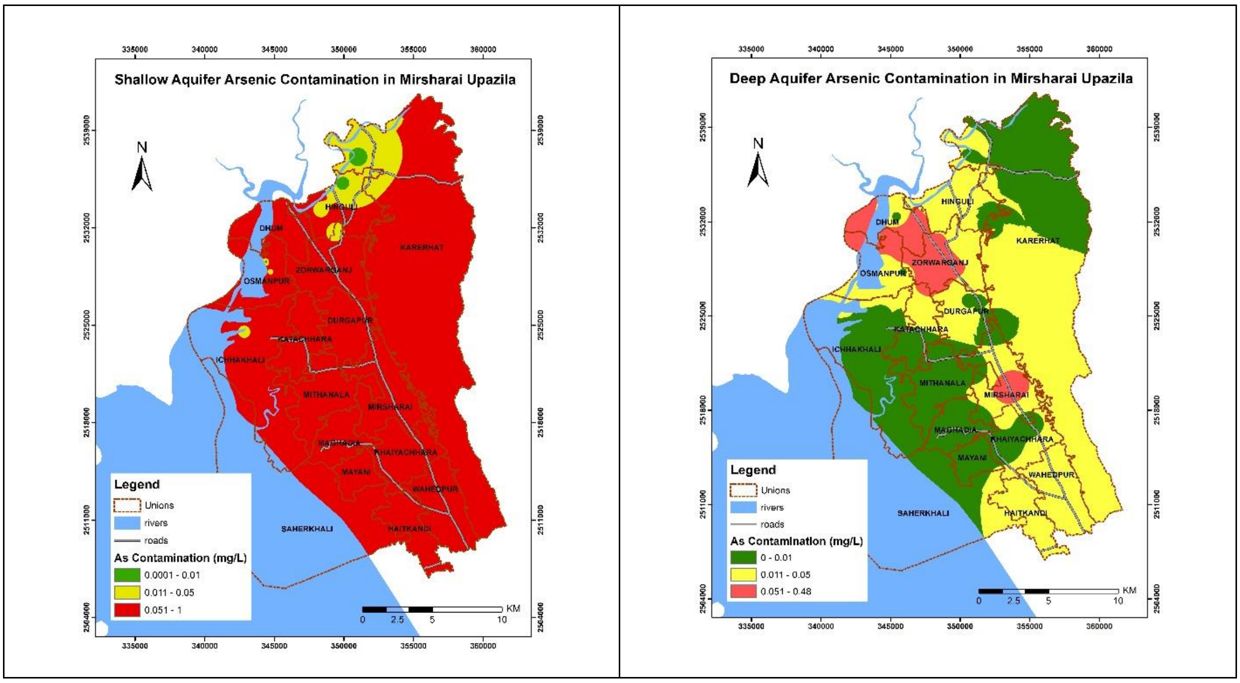

Figure 33: Arsenic distribution of Shallow and Deep Aquifer of the project area.

3.1.1. Groundwater Recharge Areas

Some preliminary assumptions about the groundwater recharge locations in the study area can be made based on the field observations. Groundwater level is the most important dataset delineating recharge zone, however, because of the erratic nature of the groundwater level data of the shallow aquifer it is really difficult to conclude anything based on groundwater level data for the shallow aquifer. However, the EC map provides a nice indication of the groundwater recharge areas as well as groundwater flow direction for the shallow aquifer. In recharge areas, the EC values are expected to be exceptionally low, and an increasing trend in EC from recharge areas towards discharge area is expected. Figure 23 (EC map) clearly suggests that the shallow aquifer receives most of its recharge in the northern part of the study area. This assumption is also supported by the arsenic concentration data. High arsenic is expected in old reduced water while there should be little or no arsenic in newly recharged oxidized water. The arsenic map of the shallow aquifer suggests that the northern part of the study area have very low arsenic concentration.

The groundwater level map of the deep aquifer readily indicates the location of the recharge area. It is also located in the north. Presence of artesian flow in some areas also indicates that some part of the deep aquifer must be exposed in the hills in the north where they receive bulk of the recharge.

The above discussed assumption has been verified using the groundwater model and found to be largely supported by the model. Figure 34 shows the distribution of model simulated recharge rate in the study area. The high recharge rate in the north is readily evident. However, the figure also indicates high recharge rate along the western boundary near the rivers and along the elevated eastern boundary. The high recharge rates along the western boundary is due to its location near a river, water infiltrates in to the shallow subsurface and quickly discharges off in to the nearby river. These recharges do not penetrate deeper in to the aquifer. Similarly, due to the presence of thick aquitard below the shallow aquifer along the eastern boundary, recharge along this elevated areas only add water to the shallow aquifer. In contrast, since all three aquifers are connected in the north and there is now aquitard present in between them, recharge in this region adds water to all three aquifers. The deep aquifer which provides suitable drinking water throughout the upazila is primarily recharged in the north. Additionally, the deep aquifer could also be recharged regionally in areas farther north. Flow in to the deep aquifer from the constant head boundary in the northwest would indicate this.

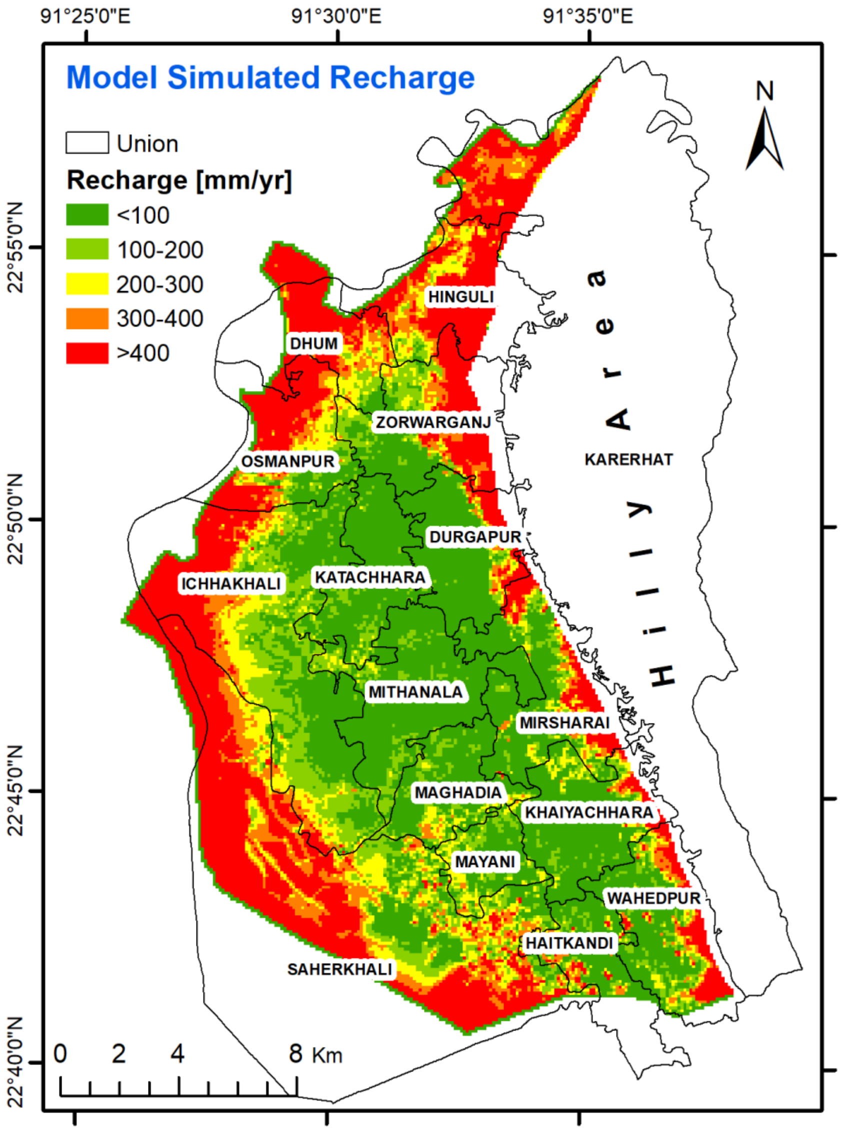

Figure 34: Model simulated recharge rate in the study area

3.2. Surface Water Resources and Flash Flood zoning and mitigation approach

3.2.1. Prospect of surface water reservoir

The eastern part of the Upazila is hilly and demarcated from the plain land in the west by a sharp boundary, which is most likely a fault. Numerous streams, locally known as chharas, originate in the hill and flows towards west and joins larger rivers/channels in the plain lands. Analysis of digital elevation model (DEM) reveals that in addition to the existing Mahamaya lake a total of four other artificial reservoir can be made in the hills (Figure 18). Two of the prospects are located north of the Mahamaya lake, and the remaining two located at the south. The northern two are larger in size than the southern two. Estimated maximum of reserve of these four reservoir together would be 52.42 million m3/year. The largest reserve can be made in Prospect-2, followed by prospect-1, prospect-3. The smallest reservoir is the prospect-4. Water reserve in individual prospect is shown in Table-5.

Water reserve calculation					
ID	Sq. km	Sq. mile	Annual Water Reserve in ft^3	Annual Water Reserve in mft^3	Annual Water Reserve in mm^3
Reservoir-1	4.87	1.88031674	646799211.3	646.7992113	18.31528391
Reservoir-2	5.31	2.05020162	705236922.3	705.2369223	19.97005288
Mohamaya Project	10.53	4.06565406	1398520676	1398.520676	39.60163029
Reservoir-3	2.65	1.0231703	351954396.3	351.9543963	9.966222248
Reservoir-4	1.11	0.42857322	147422407.5	147.4224075	4.174530829
Total Reserve in 5 reservoirs					92.02772016

Table 5: Proposed artificial and existing reservoirs reserve calculation

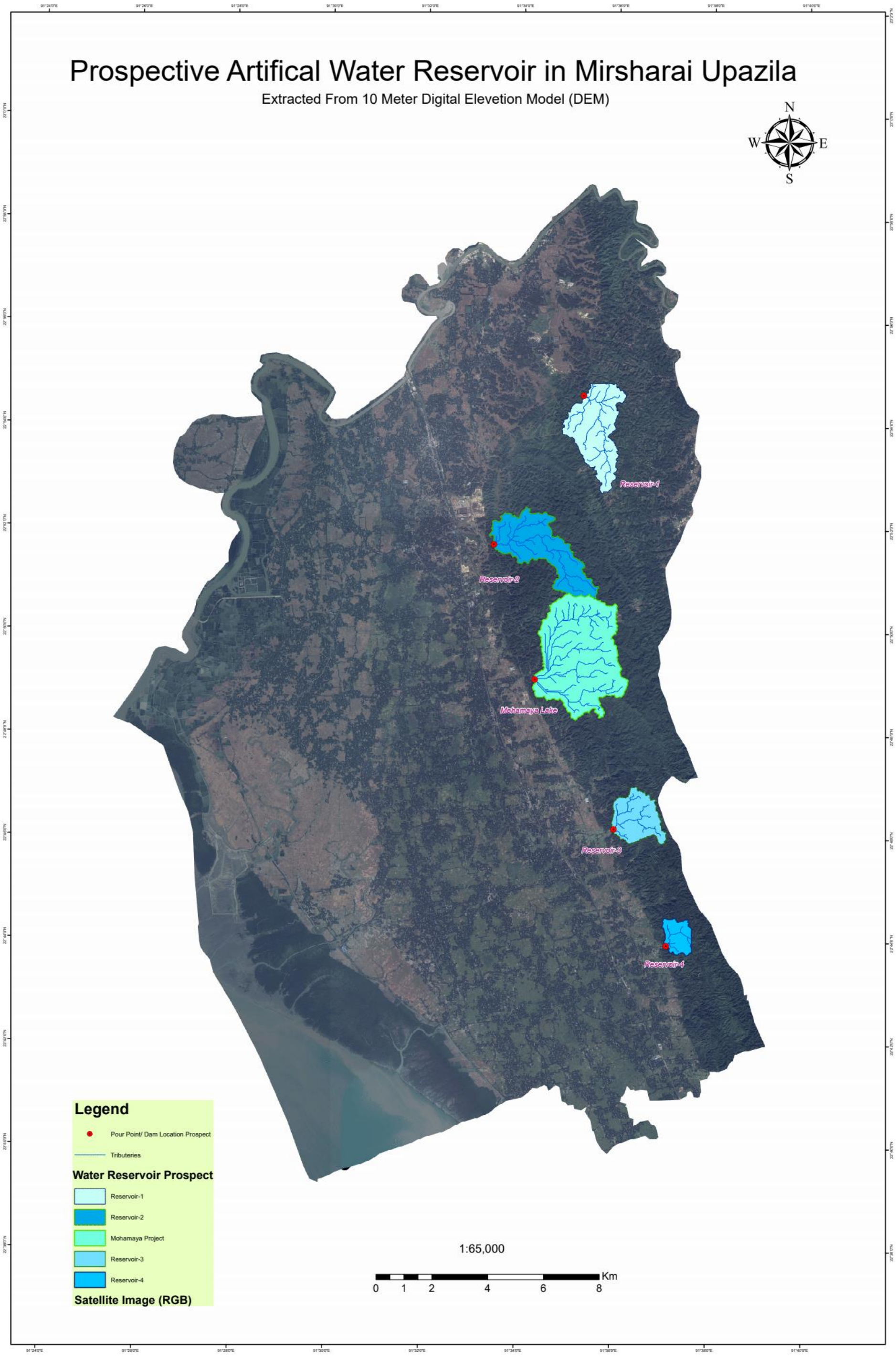

Figure 35: Prospective artificial reservoir locations

3.2.2. Flash Flood Zonation

In Mirsharai Upazila Main River is Feni; Sandwip Channel is notable; Canal is about 30 nos, most noted of which are Feni Nadi, Isakhali, Mahamaya, Domkhali, Hinguli, Molisaish, Koila Govania and Mayani Khal. All the rivers, khals, and canals are coming from eastern hilly region and falling in Bay of Bengal. In the high tide, sea water enters into the canal and goes back into sea in low tide time. Besides, these notable large rivers there are numerous small streams and channels criss-cross the Upazila (Figure 36). Based on the drainage distribution five (5) major basins/watersheds were delineated which is shown in figure 36.

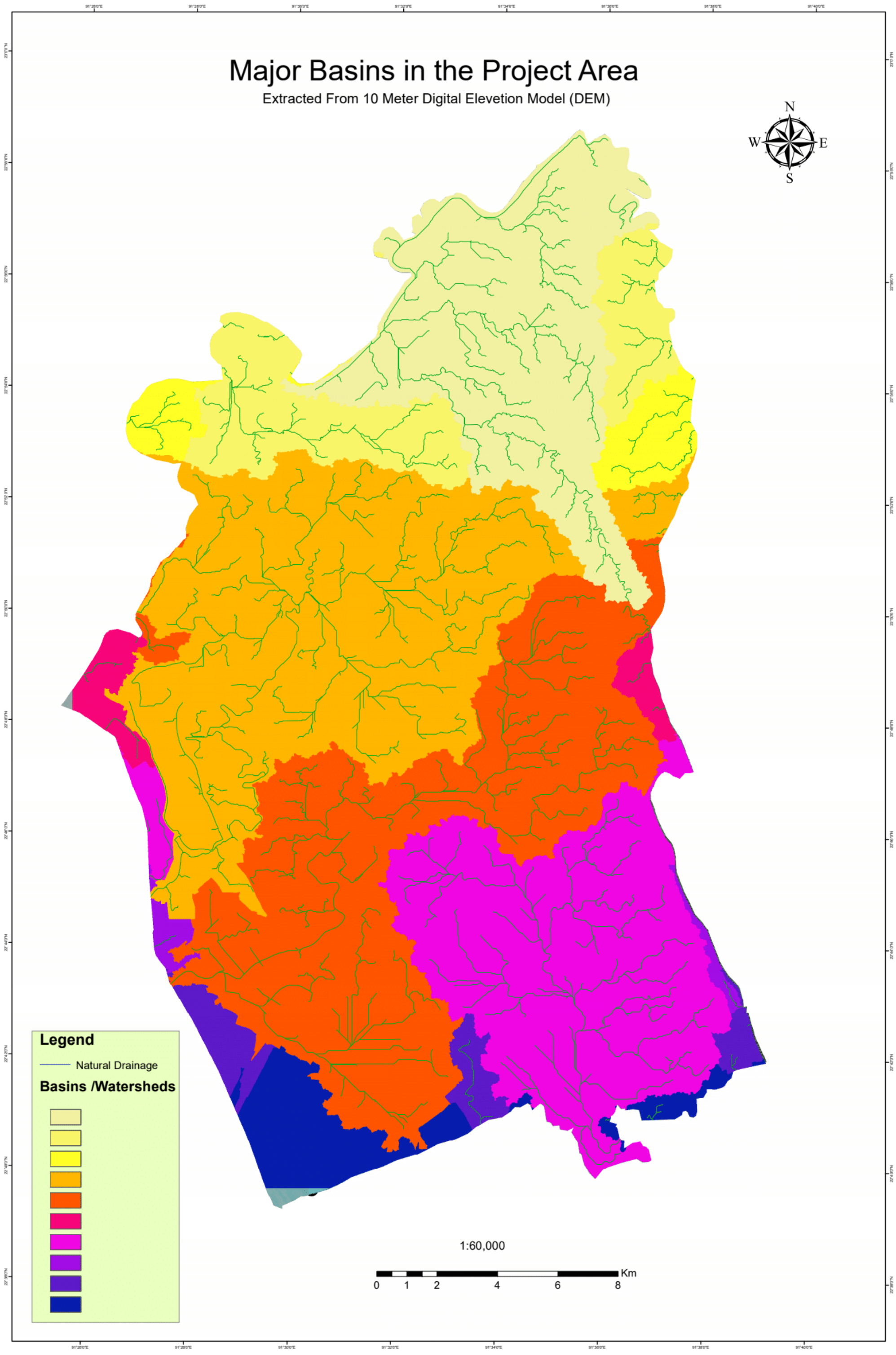

Figure 36: Major basin/watershed identified in the project area.

During the monsoon season heavy rainfall occurs in this area. As the project area is bounded by hills at eastern side and west by sea, the rainwater influx affects the project area by flash flood. By discussing with local people it is very clear that flash flood effect is prominent in monsoon season.

A flash flood susceptibility map is prepared for the entire Upazila in GIS environment considering the following factors-

i) Runoff lag time
ii) Soil type
iii) Surface slope
iv) Surface roughness
v) Drainage density
vi) Distance to main channel
vii) Land sue

Each factors were assigned a numeric value and the weighted average of these factors were calculated. Area with the highest weighted average has high susceptibility and that with the lowest average weight has the least susceptibility. It was found that only 13% of the total area of the Upazila has no risk of flash flood. The rest of the area has susceptibility of various degrees. Summary of the risk of flashflood is shown in the following table.

Table 6: Showing % of total area at various risk categories for flash flood.

Risk Category	% of total Upazila area
None	13%
Very low	28%
Low	30%
Moderate	18%
High	11%

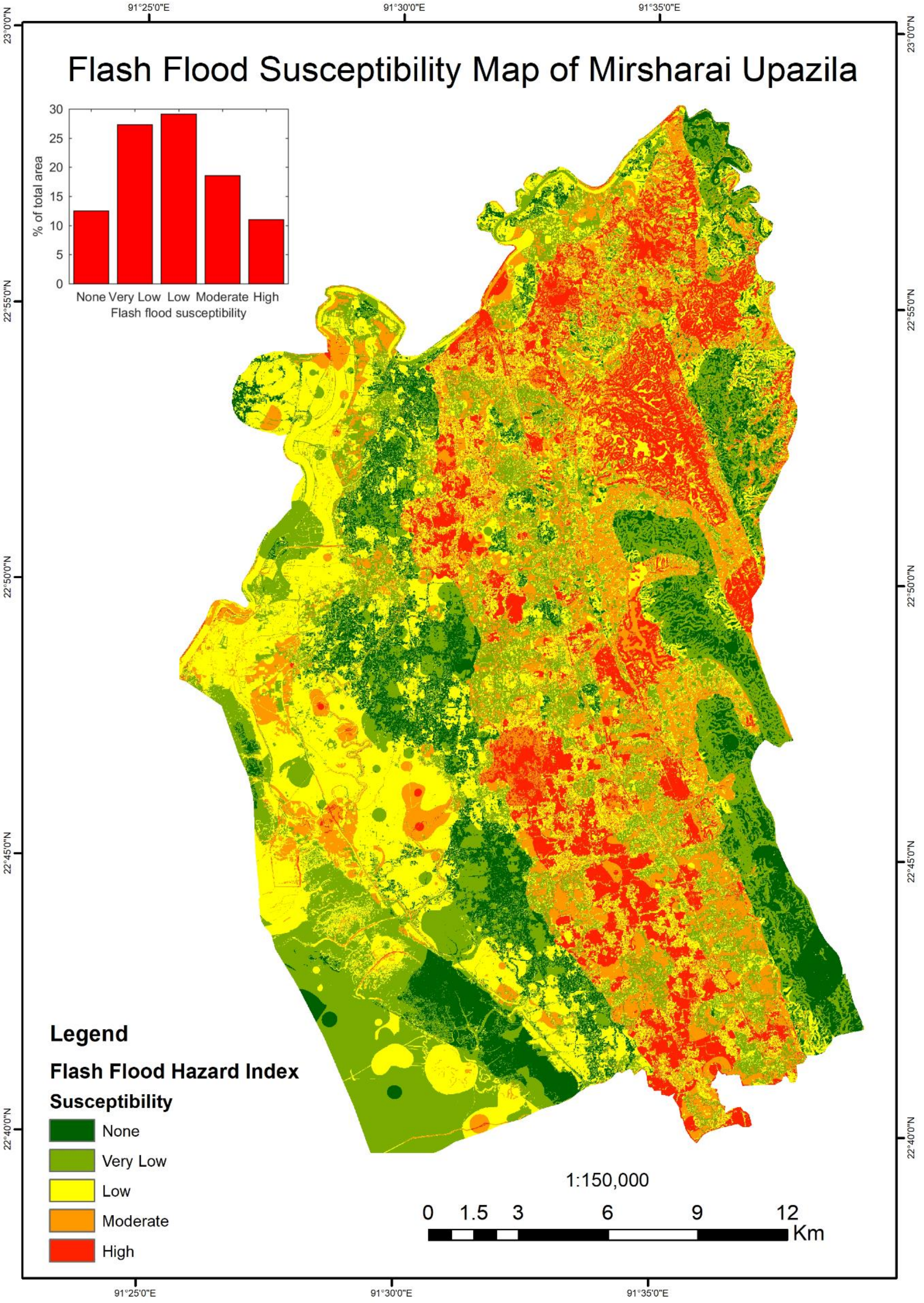

Figure 37: Flash flood susceptibility Index Map

3.3. Model Simulation

3.3.1. Current condition

The groundwater flow model was simulated in steady state to determine the current groundwater flow condition in the study area. Model simulated hydraulic head for all three aquifers (Figure 38) shows similar flow direction and generally shows the same trend as that based on the measured head data in the field.

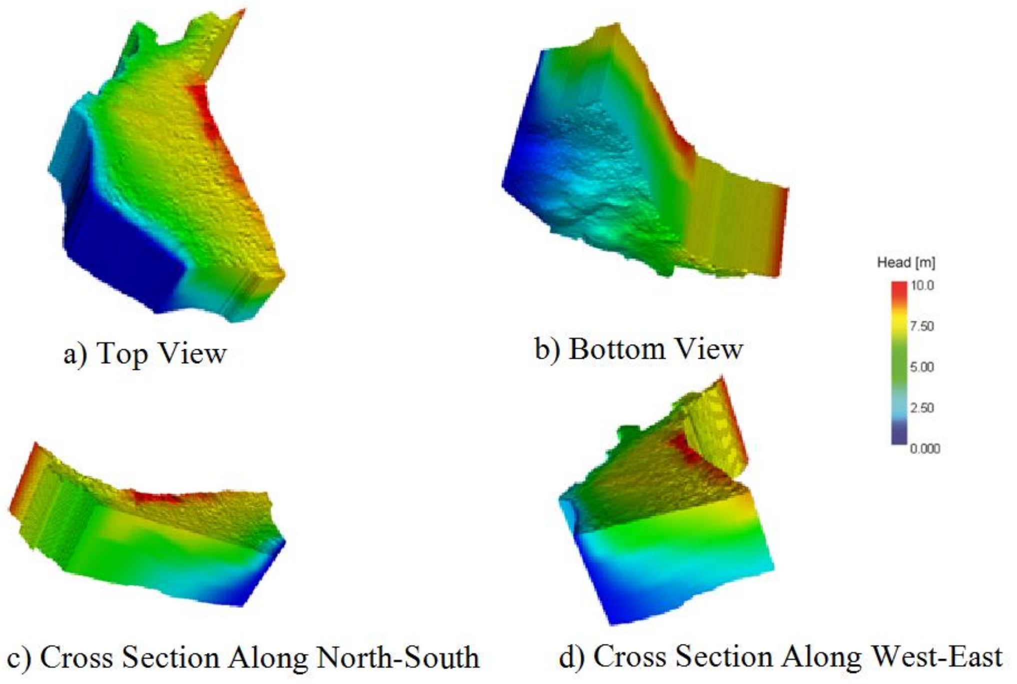
a) Top View

b) Bottom View

c) Cross Section Along North-South

d) Cross Section Along West-East

Figure 38: Model simulated hydraulic head at present condition.

3.3.2. Future Prediction

Considering the current population growth rate in Mirsharai Upazila there will be Little or no drawdown in the study area after 20 years compared to present day condition (Figure 39a). The increased withdrawal at the end of 20 years won’t be able to alter the Current flow direction, indicating there is little or no risk in the business as usual scenario.

3.3.3. High population growth rate in rural settings

Under this condition there will be a huge influx (10 time more than current population) of population in the next 20 years. Under this high pumping scenario, the model predict that there will be a total drawdown of more than 10 meters in some areas in the model (Figure 39b) which indicates that there will be a complete flow reversal in the southwest and western margin of the study area where the Sandwip channel is located. The reversal in flow direction means that there will be saltwater intrusion in the study area. Determination of the exact time frame and location of the saltwater front requires investigation in offshore region to identify the current location of saltwater front the deep aquifer in the study region,

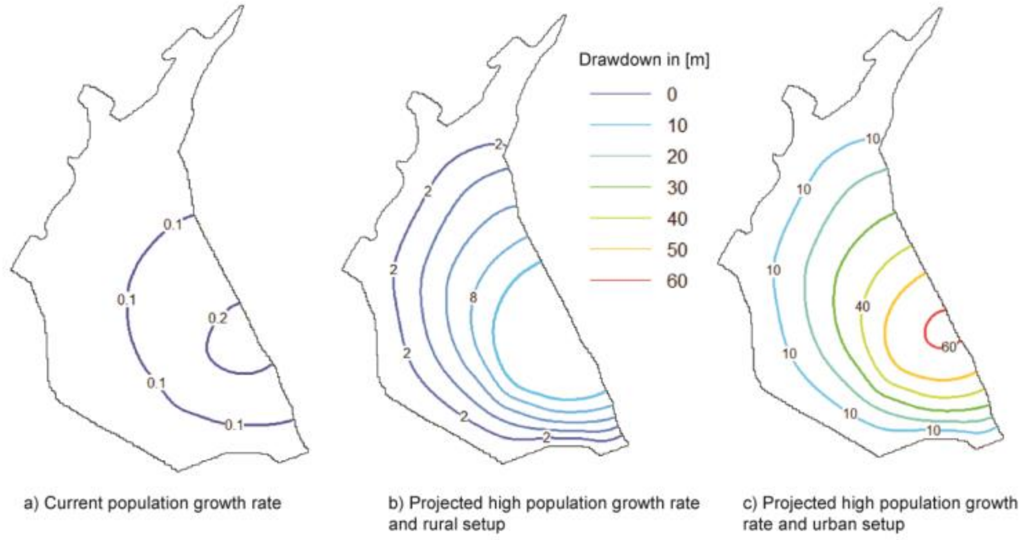

a) Current population growth rate

b) Projected high population growth rate and rural setup

c) Projected high population growth rate and urban setup

Figure 39: Model predicted drawdown for various future pumping scenarios in the deep aquifer.

which is out of the scope of this study.

3.3.4. High population growth rate in urban setting

Since per capita water consumption in urban settings is higher than in rural settings, for the same projected population growth the drawdown after 20 years become huge (as large as 60 m), completely disrupting the natural flow direction in the study area and making the aquifer vulnerable for both saltwater intrusions and compaction induced land subsidence (Figure 39c).

4. Policy Recommendation:

1. The aquifer condition in the BEZA area is not suitable for heavy groundwater withdrawal required for the project. The shallow groundwater in this part of the Upazila is brackish while the deep groundwater is fresh and occurs in a thin confined aquifer below a thick and soft clay layer. Heavy pumping from that aquifer would cause the compression of the aquitard and result in land subsidence. Besides, there is a high risk of later intrusion of sea water from the adjacent sea.
2. The water demand for BEZA might be supported by a combination of sources as outlined below-

a. Artesian condition exists in the Northeastern corner of Mirsharai Upazila. Detail investigation on the extent and yielding capacity of this artesian aquifer is recommended. It could meet a part of the water demand in the project area.
b. Water storage capacity of the Mahamaya and four other proposed surface reservoirs have been quantified in this study. These surface water sources should be able to meet a significant part of the total water demand in the BEZA project.
c. Feasibility of Feni River for a water treatment plant should be assessed for additional sources of water.
d. Feasibility of importing groundwater from adjacent Upazilas might be assessed for additional option.

The deep groundwater supplies most of the domestic water to the existing population in the Mirsharai Upazila. Modelling studies suggested that the deep aquifer recharge area lies in the northern part of the upazila. Development activities that might inhibit groundwater recharge or deteriorate the quality of recharge water should be avoided in that part of the Upazila to keep its quality and quantity unaffected to keep supporting the existing population.

5. Discussion

This study comprises of extensive field work, laboratory analysis, and modeling to assess the availability and sustainability of the groundwater resources in Mirasharai Upazila. In this upazila both surface water and groundwater are available for use. Groundwater occurs primarily in three aquifers at various depths. However, the water quality of the shallow aquifer in a large part of the upazila in the south is not suitable for drinking purpose due to the presence of both arsenic and salinity. The remaining two aquifers that occur on average below a depth of 70-100 m contain water suitable for drinking purpose. Both these deeper aquifers receive recharge in the northern part of the Upazila where all three aquifers are connected due to the lack of clay layers separating them. Presence of artesian condition in the northern part of the study area indicates that the recharge potential of the deep aquifer is very high. Development of the artesian aquifer in the north could be good option for drinking water supply throughout the Upazila, however, this need detail field and modeling investigation, which is not in the scope of the current study. Lack of clays and high recharge in the north also causes for some concern. Presence of water pollutants and contaminants in this area would be a potential threat for the groundwater to be contaminated. Care should be taken for carrying out any future development activities in the north that might discharge contaminated water on the surface and shallow subsurface.

Presence of high EC in the shallow aquifer only and not in the deep aquifer indicates that the Sandwip channel and the shallow aquifer is well connected and it does not have any connectivity with the deeper aquifers. However, the shallow salinity could also be due to inundation during storm surges in near past (100 years scale) or during the high sea level stand 5000 years before present, though, the parallel alignment of the EC contour and Sandwip channel suggest intrusion from the channel.

A groundwater flow model has been developed to assess the sustainability of the Aquifers (deeper aquifers) to supply various projected high demand scenarios in near future. Three different future groundwater withdrawals were simulated in this study, namely a) Business as usual scenario, b) High population growth in rural setting, and c) High population growth in urban setting. Model shows that for the current population growth rate there is no future risk in the development of groundwater in the study area. However, for the projected high population growth rate both rural and urban settings makes the aquifers vulnerable for saltwater intrusion and pumping induced land subsidence. The two freshwater aquifers (aquifer-2 and 3) in the study area are underlain by very soft clays of 10-30 m thick. Pumping induced drawdown in the underlying aquifers would induce vertical migration of water from these aquitard to the adjacent aquifers leading to a release in fluid pressure in the aquitard causing compaction of the aquitard. Even a 10% compaction may cause land subsidence of 2-3 m in the study area, especially in the south. Detail geotechnical and modelling exercise is required to characterize this risk in this region. The current model is very simplified and based on a number of assumptions, future monitoring of head in the study area is required to validate and update the model in future.

There is one important concern about deep pumping in the southern part of the study area, where the aquitard between the shallow and the deep aquifer is thicker than 50 m. Heavy pumping from below that aquitard would cause a drop in pressure in the aquifer, and would initiate draining the overlying aquitard. The aquitard is composed of very soft marine clay. Upon drainage such clay layers have potential to lose more than 50% of its thickness causing subsidence. On the other hand, this thick aquitard can provide protection against downward migration of brackish water in the deep aquifer if the pumping in the deep aquifer in this part of the study area kept low. The current model can be used to predict the possibility of the migration of shallow high saline water to deep aquifer but it cannot be used to predict land subsidence. Land subsidence prediction requires more complex modelling which is not in the scope of this study.

6. Acknowledgement

Firstly, we are grateful to almighty Allah for giving me the excellent opportunity of doing this project work. We are also very grateful to Urban Development Directorate (UDD) under the Ministry of Housing and Public Works, Government of the People’s Republic of Bangladesh for selecting our consulting firm “Center for Geoservices and Research” as the consultant for the Hydro-Geological survey under Mirsharai Upazila Development Plan (MUDP).

“Center for Geoservices and Research” would like to honor Dr. Kazi Matin Uddin Ahmed, Professor and Chairman of Department of Geology, University of Dhaka, Dr. Md, Aziz Hasan, Professor of Department of Geology, University of Dhaka, Dr. A.S.M Woobaid Ullah, Professor of Department of Geology, University of Dhaka for their proper guidance and suggestion during the field and post field duration. Special thanks to Dr. Mahfuzur Rahman Khan, Associate Professor, Department of Geology, University of Dhaka for his huge effort and expertise for the Groundwater Modelling.

Special thanks to Department of Geology for giving the Laboratory facilities to complete Geotechnical and Geochemical analysis of the samples collected during field. Also thanks to the staffs of the laboratories.

Finally thanks to all the Geologists, Hydro-Geologists and staffs of Center for Geoservices and Research.

7. References

1. Acharyya, S.K., Lahiri, S., Raymahashay, B.C. and Bhowmik, A., 2000. Arsenic toxicity of groundwater in parts of the Bengal basin in India and Bangladesh: the role of Quaternary stratigraphy and Holocene sea-level fluctuation. Environmental Geology, 39(10), pp.1127-1137.
2. Ahmed, Z.U., Panaullah, G.M., DeGloria, S.D., Duxbury, J.M., 2011b. Factors affecting paddy soil arsenic concentration in Bangladesh: Prediction and uncertainty of geo-statistical risk mapping. Sci. Total Env., 412-413:324-35.
3. Ahmed, K.M., Bhattacharya, P., Hasan, M.A., Akhter, S.H., Alam, S.M., Bhuyian, M.H., Imam, M.B., Khan, A.A. and Sracek, O., 2004. Arsenic enrichment in groundwater of the alluvial aquifers in Bangladesh: an overview. Applied Geochemistry, 19(2), pp.181-200.
4. Ahmed, Z.U., Panaullah, G.M., Duxbury, J.M., Lauren, G.J., Meisner, C.A., DeGloria, S.D., Woodbury, P.B., 2013. Arsenic contamination in Bangladesh: Spatial relationship between arsenic exposure from groundwater and rice, and incidence of arsenicosis. Environmental Health, March 3-6, Boston, MA.
5. Ahmed, M.J., Ahsan, A., Haque, M.R., Siraj, S., Bhuiyan, M.H.R., Bhattacharjee, S.C. and Islam, S., 2010. Physicochemical assessment of surface and groundwater quality of the greater Chittagong region of Bangladesh. Pakistan Journal of Analytical & Environmental Chemistry, 11(2), p.11.
6. Alyamani, M.S. and Şen, Z., 1993. Determination of hydraulic conductivity from complete grain-size distribution curves. Groundwater, 31(4), pp.551-555.
7. Ayers, R.S. and Westcot, D.W., 1989. Salinity problems. Water quality for agriculture. FAO, Rome, Italy, pp.1-32.
8. Baalousha, H., Mckay, G., Haik, Y., Siddique, A., Koç, M., Francis, L., Saleem, J., Abdulrahim, H.K.M. and Al-Adwan, A., 2013. FUNDAMENTALS OF GROUNDWATER MODELLING. Jordan Journal of Applied Science, 15(15), pp.347-360.
9. Bahar, M.M. and Reza, M.S., 2010. Hydrochemical characteristics and quality assessment of shallow groundwater in a coastal area of Southwest Bangladesh. Environmental Earth Sciences, 61(5), pp.1065-1073.
10. Bangladesh Bureau of Statistics, Population and Housing Census-2011.

11. BGS-DPHE, 2001. Arsenic Contamination of Groundwater in Bangladesh, British Geological Survey (BGS) and Department of Public Health Engineering (DPHE) Govt. of Bangladesh; rapid investigation phase, Final Report.
12. Chowdhury, S.Q., Chittagong City, BANGLAPEDIA, National Encyclopaedia of Bangladesh, Asiatic Society of Bangladesh, Dhaka, Bangladesh. Assessed on 14 September, 2013.
13. Deshpande, S.M. and Aher, K.R., 2012. Evaluation of groundwater quality and its suitability for drinking and agriculture use in parts of Vaijapur, District Aurangabad, MS, India. Research Journal of Chemical Sciences.
14. Dittmar, J., Voegelin, A., Roberts, L.C., Hug, S.J., Saha, G.C., Ali, M.A., 2007. Spatial distribution and temporal variability of arsenic in irrigated rice fields in Bangladesh. Paddy Soil. Environ. Sci. Technol . 41, 5967-72.
15. DoE, 1997. Environmental Quality Slandered for Bangladesh, Department of Environment, Government of Bangladesh. pp.35.
16. Duxbury, J.M., Panaullah, G.M., Zavala, Y.J., Loeppert, R.U., Ahmed, Z.U., 2009. Impact of use As-contaminated groundwater on soil As content and paddy rice production in Bangladesh.
17. Feasibility study for Mirershorai Economic Zone, Bangladesh Economic Zones Authority (BEZA), July, 2014.
18. Fetter, C.W., (1994): Applied Hydrogeology, Fourth Edition, Prentic Hall. pp. 190-205.
19. Flanagan, S.V., Johnstan, R.B., Zheng, Y., 2012. Arsenic in tube well water in Bangladesh: health and economic impacts and implications for arsenic mitigation. Bulletin of the World Health Organization 2012;90:839-846. doi: 10.2471/BLT.11.101253.
20. Freeze, R.A. and Cheery, J.A., 1979. Groundwater. pp 82-87.
21. Garrels, R.M., 1976. A survey of low temperature water-mineral relation, Interpretation of Environmental Isotop and Hydrochemical Data In Groundwater Hudrology, International Atomic Energy Agency, Vienna, pp. 65-68
22. Groundwater Investigation in Mirsharai Economic Zone, Department of Public Health Engineering (DPHE), December 2015
23. Guidline for drinking water quality, 2nd ed. Vol. 2, Health criteria and other supporting information, World Health Organisation, Geneva, 1996

24. Haque, M.A., Islam, M.S., Zahid, A., 2012. Groundwater irrigation and crop economy in the lower Gangatic Plain at Madbarer Char, Madripur, South-Central Bangladesh. J. Asiatic. Soc. Bangladesh Sci., 38(1): 29-39
25. Hem, J.D. and Geological Survey (US), 1989. Study and interpretation of the chemical characteristics of natural water, 3rd Edition, USGS WSP2254, Washington, D. C
26. Hounslow, A.W., 1995. Water quality data, analysis and interpretation, Lewis Publishers, New York.
27. Hu, R.L., Yue, Z.Q., Wang, L.U. and Wang, S.J., 2004. Review on current status and challenging issues of land subsidence in China. Engineering Geology, 76(1-2), pp.65-77.
28. Islam, M.A., Zahid, A., Rahman, M.M., Rahman, M.S., Islam, M.J., Akter, Y., Shammi, M., Bodrud-Doza, M. and Roy, B., 2017. Investigation of groundwater quality and its suitability for drinking and agricultural use in the south central part of the coastal region in Bangladesh. Exposure and Health, 9(1), pp.27-41.
29. Joshi, P.K., L. Joshi, R.K. Singh, J. Thakur, K. Singh and A.K. Giri, (2003) Analysis of Productivity Changes and Future Sources of Growth for Sustaining Rice- Wheat Cropping System. National Agricultural Technology Project ((PSR 15;4.2), New Delhi: National Centre for Agricultural Economics and Policy Research(NCAP).
30. Karim, M.F. Ahmed, S. and Olsen, H.W., Engineering geology of Chittagong City, Bangladesh, Geological Survey of Bangladesh (GSB) Report, Unpublished, 1990
31. Kelley, P.L., 1963. Nonlinear effects in solids. Journal of Physics and Chemistry of Solids, 24(5), pp.607-616.
32. Lee, S.H., Levy, D.A., Craun, G.F., Beach, M.J. and Calderon, R.L., 2002. Surveillance for waterborne-disease outbreaks--United States, 1999-2000. Morbidity and mortality weekly report. Surveillance summaries (Washington, DC: 2002), 51(8), pp.1-47.
33. Malek, A. U. (2014). Arsenic Contamination of Tube Well Water in Chittagong City, Bangladesh- A Case Study. International Journal of Scientific and Engineering Research , 796.
34. McArthur, J.M., Ravenscroft, P., Safiulla, S. and Thirlwall, M.F., 2001. Arsenic in groundwater: testing pollution mechanisms for sedimentary aquifers in Bangladesh. Water Resources Research, 37(1), pp.109-117.

35. Md. Abdul Hamid Mirdad, S. K. (2014). Investigation of ground water table in the South-East (Chittagong) part of Bangladesh. American Journal of Civil Engineering .
36. Piper, A.M., 1944. A graphic procedure in the geochemical interpretation of water-analyses. Eos, Transactions American Geophysical Union, 25(6), pp.914-928.
37. Raghunath, H.M., 1987. Ground water. New Age International.
38. Richards LA (Ed.) (1954) ‘Diagnosis and improvement of saline and alkali soils.’ Agriculture Handbook 60. (USDA: Washington, DC)
39. Sawyer, C.N., McCarty, P.L. and Parkin, G.F., 1994. Chemistry for environmental engineering (Vol. 4). New York: McGraw-Hill.
40. S. Andrea, (2014), Estimation of Hydraulic Conductivity From Grain Size Analyses, Master’s Thesis 2014:1
41. Shamsudduha, M., Chandler, R.E., Taylor, R., Ahmed, K.M., 2009. Recent trends in groundwater levels in a highly seasonal hydrological system: the Ganges-Brahmaputra-Meghna Delta. Hydrol. Earth Syst. Sci., 13, 2373–2385.
42. Shamsudduha, M., Uddin, A., Saunders, J.A. and Lee, M.K., 2008. Quaternary stratigraphy, sediment characteristics and geochemistry of arsenic-contaminated alluvial aquifers in the Ganges–Brahmaputra floodplain in central Bangladesh. Journal of Contaminant Hydrology, 99(1-4), pp.112-136.
43. Zahid, A. and Ahmed, S.R.U., 2006. Groundwater resources development in Bangladesh: Contribution to irrigation for food security and constraints to sustainability. Groundwater Governance in Asia Series-1, pp.25-46.

APPENDICES

APPENDIX-I: LITHOLOGICAL DATA FROM MONITORING WELL

Client: Urban Development Directorate (UDD)

Project: Mirsharai Upazila Development Plan (MUDP)

Bore Hole ID: MW-01

Location: Mehedi Nagar, Hinguli, Mirsharai.

Co-ordinate: 22.88738° N, 91.55460° E

Depth of Boring: 219 Meter

Ground Water Level: 6.53 m

Method of Boring: Rotary Wash Boring

Boring Diameter: 3"/1.5"

Date: 31/01/2018

Depth Bellow GL (m)	Type of Sample	Sample No	Thickness (m)	Lithologic Description	Layer Change
3.0m	▬	D1	3	Yellowish brown,very fine to medium grained clayey sand, moderately sorted, subangular to subrounded, trace mica.	
6.0m	▬	D2	15	Light yellowish to yellowish brown, occationally gray, fine to medium grained sand, moderately sorted, subangular to sub rounded, trace mica.	
9.0m	▬	D3			
12.0m	▬	D4			
15.0m	▬	D5			
18.0m	▬	D6			
21.0m	▬	D7	3	Light yellowish brown, very fine to medium grained sand, poorly sorted subangular to subrounded, trace clay and mica.	
24.0m	▬	D8	9	Light yellowish brown, medium grained sand, moderately sorted, subangular to subrounded, dark color minerals present, trace mica.	
27.0m	▬	D9			

30.0m	D10			
33.0m	D11	6	Yellowish brown, very fine to fine grained sand, well sorted, dark color minerals present, trace mica.	
36.0m	D12			
39.0m	D13	3	Reddish brown, occationally gray, fine to medium grained clayey sand, poorly sorted, dark color minerals present, trace mica.	
42.0m	D14			
45.0m	D15			
48.0m	D16			
51.0m	D17			
54.0m	D18			
57.0m	D19			
60.0m	D20			
63.0m	D21			
		51	Yellowish brown, occationally reddish brown, very fine to medium grained sand, moderately sorted, subangular, dark	

			medium grained sand, moderately sorted, subangular, dark color minerals present, trace mica.
66.0m	D22		
69.0m	D23		
72.0m	D24		
75.0m	D25		
78.0m	D26		
81.0m	D27		
84.0m	D28		
87.0m	D29		
90.0m	D30		
93.0m	D31	12	Gray with yellowish brown patches, silty clay, moderately sticky.
96.0m	D32		
99.0m	D33		

102.0m	D34		
105.0m	D35	36	Light yellowish brown, yellowish brown, reddish brown, medium grained sand, well sorted, subrounded, dark color minerals, trace mica.
108.0m	D36		
111.0m	D37		
114.0m	D38		
117.0m	D39		
120.0m	D40		
123.0m	D41		
126.0m	D42		
129.0m	D43		
132.0m	D44		
135.0m	D45		

138.0m	D46			
141.0m	D47	3	Yellowish brown, fine to medium grainde sand, moderately sorted, subangular to subrounded, dark color minerals present, trace mica.	
144.0m	D48	39	Light yellowish brown to yellowish brown, medium to coarse grained sand, moderately sorted, subangular to subrounded, trace mica.	
147.0m	D49			
150.0m	D50			
153.0m	D51			▨
156.0m	D52			▨
159.0m	D53			
162.0m	D54			
165.0m	D55			▨
168.0m	D56			▨
171.0m	D57			

174.0m	D58		
177.0m	D59		
180.0m	D60		
183.0m	D61	12	Light yellowish, fine to medium grainded, moderately sorted, subangular to subrounded, trace clay.
186.0m	D62		
189.0m	D63		
192.0m	D64		
195.0m	D65	15	Gray to dark gray, fine to medium grained sand, poorly sorted, trace clay.
198.0m	D66		
201.0m	D67		
204.0m	D68		

207.0m	■	D69			
210.0m	■	D70	3	Dark gray, very fine to fine grained clayey sand.	
213.0m	■	D71	9	Light yellowish gray, medium to coarse graindеd sand, poorly sorted, subangular to angular.	
216.0m	■	D72			
219.0m	■	D73			

Client: Urban Development Directorate (UDD)
Project: Mirsharai Upazila Development Plan (MUDP)
Bore Hole ID: MW-02
Location: Vanguni Bazar Jame Moshjid, Ichakhali, Mirsharai.
Co-ordinate: 22.82665° N, 91.48352° E
Depth of Boring: 222 Meter
Ground Water Level: 3.45 m
Method of Boring: Rotary Wash Boring
Boring Diameter: 1.5"
Date: 07/02/2018

Depth Bellow GL (m)	Type of Sample	Sample No	Thickness (m)	Lithologic Description	Layer Change
3.0m	■	D1	6	Dark gray clay, moderately sticky.	
6.0m	■	D2			
9.0m	■	D3	15	Gray, very fine to fine grained sand, trace mica.	
12.0m	■	D4			
15.0m	■	D5			
18.0m	■	D6			
21.0m	■	D7			
24.0m	■	D8			
27.0m	■	D9			

30.0m	D10	42	Light gray to gray, yellowish gray, medium to coarse grained sand, moderately sorted, subangular to subrounded, dark color minerals present, trace mica.
33.0m	D11		
36.0m	D12		
39.0m	D13		
42.0m	D14		
45.0m	D15		
48.0m	D16		
51.0m	D17		
54.0m	D18		
57.0m	D19		
60.0m	D20		
63.0m	D21		
		3	Gray, clayey fine to medium grained sand

66.0m	D22	[illegible]	Gray, clayey fine to medium grained sand.		
69.0m	D23	12	Gray to Yellowish brown, medium grained sand, poorly sorted, silt and black color minerals present.		
72.0m	D24				
75.0m	D25				
78.0m	D26				
81.0m	D27	12	Gray, medium to coarse grained sand, poorly sorted, occationally clayey.		
84.0m	D28				
87.0m	D29				
90.0m	D30				
93.0m	D31	12	Gray, fine to medium sand well sorted, rounded, trace mica.		
96.0m	D32				
99.0m	D33				

102.0m	D34		
105.0m	D35	12	Yellowish brown, fine to coarse grained sand, moderately sorted, trace mica, dark color minerals and clay.
108.0m	D36		
111.0m	D37		
114.0m	D38		
117.0m	D39	3	Dark gray clay, moderately sticky with silt.
120.0m	D40	6	Gray, fine to medium grained clayey sand.
123.0m	D41		
126.0m	D42	6	Light gray, medium to coarse grained sand, well sorted, rounded.
129.0m	D43		
132.0m	D44		
135.0m	D45		

138.0m	D46	15	Light gray, medium to fine grained sand woth silt and trace clay.		
141.0m	D47				
144.0m	D48				
147.0m	D49	21	Gray, light yellowish brown, medium grained sand, moderately sorted, subrounded trace clay.		
150.0m	D50				
153.0m	D51				
156.0m	D52				
159.0m	D53				
162.0m	D54				
165.0m	D55				
168.0m	D56				
171.0m	D57				

		15	Gray, clayey fine to very fine grained sand, dark color minerals present.	
174.0m	D58			
177.0m	D59			
180.0m	D60			
183.0m	D61			
186.0m	D62			
189.0m	D63			
192.0m	D64			
195.0m	D65	30	Light brownish gray, medium to fine grained sand, dark color m	
198.0m	D66			
201.0m	D67			
204.0m	D68			▨

207.0m	D69			▨
210.0m	D70			
213.0m	D71	12	Brownish gray to gray, very fine to medium grained sand, well sorted, dark color minerals present, trace clay.	
216.0m	D72			
219.0m	D73			
222.0m	D74			

Client: Urban Development Directorate (UDD)
Project: Mirsharai Upazila Development Plan (MUDP)
Bore Hole ID: MW-03
Location: West Kismot Jafrabad, Mirsharai Pourosova, Mirsharai.
Co-ordinate: 22.78856° N, 91.55094° E
Depth of Boring: 204 Meter
Ground Water Level: 4.0 m
Method of Boring: Rotary Wash Boring
Boring Diameter: 3"/1.5"
Date: 11/02/2018

CENTER FOR GEOSERVICES & RESEARCH

Depth Bellow GL (m)	Type of Sample	Sample No	Thickness (m)	Lithologic Description	Layer Change
3.0m	▬	D1	6	Light brown to gray clay.	
6.0m	▬	D2			
9.0m	▬	D3	39	Gray to light brown, medium grained sand, moderately sorted, subangular to subrounded, dark color minerals present, trace mica.	
12.0m	▬	D4			
15.0m	▬	D5			
18.0m	▬	D6			
21.0m	▬	D7			
24.0m	▬	D8			
27.0m	▬	D9			

30.0m	D10		
33.0m	D11		
36.0m	D12		
39.0m	D13		
42.0m	D14		
45.0m	D15		
48.0m	D16	9	Brown, silt with fine grained sand.
51.0m	D17		
54.0m	D18		
57.0m	D19		
60.0m	D20		
63.0m	D21		
		21	Light gray to brown, fine grained sand, dark color minerals

66.0m	D22	21	present, trace mica.
69.0m	D23		
72.0m	D24		
75.0m	D25		
78.0m	D26	15	Light brown to gray, fine to medium grained sand, moderately sorted, subangular to subrounded, dark color minerals present, trace mica.
81.0m	D27		
84.0m	D28		
87.0m	D29		
90.0m	D30		
93.0m	D31	6	Light gray, medium grained sand, moderately sorted, subangular to subrounded, trace mica.
96.0m	D32		
99.0m	D33		

102.0m	D34	18	Light brown to gray, fine grained sand, dark color minerals present, trace mica.
105.0m	D35		
108.0m	D36		
111.0m	D37		
114.0m	D38		
117.0m	D39	24	Light brown to gray silt with very fine sand.
120.0m	D40		
123.0m	D41		
126.0m	D42		
129.0m	D43		
132.0m	D44		
135.0m	D45		

138.0m	D46		
141.0m	D47		
144.0m	D48		
147.0m	D49		
150.0m	D50	24	Light brown clay with silt.
153.0m	D51		
156.0m	D52		
159.0m	D53		
162.0m	D54		
165.0m	D55		
168.0m	D56	12	Light brown to gray, fine sand with silt, trace mica.
171.0m	D57		

174.0m	D58			
177.0m	D59	6	Light brown silt with clay.	
180.0m	D60			
183.0m	D61	15	Light brown, fine to medium grained sand, moderately sorted, subangular to subrounded, trace mica.	
186.0m	D62			
189.0m	D63			▨
192.0m	D64			▨
195.0m	D65			▨
198.0m	D66	9	Light brown to gray clay.	
201.0m	D67			
204.0m	D68			

Client: Urban Development Directorate (UDD)
Project: Mirsharai Upazila Development Plan (MUDP)
Bore Hole ID: MW-04
Location: Char Shorot, Ichakhali, Mirsharai.
Co-ordinate: 22.733950° N, 91.503290° E
Depth of Boring: 216 Meter
Ground Water Level: 4.18 m
Method of Boring: Rotary Wash Boring
Boring Diameter: 1.5"
Date: 07/02/2018

Depth Bellow GL (m)	Type of Sample	Sample No	Thickness (m)	Lithologic Description	Layer Change
3.0m	▬	D1	39	Light brown to gray, very fine to fine sand with silt and clay, dark color minerals present, trace mica.	
6.0m	▬	D2			
9.0m	▬	D3			
12.0m	▬	D4			
15.0m	▬	D5			
18.0m	▬	D6			
21.0m	▬	D7			
24.0m	▬	D8			

27.0m	D9				
30.0m	D10				
33.0m	D11				
36.0m	D12				
39.0m	D13				
42.0m	D14	9	Light brown to gray, silty clay.		
45.0m	D15				
48.0m	D16				
51.0m	D17	6	Light brown to gray, fine to medium grained sand with silt, moderately sorted, trace mica.		
54.0m	D18				
57.0m	D19				
60.0m	D20				

63.0m	D21	36	Light brown clayey fine sand, dark color minerals present, trace mica.
66.0m	D22		
69.0m	D23		
72.0m	D24		
75.0m	D25		
78.0m	D26		
81.0m	D27		
84.0m	D28		
87.0m	D29		
90.0m	D30		
93.0m	D31		
96.0m	D32		

99.0m	■	D33	48	Light brown to gray, silty fine sand, dark color minerals present, trace mica.		
102.0m	■	D34				
105.0m	■	D35				
108.0m	■	D36				
111.0m	■	D37				
114.0m	■	D38				
117.0m	■	D39				
120.0m	■	D40				
123.0m	■	D41				
126.0m	■	D42				
129.0m	■	D43				
132.0m	■	D44				

135.0m	D45			
138.0m	D46			
141.0m	D47	15	Light brown to gray, fine to medium grained sand with silt, moderately sorted, trace mica.	
144.0m	D48			
147.0m	D49			
150.0m	D50			
153.0m	D51			
156.0m	D52	12	Light brown to gray, medium to fine grained sand, moderately sorted, trace mica.	
159.0m	D53			
162.0m	D54			
165.0m	D55			
168.0m	D56			

171.0m	D57	15	Light brown to gray, medium grained sand, moderately sorted, trace mica.	
174.0m	D58			
177.0m	D59			
180.0m	D60			
183.0m	D61	12	Light brown to gray, medium to fine grained sand with clay, moderately sorted, trace mica.	
186.0m	D62			
189.0m	D63			
192.0m	D64			
195.0m	D65	18	Light brown to gray, medium grained sand, moderately sorted, subangular to subrounded, trace mica.	▨
198.0m	D66			▨
201.0m	D67			▨

204.0m	D68		
207.0m	D69		
210.0m	D70		
213.0m	D71	6	Grayish to light brown, clay with silt.
216.0m	D72		

Project: Mirsharai Upazila Development Plan (MUDP)
Client: Urban Development Directorate (UDD)
Bore Hole ID: MW-05
Location: East Shaherkhali, Haitkandi, Mirsharai.
Co-ordinate: 22.70814° N, 91.56847° E
Depth of Boring: 159 Meter
Ground Water Level: 3.59 m
Method of Boring: Rotary Wash Boring
Boring Diameter: 1.5"
Date: 15/02/2018

Depth Bellow GL (m)	Type of Sample	Sample No	Thickness (m)	Lithologic Description	Layer Change
3.0m	■	D1			
6.0m	■	D2			
9.0m	■	D3			
12.0m	■	D4			
15.0m	■	D5			
18.0m	■	D6			
21.0m	■	D7			
24.0m	■	D8			
			48	Gray, fine grainde sand with silt,dark color minerals present, trace mica.	

27.0m	D9
30.0m	D10
33.0m	D11
36.0m	D12
39.0m	D13
42.0m	D14
45.0m	D15
48.0m	D16
51.0m	D17
54.0m	D18
57.0m	D19
60.0m	D20

63.0m	■	D21				
66.0m	■	D22				
69.0m	■	D23	42	Brown to gray, silty clay		
72.0m	■	D24				
75.0m	■	D25				
78.0m	■	D26				
81.0m	■	D27				
84.0m	■	D28				
87.0m	■	D29				
90.0m	■	D30				
93.0m	■	D31				
96.0m	■	D32	12	Brownish gray, medium to fine grained sand with silt.		

99.0m	D33		
102.0m	D34		
105.0m	D35	45	Brownish gray, silty clay with very fine sand.
108.0m	D36		
111.0m	D37		
114.0m	D38		
117.0m	D39		
120.0m	D40		
123.0m	D41		
126.0m	D42		
129.0m	D43		
132.0m	D44		

135.0m	■	D45			
138.0m	■	D46			
141.0m	■	D47			
144.0m	■	D48			
147.0m	■	D49			
150.0m	■	D50	9	Gray, medium to fine grained sand, moderately sorted, subrounded, dark color minerals present.	▒
153.0m	■	D51			
156.0m	■	D52			
159.0m	■	D53	3	Gray, silty sand with clay.	

APPENDIX-II: VERTICAL ELECTRICAL SOUNDING (VES) INTERPRETATION DATA

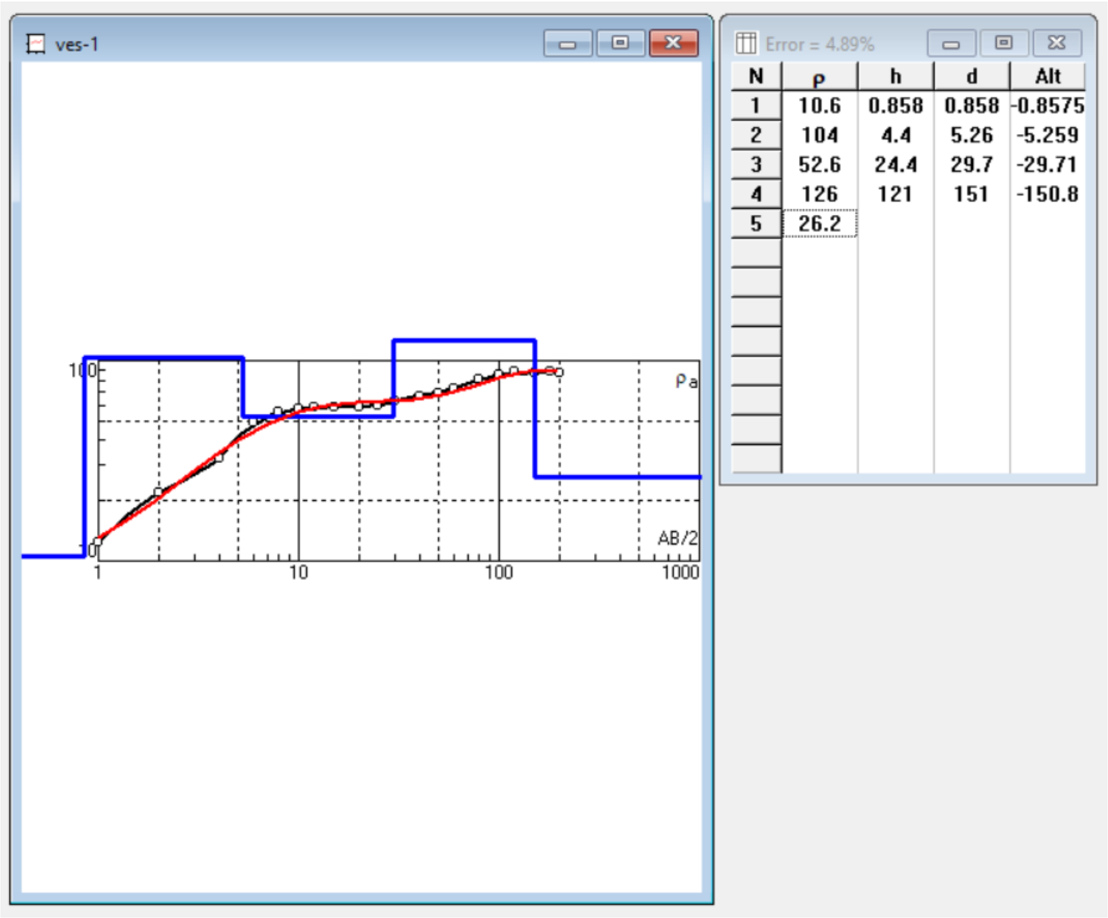

N	ρ	h	d	Alt
1	10.6	0.858	0.858	-0.8575
2	104	4.4	5.26	-5.259
3	52.6	24.4	29.7	-29.71
4	126	121	151	-150.8
5	26.2			

Rho	Thickness	Depth	Lithology
10.6	1	1	Alternating top
104	4.5	5.5	Coarse Sands
53	24.5	30	Medium Sands
126	121	151	Coarse Sands

VES-03

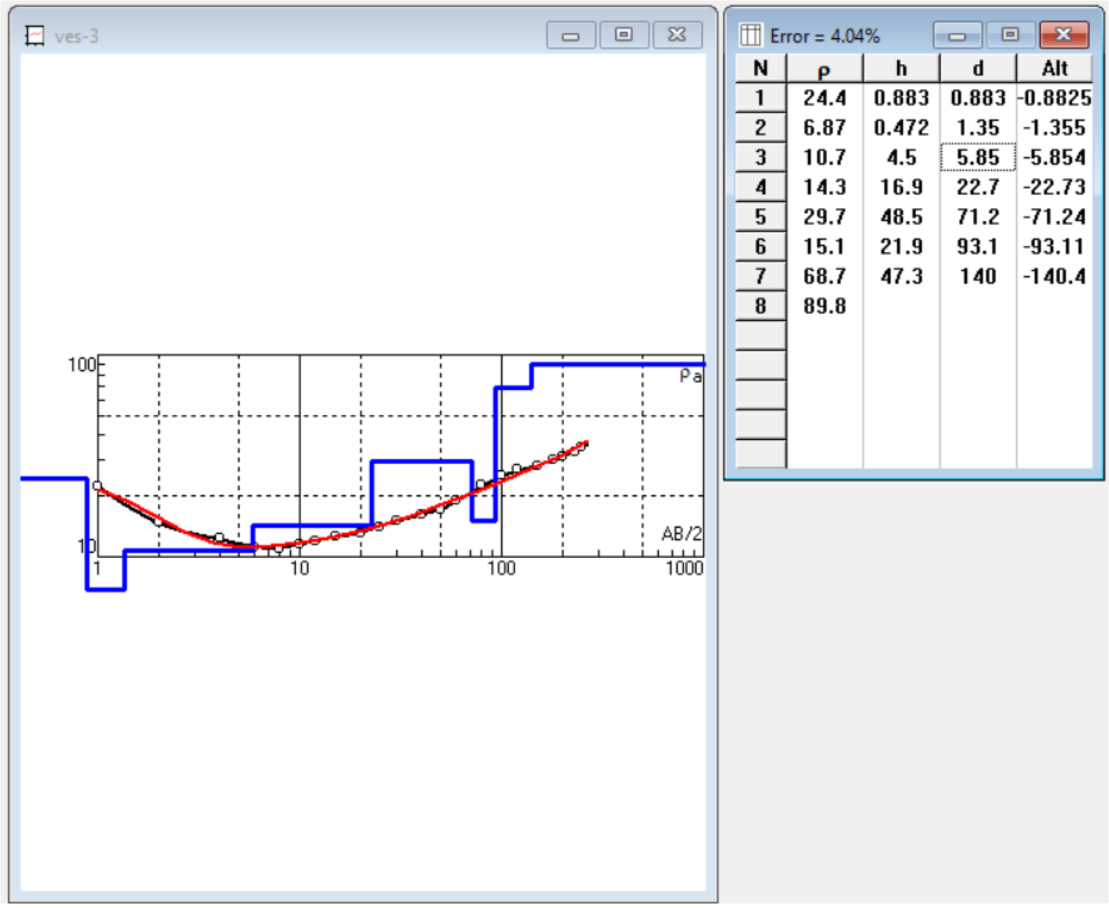

Error = 4.04%

N	ρ	h	d	Alt
1	24.4	0.883	0.883	-0.8825
2	6.87	0.472	1.35	-1.355
3	10.7	4.5	5.85	-5.854
4	14.3	16.9	22.7	-22.73
5	29.7	48.5	71.2	-71.24
6	15.1	21.9	93.1	-93.11
7	68.7	47.3	140	-140.4
8	89.8			

Rho	Thickness	Depth	Lithology
24.4	1	1	Top soil
6.8-10.7	5	6	Silty sand/silts
14.3 - 29.7	64	71	Relatively fresh sand
15.1	22	93	Silts/Sandy clay
68	41	141	FW sands

VES-04

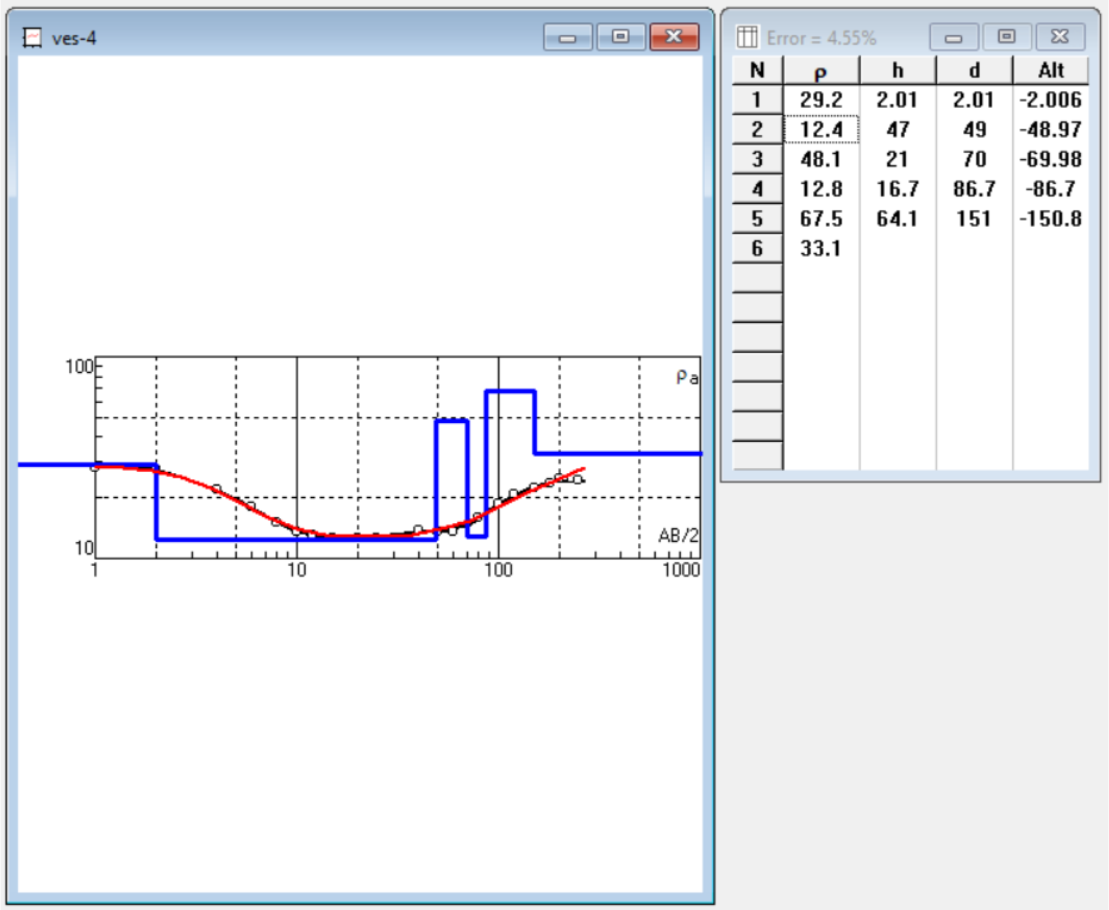

N	ρ	h	d	Alt
1	29.2	2.01	2.01	-2.006
2	12.4	47	49	-48.97
3	48.1	21	70	-69.98
4	12.8	16.7	86.7	-86.7
5	67.5	64.1	151	-150.8
6	33.1			

Rho	Thickness	Depth	Lithology
29.2	2	2	Top soil
12.4 - 48.1	68	70	Top brackish, bottom fw Sands
13	17	87	Silts/clay
68	63	150	FW sands

VES-06

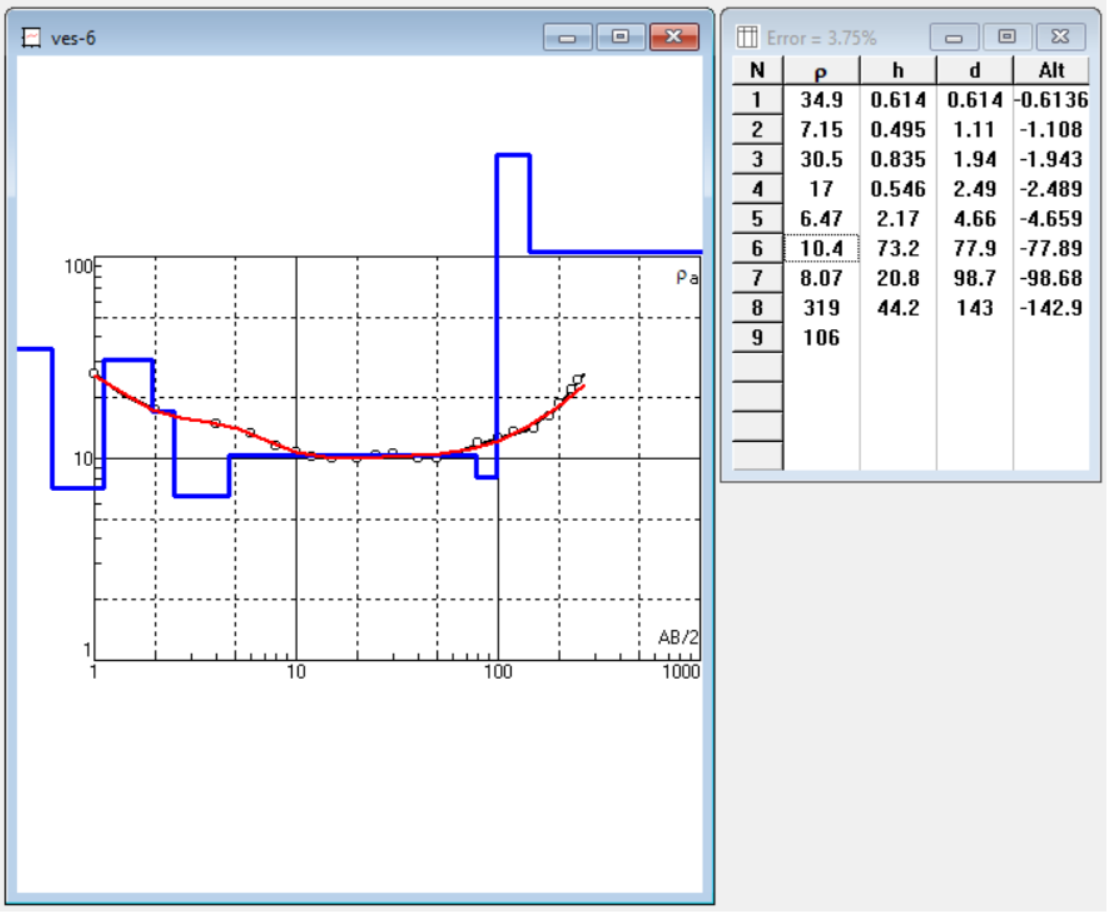

N	ρ	h	d	Alt
1	34.9	0.614	0.614	-0.6136
2	7.15	0.495	1.11	-1.108
3	30.5	0.835	1.94	-1.943
4	17	0.546	2.49	-2.489
5	6.47	2.17	4.66	-4.659
6	10.4	73.2	77.9	-77.89
7	8.07	20.8	98.7	-98.68
8	319	44.2	143	-142.9
9	106			

Rho	Thickness	Depth	Lithology
7-35	5	5	Alternating top
10.4	73	78	Brackish Sands
8	21	99	Silts/clay
309	45	144	FW sands

VES-07

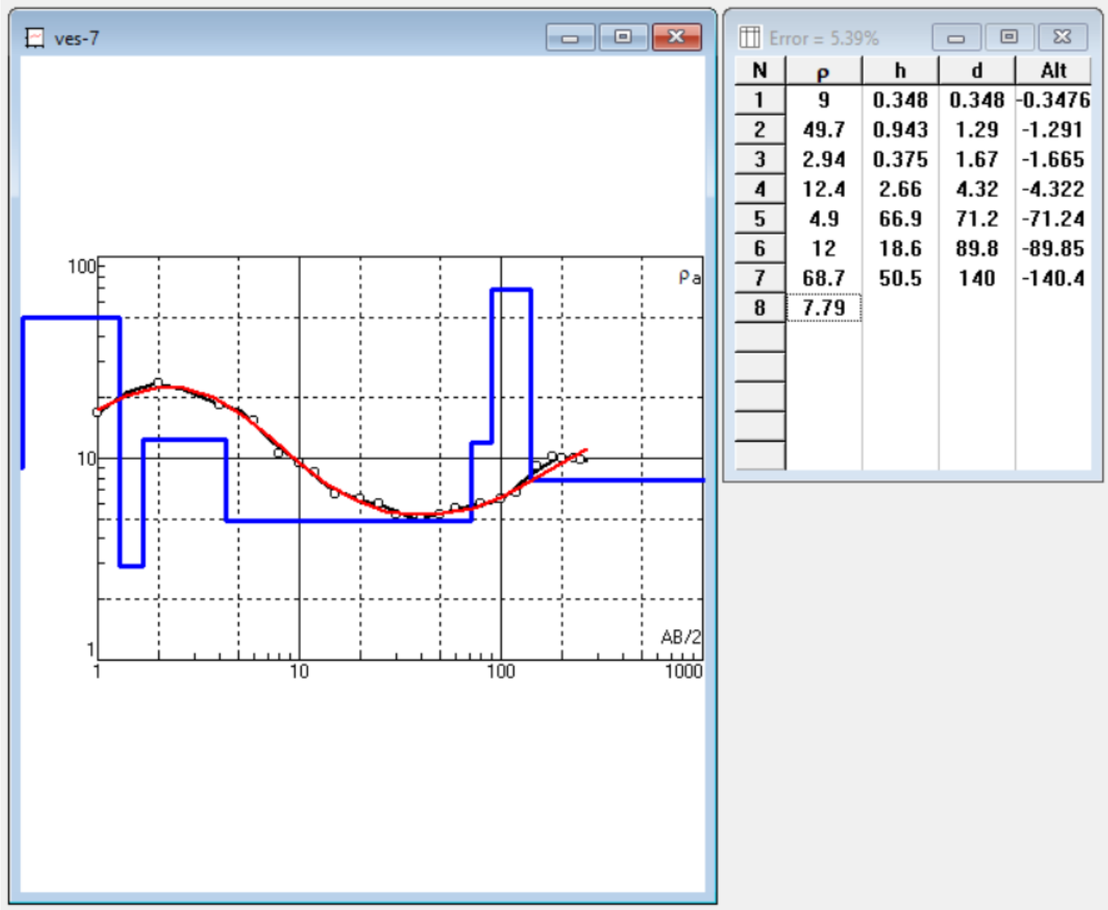

Error = 5.39%

N	ρ	h	d	Alt
1	9	0.348	0.348	-0.3476
2	49.7	0.943	1.29	-1.291
3	2.94	0.375	1.67	-1.665
4	12.4	2.66	4.32	-4.322
5	4.9	66.9	71.2	-71.24
6	12	18.6	89.8	-89.85
7	68.7	50.5	140	-140.4
8	7.79			

Rho	Thickness	Depth	Lithology
2.94-50	5	5	Top soil/silts/clay alteration
4.9	67	72	Brackish Sands
12	13	90	Silts/clay
69	50	143	FW sands

VES-08

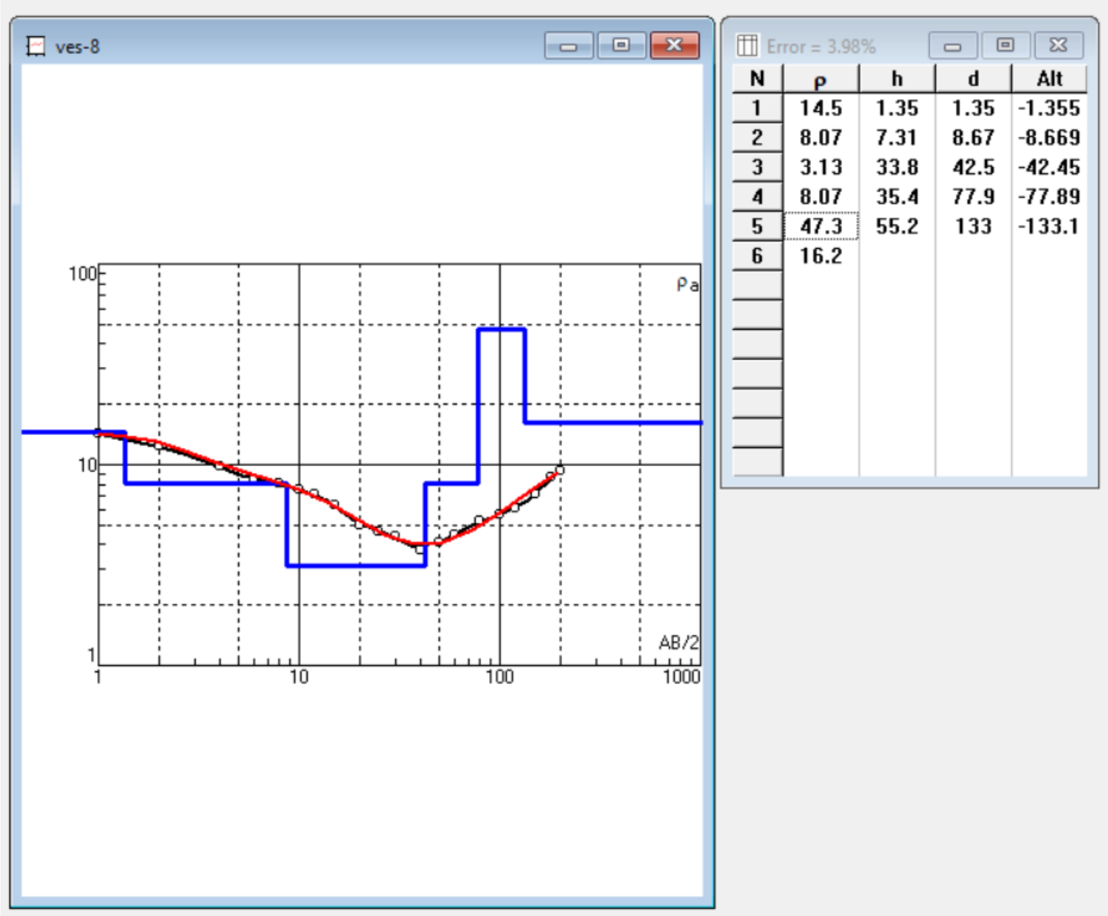

N	ρ	h	d	Alt
1	14.5	1.35	1.35	-1.355
2	8.07	7.31	8.67	-8.669
3	3.13	33.8	42.5	-42.45
4	8.07	35.4	77.9	-77.89
5	47.3	55.2	133	-133.1
6	16.2			

Rho	Thickness	Depth	Lithology
14.5	1.5	1.5	Top soil
3.1-8	41	42.5	Brackish Sand
8.07	35.5	78	Clay
47	55	133	FW Sand

VES-10

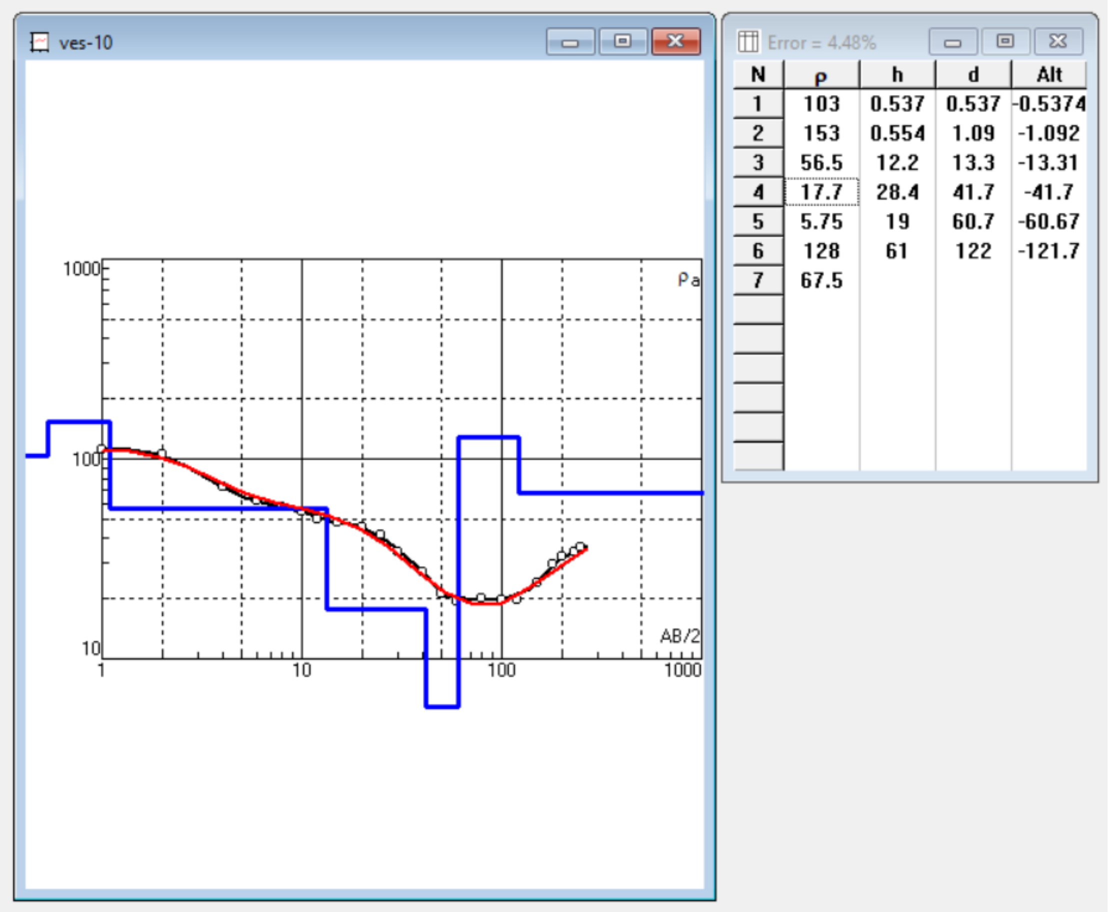

Error = 4.48%

N	ρ	h	d	Alt
1	103	0.537	0.537	-0.5374
2	153	0.554	1.09	-1.092
3	56.5	12.2	13.3	-13.31
4	17.7	28.4	41.7	-41.7
5	5.75	19	60.7	-60.67
6	128	61	122	-121.7
7	67.5			

Rho	Thickness	Depth	Lithology
103-153	1	1	Top soil
18-56	41	42	Relatively FW Sand
5.85	19	61	Clay
128	61	122	FW Sand

VES-12

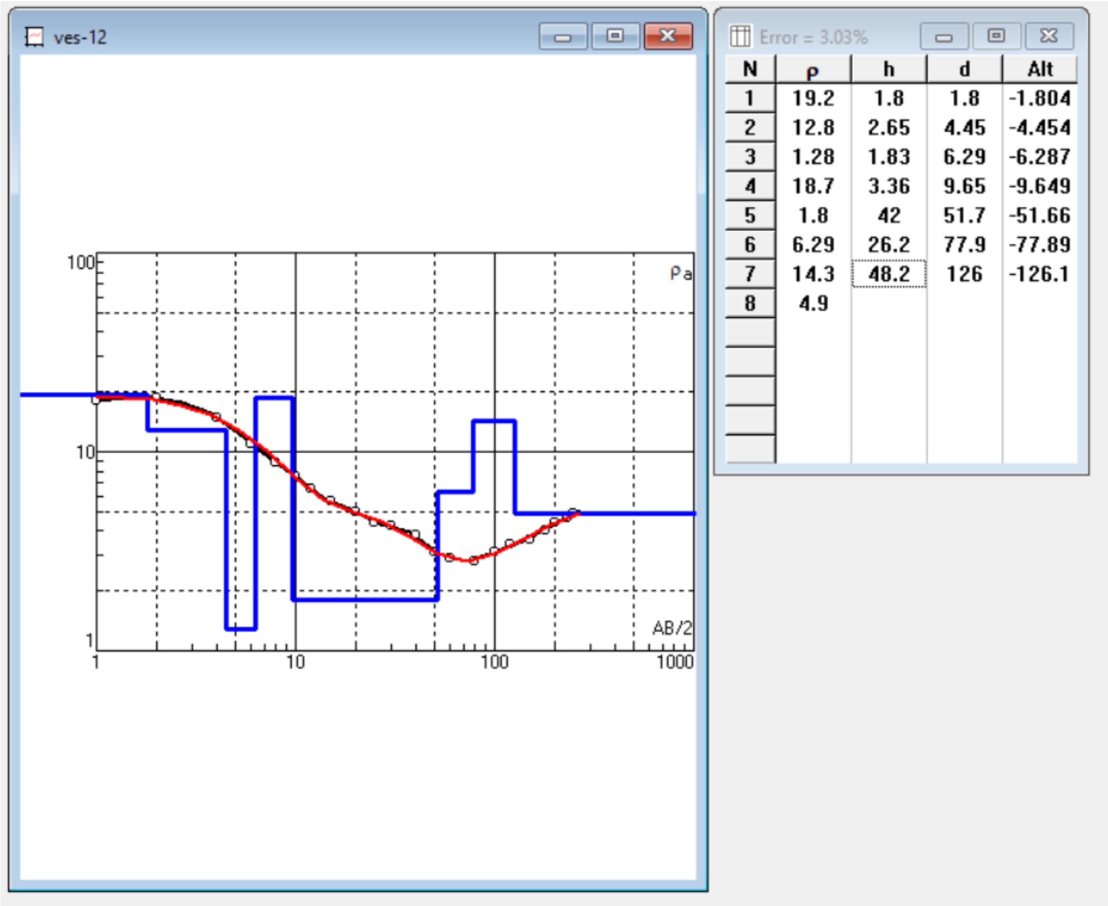

Error = 3.03%

N	ρ	h	d	Alt
1	19.2	1.8	1.8	-1.804
2	12.8	2.65	4.45	-4.454
3	1.28	1.83	6.29	-6.287
4	18.7	3.36	9.65	-9.649
5	1.8	42	51.7	-51.66
6	6.29	26.2	77.9	-77.89
7	14.3	48.2	126	-126.1
8	4.9			

Rho	Thickness	Depth	Lithology
19.2	2	2	Top soil
1.8-18.7	50	52	Brackish Sand
6.3	26	78	Clay
70	48	126	FW Sand

VES-13

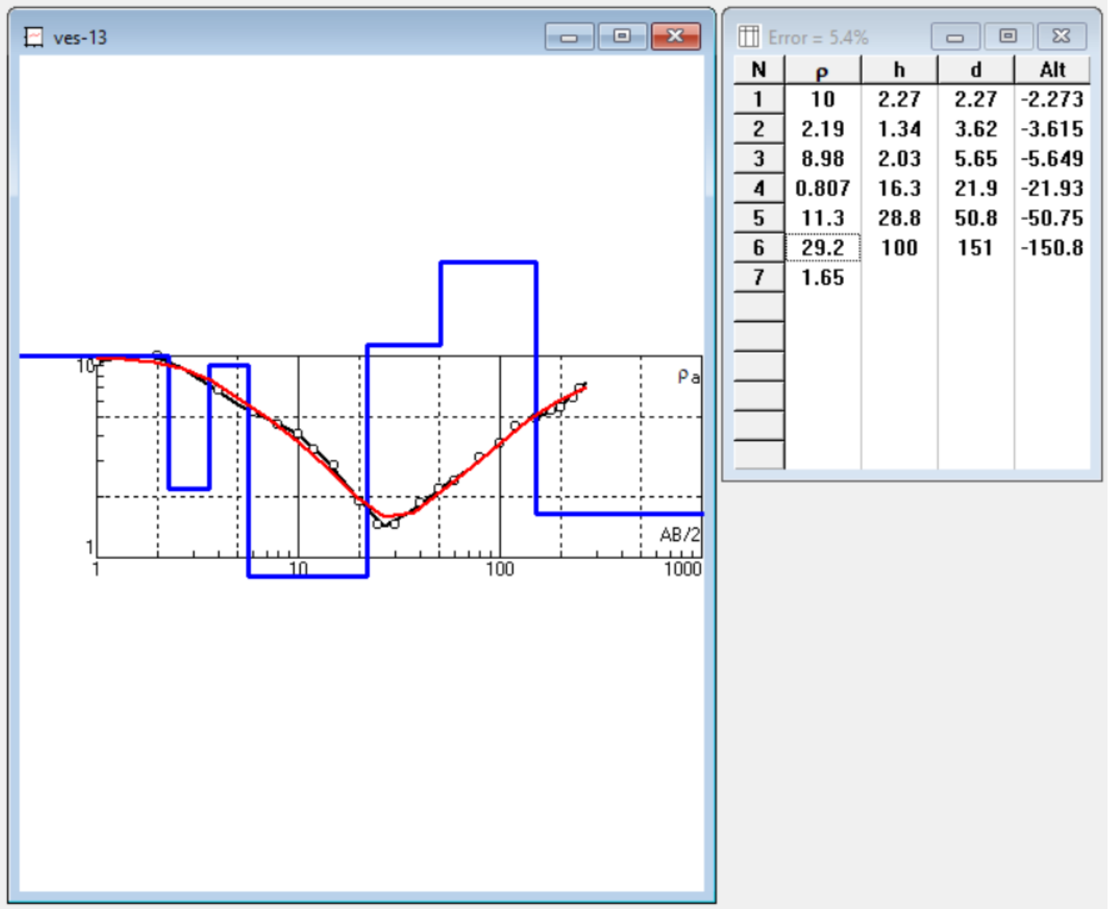

Error = 5.4%

N	ρ	h	d	Alt
1	10	2.27	2.27	-2.273
2	2.19	1.34	3.62	-3.615
3	8.98	2.03	5.65	-5.649
4	0.807	16.3	21.9	-21.93
5	11.3	28.8	50.8	-50.75
6	29.2	100	151	-150.8
7	1.65			

Rho	Thickness	Depth	Lithology
10	2	2	Top soil
0.8-2.2	20	22	Brackish Sand
11.3	29	51	Clay
30	100	151	FW Sand

VES-14

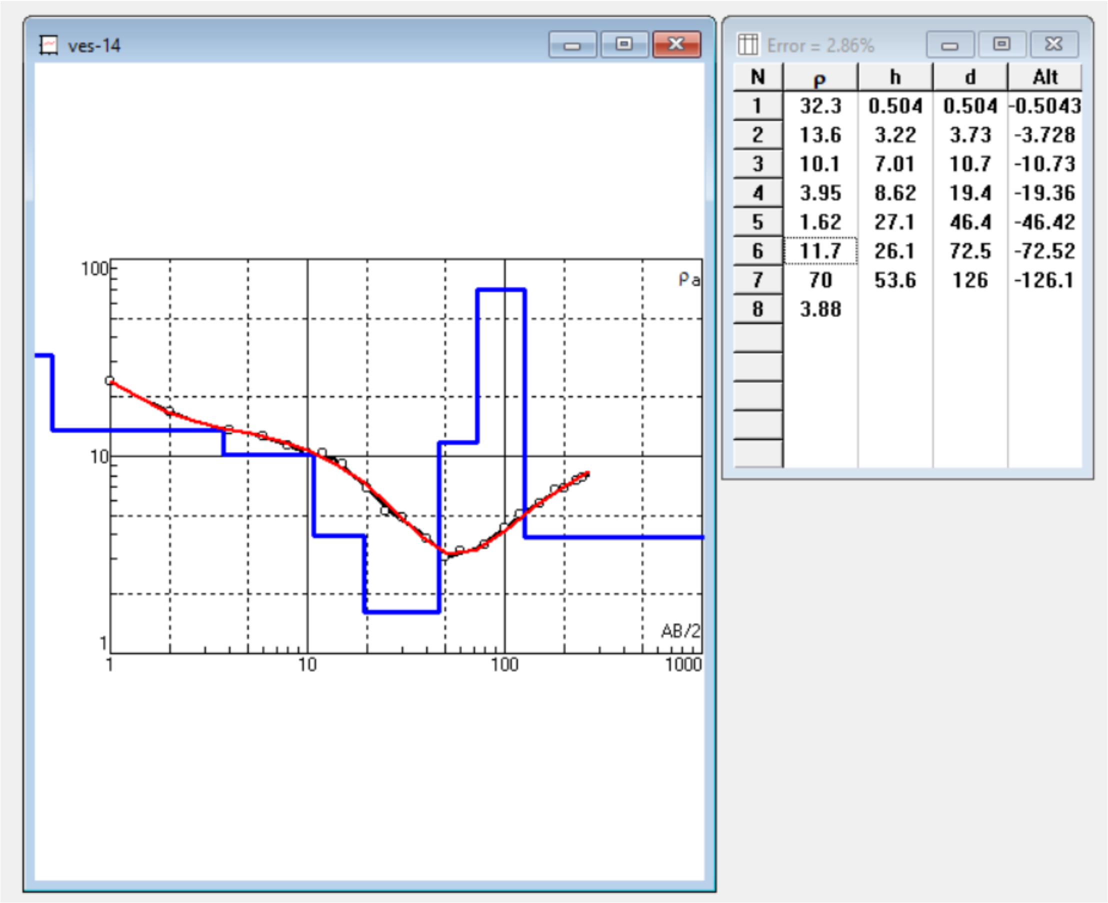

Error = 2.86%

N	ρ	h	d	Alt
1	32.3	0.504	0.504	-0.5043
2	13.6	3.22	3.73	-3.728
3	10.1	7.01	10.7	-10.73
4	3.95	8.62	19.4	-19.36
5	1.62	27.1	46.4	-46.42
6	11.7	26.1	72.5	-72.52
7	70	53.6	126	-126.1
8	3.88			

Rho	Thickness	Depth	Lithology
32.3	0.5	0.5	Top soil
1.6-13	46	46.5	Brackish Sand
11.7	26.5	73	Clay
70	53	126	FW Sand

VES-16

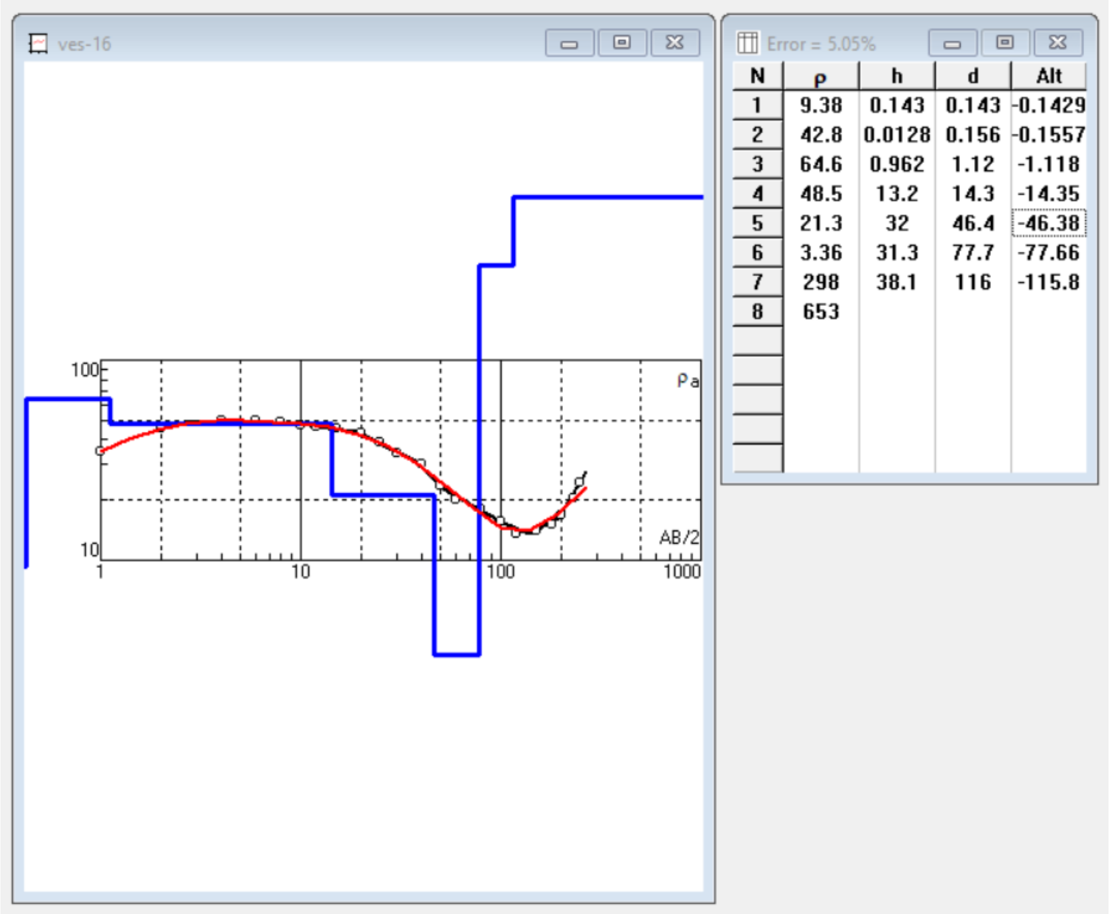

Error = 5.05%

N	ρ	h	d	Alt
1	9.38	0.143	0.143	-0.1429
2	42.8	0.0128	0.156	-0.1557
3	64.6	0.962	1.12	-1.118
4	48.5	13.2	14.3	-14.35
5	21.3	32	46.4	-46.38
6	3.36	31.3	77.7	-77.66
7	298	38.1	116	-115.8
8	653			

Lithology

Rho	Thickness	Depth	Lithology
9.38	1	1	Top soil
21-64	45	46	Relatively FW Sand
3.4	31	77	Clay
298	37	110	FW Sand

VES-20

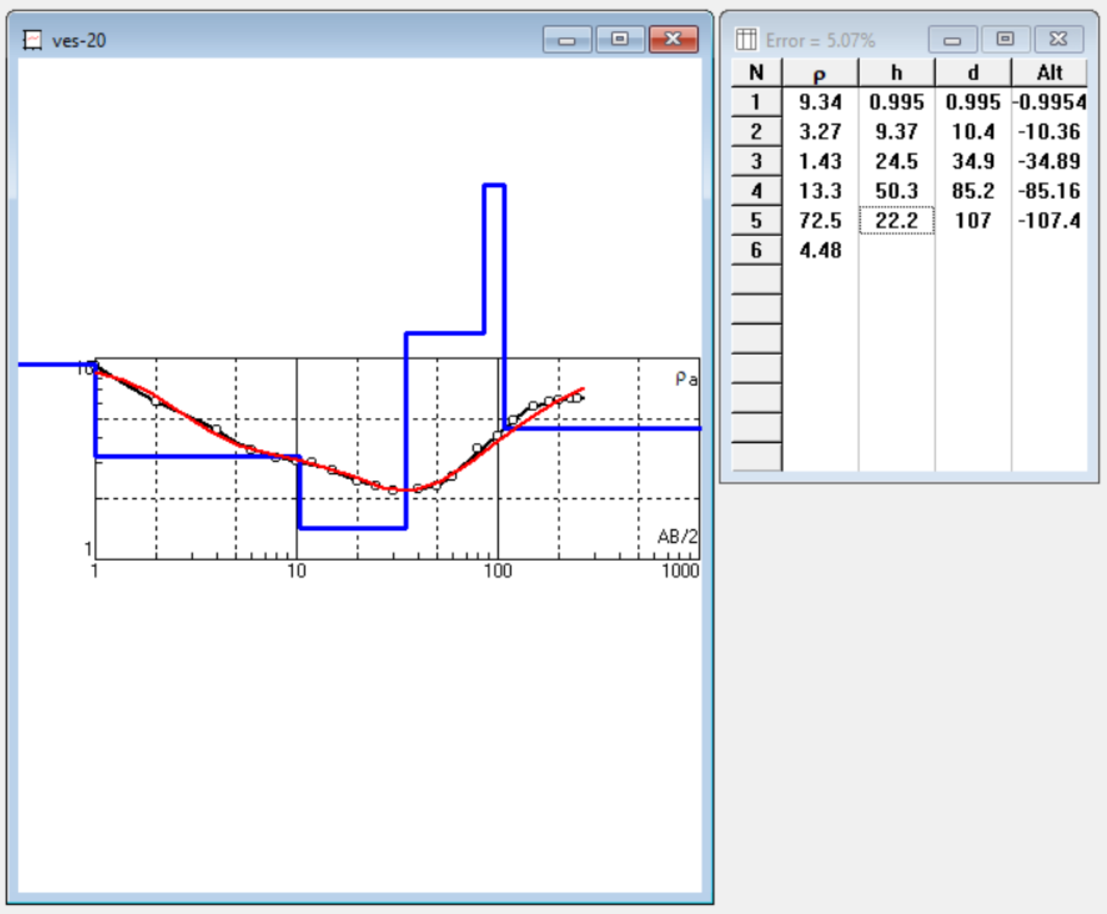

Error = 5.07%

N	ρ	h	d	Alt
1	9.34	0.995	0.995	-0.9954
2	3.27	9.37	10.4	-10.36
3	1.43	24.5	34.9	-34.89
4	13.3	50.3	85.2	-85.16
5	72.5	22.2	107	-107.4
6	4.48			

Rho	Thickness	Depth	Lithology
9.34	1	1	Top soil
1.43-3.27	34	35	Brackish Sand
13.3	50	86	Clay
72.5	22	108	FW Sand

APPENDIX-III: FIELD WATER QUALITY DATA (PHYSICO-CHEMICAL)

Detail Field Data Field Parameter for water

Sl No.	Type	Union Name	Village	Lattitude	Longitude	Depth	EC(mS/cm)	Temp (°C)	pH	Eh	Arsenic
1	DOBH	Kaherhat	Bhalukia	22.93435	91.55141	650+	0.15	25.3	5.04	195	0.01
2	WQP	Kaherhat	Bhalukia	22.9336	91.5495	180	0.24	25.6	6.3	-36	0.01
3	DOBH	Kaherhat	Bhalukia	22.93901	91.54931	550+	0.05	24.7	5.65	130	0.025
4	WQP	Kaherhat	Bhalukia	22.93623	91.54981	520+	0.05	25.3	5.46	157	0.01
5	WQP	Kaherhat	Bhalukia	22.93497	91.54753	90	0.28	25.3	6.45	70	0.01
6	WQP	Hinguli	Hinguli	22.91796	91.54876	380	0.08	25	5.8	154	0.01
6(1)	WQP	Hinguli	Purba Hinguli Taltola	22.91301	91.5461	45	0.15	21.5	6.72	104	0.01
7	WQP	Hinguli	Madhya Azamnagar	22.918	91.54183	120+	0.27	26	6.7	-29	0.025
8	WQP	Hinguli	Madhya Azamnagar	22.91763	91.53693	780	0.06	26.6	5.51	120	0.01
9	WQP	Hinguli	Jamalpur	22.89365	91.52956	700+	0.15	25.5	6.1	32	0.01
10	WQP	Hinguli	Gonokchara	22.90011	91.52068	600+	0.22	25.7	6.65	-36	0.01
11	WQP	Hinguli	Jamalpur	22.88452	91.51921	680	0.48	26.2	6.82	-39	0.025
12	WQP	Hinguli	Gonokchara	22.90021	91.52044	75	2.41	24.3	6.95	-93	0.025
13	WQP	Dhum	Mobarakgona	22.89305	91.49841	80	0.79	26	7.65	-152	0.2
14	WQP	Dhum	Dakhin Neharpur	22.87304	91.50825	750+	0.48	25.5	7.5	-85	0.05
15	WQP	Dhum	Dakhin Neharpur	22.87406	91.50868	70+	1.88	23.5	7.8	-150	0.5
16	WQP	Zorarganj	Paragalpur	22.8704	91.51942	30	1.66	24.4	6.54	-107	0.1
17	DOBH	Zorarganj	Paragalpur	22.87026	91.51968	440	0.6	25	7.49	-120	0.05
18	WQP	Zorarganj	Paragalpur	22.87236	91.51861	400	0.49	25.3	7.28	-105	0.05
19	WQP	Zorarganj	Uttar Sonapahar	22.8855	91.53113	730	0.29	24.5	6.42	-42	0.025
20	WQP	Zorarganj	Uttar Sonapahar	22.8855	91.53113	80	0.26	24.4	6.6	-30	0.01
21	WQP	Zorarganj	Sonapahar	22.87648	91.53789	190	0.4	23	6.96	-38	0.01
22	WQP	Osmanpur	Osmanpur	22.860048	91.48688	800	0.24	26.4	6.52	-58	0.025
23	WQP	Osmanpur	Osmanpur	22.860048	91.48688	100	3	26.4	7.44	-57	0.025
24	WQP	Osmanpur	Morgang	22.870525	91.491221	725	0.33	27.1	6.82	-93	0.05

Sl No.	Type	Union Name	Village	Lattitude	Longitude	Depth	EC(mS/cm)	Temp (°C)	pH	Eh	Arsenic
25	WQP	Osmanpur	Morgang	22.870525	91.491221	90	1.96	27	6.71	-112	0.5
26	WQP	Katachara	Katachara	22.816762	91.50793	600	12.67	25	6.45	-10	0.01
27	WQP	Katachara	Katachara	22.816762	91.50793	50	2.6	24.4	7.09	-100	0.3
28	WQP	Ichakhali	Vanguni bazar	22.86669	91.48346	60	5.13	27.6	7.1	-121	0
29	CGRMW	Ichakhali	Vanguni bazar	22.82665	91.48352	660	0.52	30.5	6.73	-114	0
30	WQP	Ichakhali	Vanguni bazar	22.82305	91.48273	60	3.56	26.2	6.96	-123	0.3
31	WQP	Ichakhali	Vanguni bazar	22.8231	91.48378	600	0.85	25.9	6.83	-96	0.01
32	WQP	Ichakhali	Jamadar gram	22.82264	91.471071	500(?)	4.57	28.2	6.47	-89	0
33	WQP	Ichakhali	Jamadar gram	22.82116	91.46944	40	8.54	28	6.8	-75	0.01
34	DNBH	Ichakhali	Neel Laxirchar	22.76384	91.47594	715	0.48	27.1	7.15	-114	0
35	DNBH	Ichakhali	Char Shorot	22.74888	91.49224	540	0.6	26.3	7.39	-104	0
36	WQP	Ichakhali	Char Shorot	22.74888	91.49224	40	4.09	25.8	7.06	-97	0.3
37	CGRMW	Ichakhali	Char Shorot	22.73395	91.50329	580	0.65	26	7.9	-62	0
38	WQP	Ichakhali	Char Shorot	22.73407	91.50385	50	9.54	25.2	7.01	-104	0.3
39	WQP	Saherkhali	Purba Sheherkhali	22.70835	91.56799	450	0.95	25.7	7.22	-82	0.025
40	WQP	Mayani	Paschim Mayani	22.7197	91.54507	400	0.61	26.3	7.29	-106	0
41	WQP	Mayani	Paschim Mayani	22.71936	91.54507	30	4.78	26	7.29	-163	0.3
42	WQP	Maghadia	Hasim Nagar	22.75491	91.51962	420	0.73	26.8	7.86	-68	0
43	WQP	Maghadia	Hasim Nagar	22.75505	91.51945	50	4.16	26.4	7.17	-120	0.3
44	WQP	Maghadia	Khurma Wala	22.7574	91.55304	450	0.74	26.8	7.54	-109	0
45	WQP	Mayani	Purba Mayani	22.73702	91.57252	520	0.59	26.6	7.13	-112	0
46	WQP	Mayani	Purba Mayani	22.73701	91.5723	50	2.11	25.9	6.65	-75	0.3
47	CGRMW	Saherkhali	Purba Saherkhali	22.70814	91.56847	520	-	-	-	-	-
48	WQP	Wahedpur	Podua	22.71861	91.59342	520	0.79	26.3	7.77	-103	0.05
49	WQP	Wahedpur	Podua	22.71893	91.59326	40	3.49	25.7	7.56	-167	1
51	DPHEOBS	Mirasarai	Borotakia Bazar	22.75539	91.58611	172	2.42	25.7	6.6	-62	0

Sl No.	Type	Union Name	Village	Lattitude	Longitude	Depth	EC(mS/cm)	Temp (°C)	pH	Eh	Arsenic
52	WQP	Mirasarai	Borotakia Bazar	22.7557	91.58601	65	1.16	26.3	7.83	-112	0.5
53	WQP	Karerhat	Bhalukia	22.93518	91.5473	550	0.09	25.9	5.12	130	0
54	WQP	Karerhat	Bhalukia	22.93485	91.54682	100	0.32	26.3	6.04	6	0
55	WQP	Hinguli	Madhya Azamnagar	22.91764	91.53634	70	0.38	26	6.38	-27	0
56	CGRMW	Hinguli	Mehedi nagar	22.88738	91.5546	510	-	-	-	-	-
57	WQP	Hinguli	Mehedi nagar	22.88738	91.5546	35	0.15	24.9	5.98	-36	0.1
58	WQP	Dhum	Mobarakgona	22.89198	91.49336	550	0.26	25.2	6.44	-36	0
59	WQP	Dhum	Mobarakgona	22.8917	91.49368	60	1.95	25.4	7.09	-114	0.5
60	ARTW	Karerhat	Oli Nagar	22.9470518	91.569671	700+	0.19	26.9	6.54	55	0
61	ARTW	Karerhat	Oli Nagar	22.9480123	91.5696116	700+	0.16	26.9	6.36	77	0
62	ARTW	Karerhat	Oli Nagar	22.9473261	91.5684257	700+	0.15	26.6	6.42	88	0
63	WQP	Osmanpur	Shahedpur	22.85519	91.49814	850	0.83	26.4	6.14	-51	0
64	WQP	Osmanpur	Shahedpur	22.85543	91.49799	65	2.96	25.5	7.15	-145	0.5
65	WQP	Durgapur	Zoroddorpur	22.83592	91.52926	550	0.46	29	6.87	-90	0.05
66	WQP	Durgapur	Zoroddorpur	22.83592	91.52926	60	1.7	29.5	7.17	-109	0.5
67	WQP	Durgapur	Gopalpur	22.83647	91.54332	200	0.4	26	6.85	-84	0
68	WQP	Mithanala	Mithanala	22.79584	91.52528	600	0.67	26.4	7.52	-57	0
69	WQP	Mithanala	Mithanala	22.79567	91.52532	45	2.1	25.6	6.41	-68	0.2
70	WQP	Mithanala	Rahmatabaz	22.78786	91.50078	700	0.71	27.9	7.42	-102	0
71	WQP	Mithanala	Rahmatabaz	22.78824	91.50121	40	4.31	26.2	7.1	-104	0.5
72	WQP	Mithanala	Jafrabad	22.788869	91.55077	50	1.2	25	7.13	-126	0.5
73	CGRMW	Mithanala	Jafrabad	22.78856	91.55094	635	-	-	-	-	-
74	WQP	Mirasarai	Mirasarai	22.77744	91.57247	700	0.51	26.1	7.17	-52	0.1
75	WQP	Mirasarai	Gorias	22.81847	91.56419	600	0.27	25.4	6.49	11	0
76	WQP	Mirasarai	Mirasarai	22.77744	91.57247	60	0.57	25	7.15	-95	0.3

APPENDIX-IV: SLUG TEST INTERPRETATION DATA

Graqphical Curves Obtained from Slug Tests

Serial_number: 35

Project ID: DNBH-03

Location: Char Shorot, Economic zone, Ichakhali

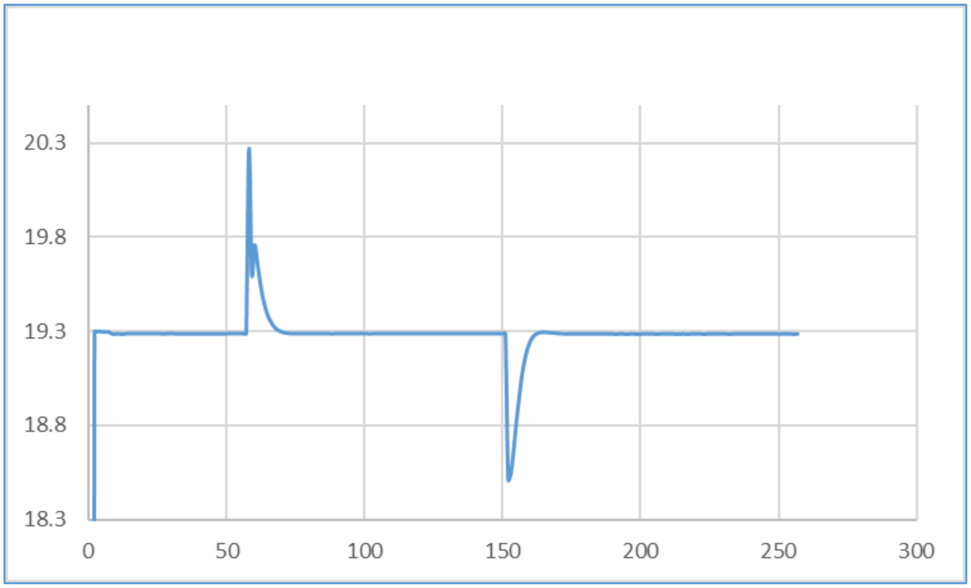

Figure-1: Overdamped Response

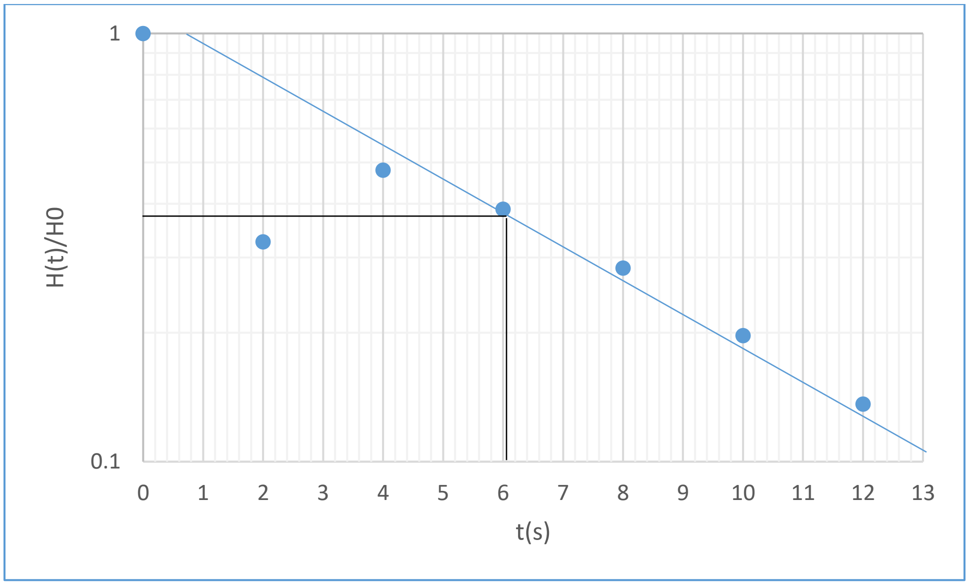

Figure-2: Rising Head curve

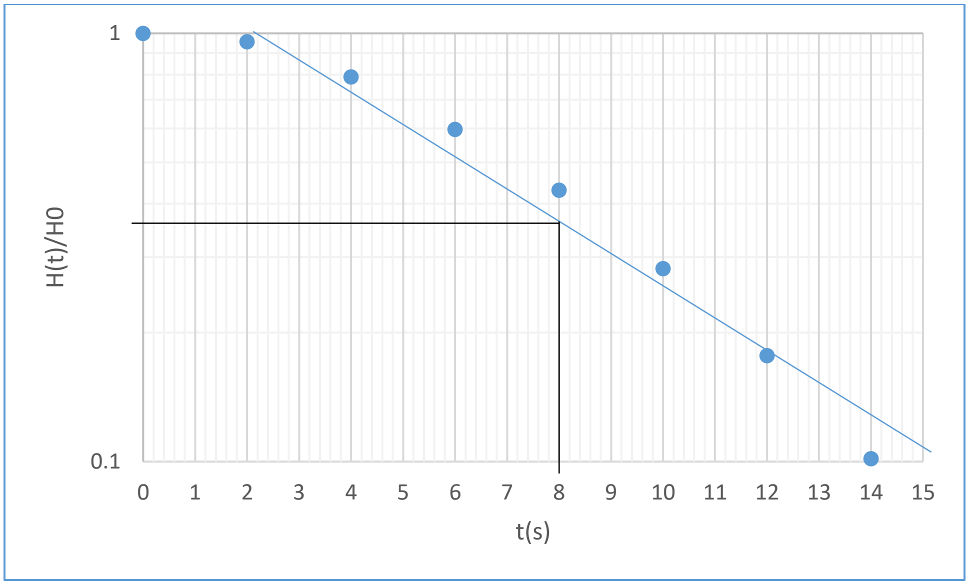

Figure-3: Falling Head curve

Serial_number: 36

Project ID: DNBH-03_S

Location: Char Shorot**,** Economic zone, Ichakhali.

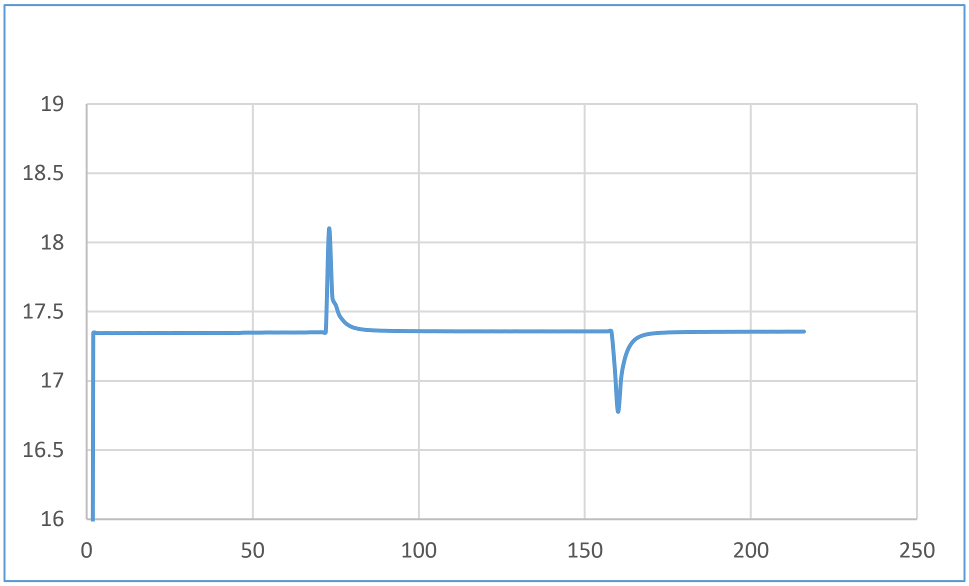

Figure-4: Overdamped Response

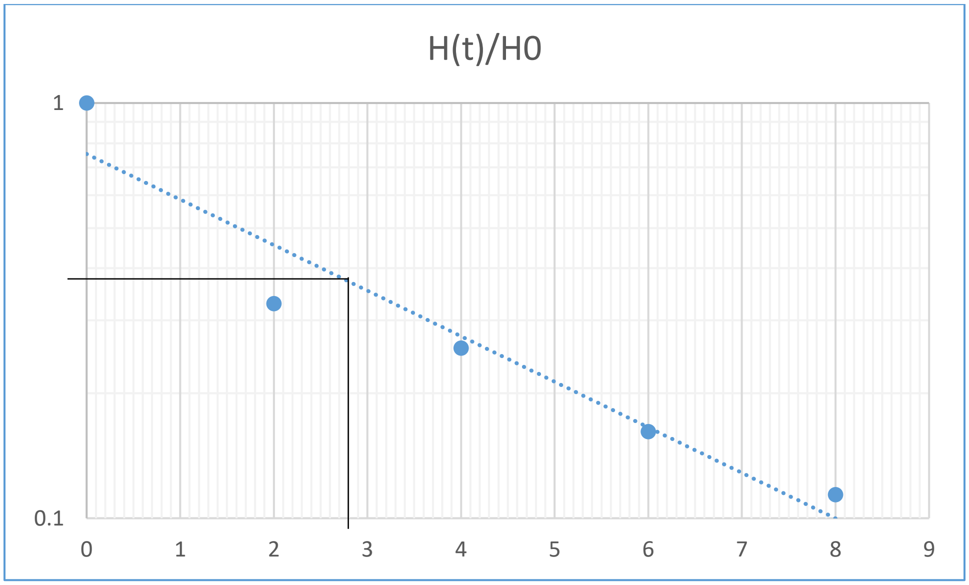

Figure-5: Rising Head curve

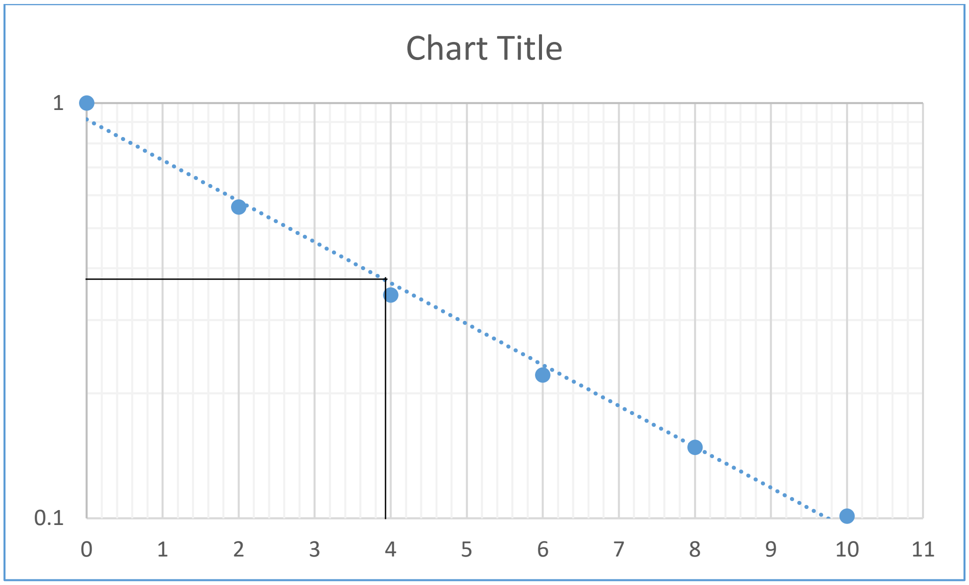

Figure-6: Falling Head curve

Serial_number: 50

Project ID: DPHEOBS

Location: Baratakia Bazar, Mirsharai.

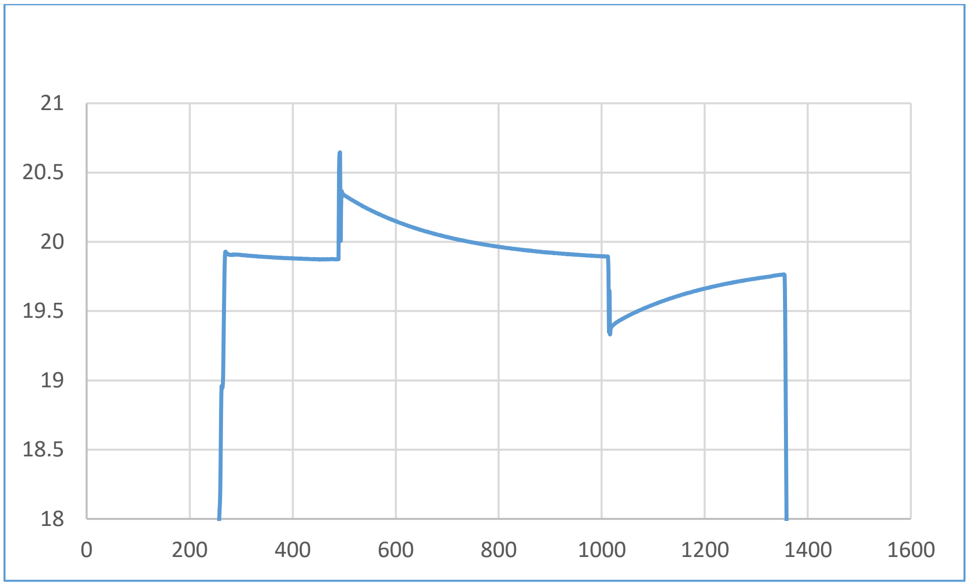

Figure-7: Overdamped Response

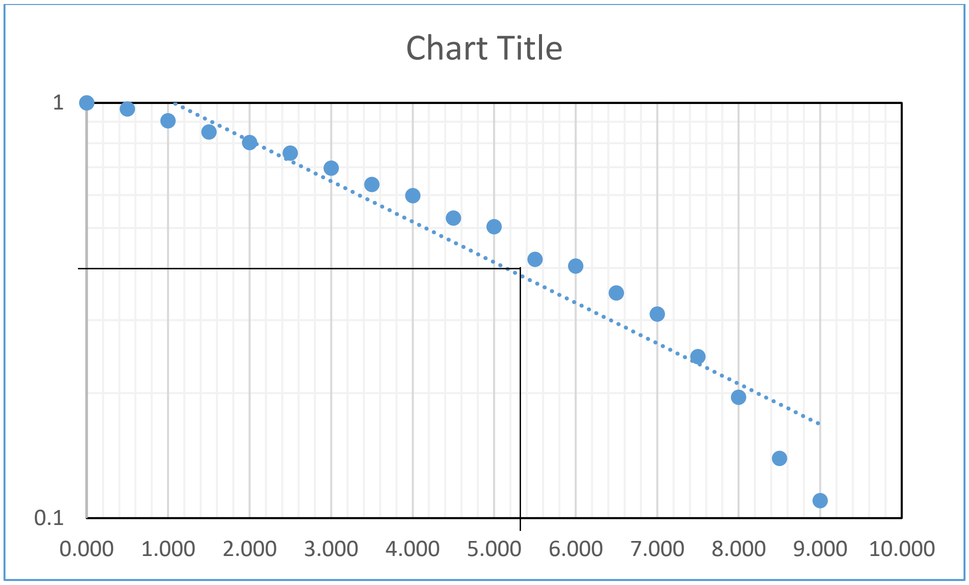

Figure-8: Rising Head curve

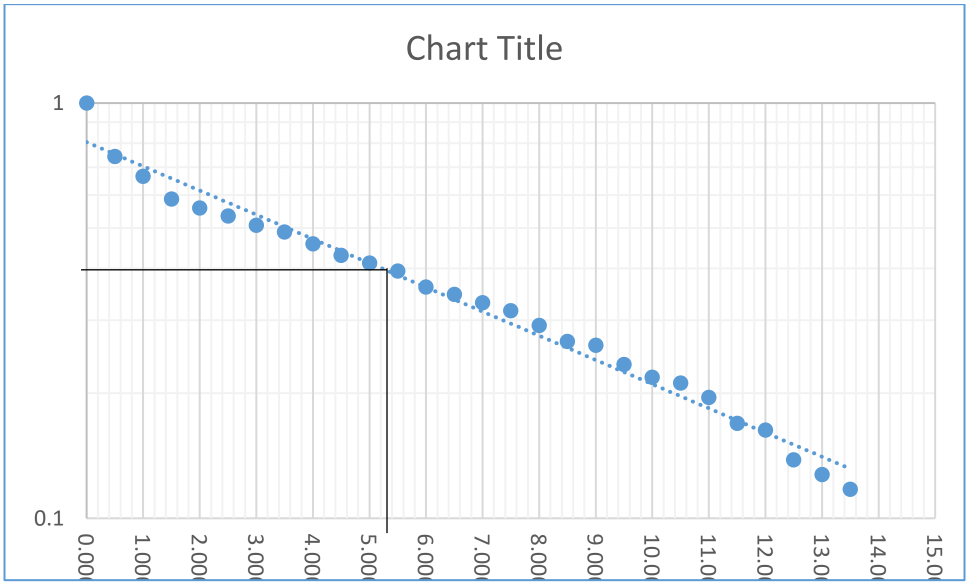

Figure-9: Falling Head curve

Serial_number: 51

Project ID: DPHEOBS_S

Location: Baratakia Bazar, Mirsharai.

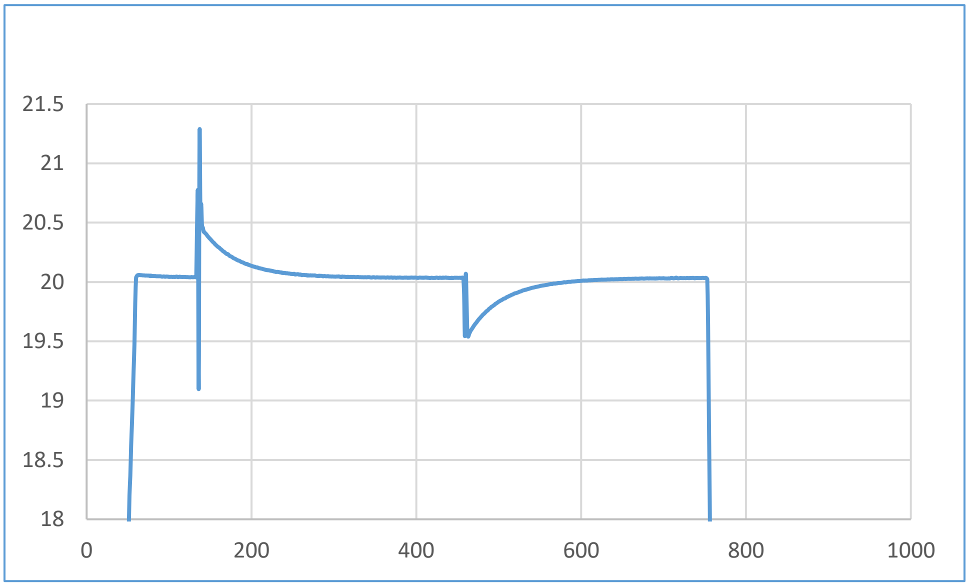

Figure-10: Overdamped Response

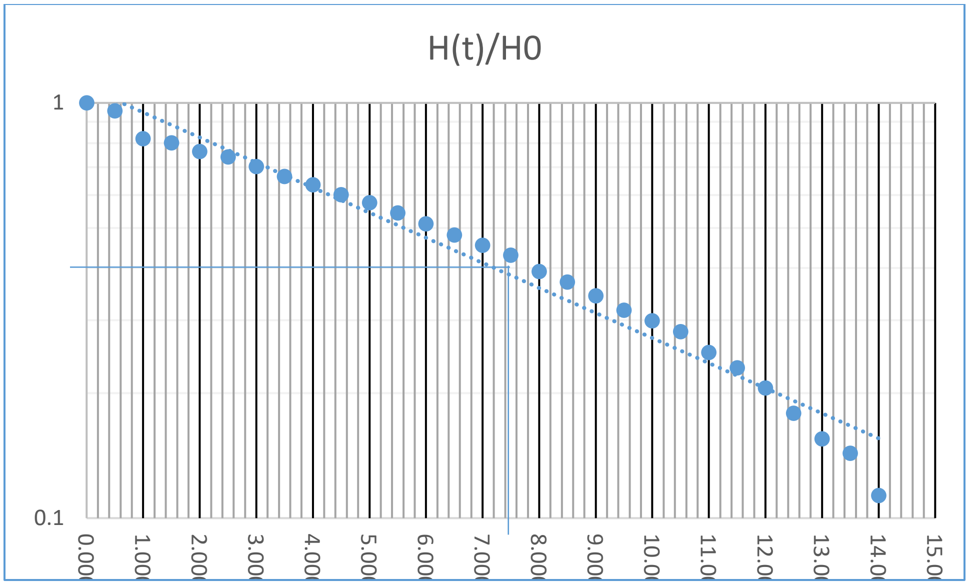

Figure-11: Rising Head curve

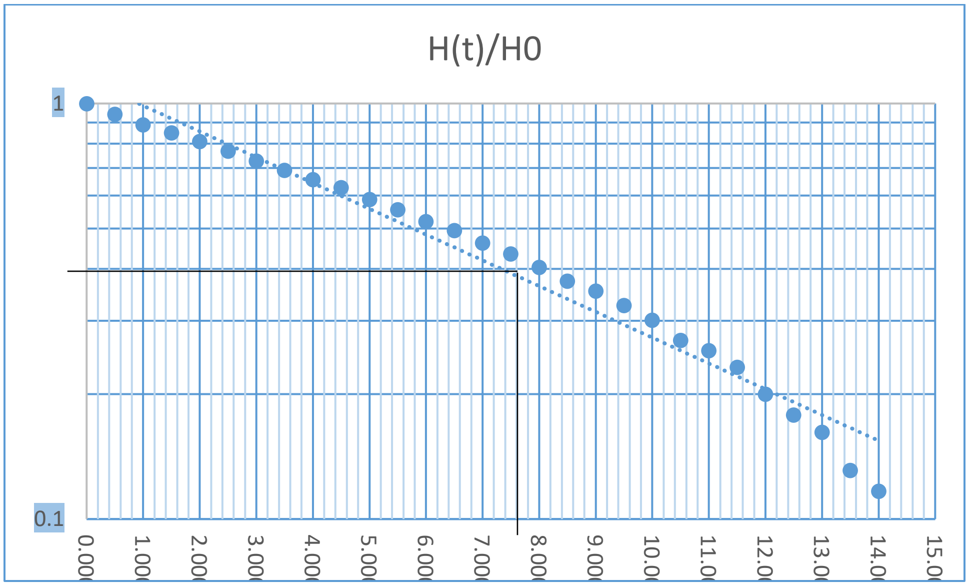

Figure-12: Falling Head curve

Serial_number: 33

Project ID: SLN33

Location: Jamadargram, Ichakhali.

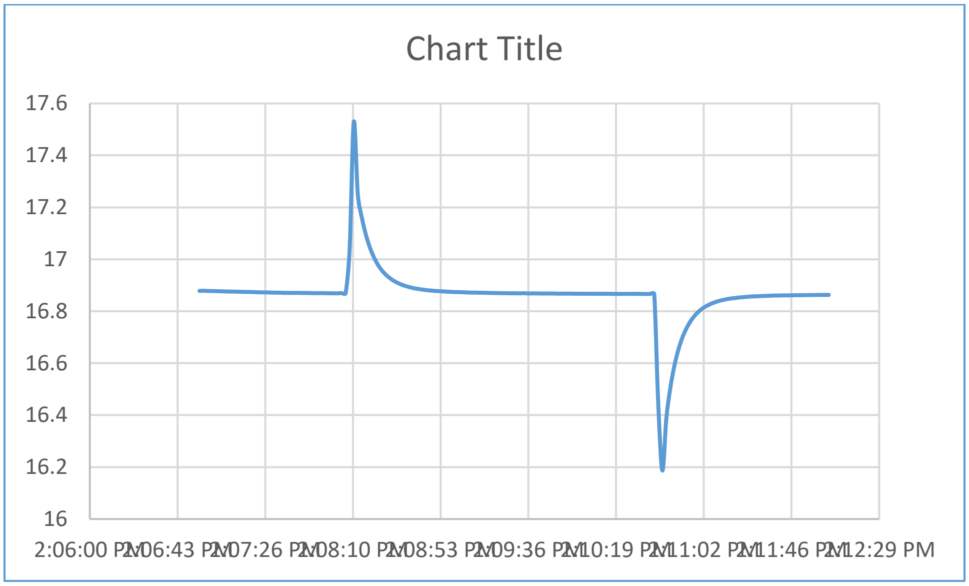

Figure-13: Overdamped Response

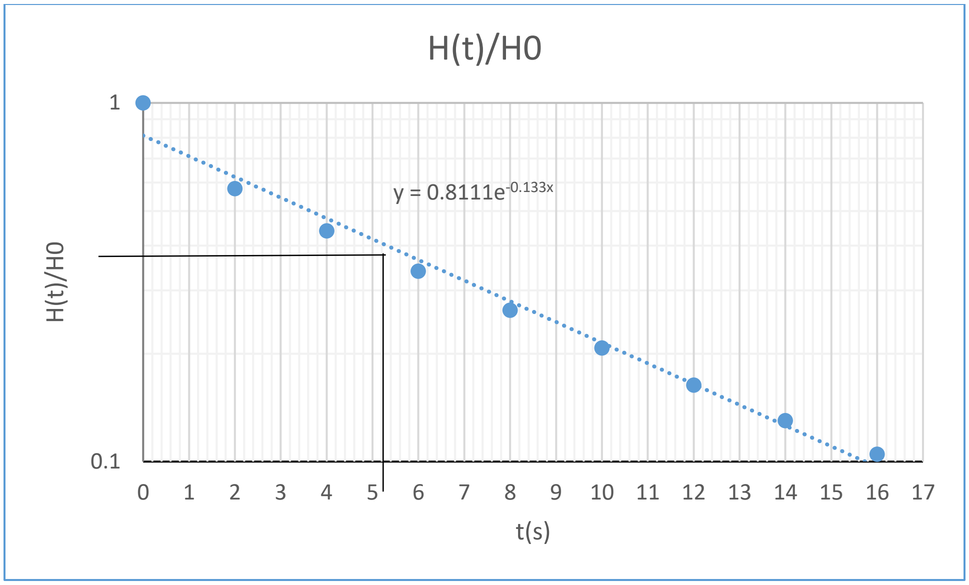

Figure-14: Rising Head curve

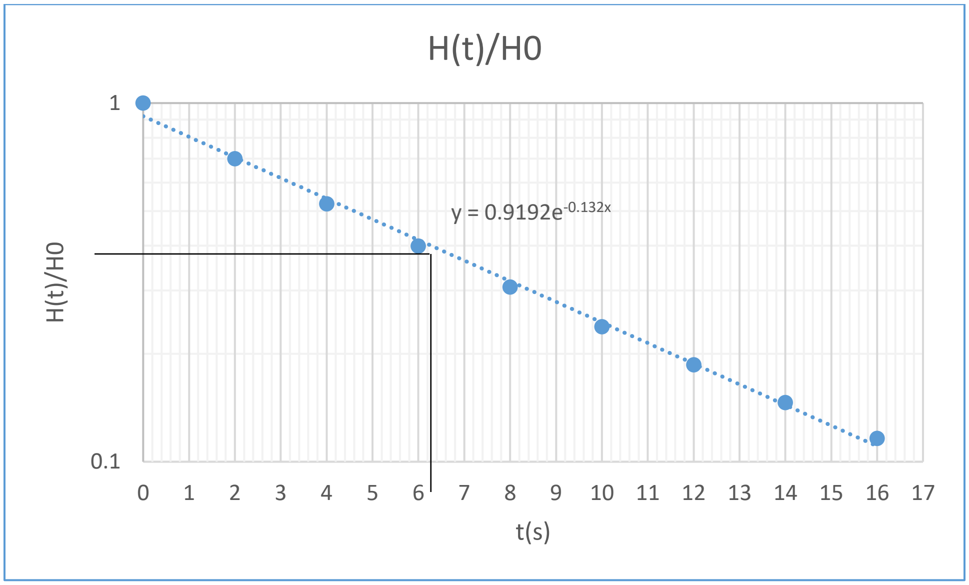

Figure-15: Falling Head curve

Serial_number: 39

Project ID: SLN39

Location: Purba Shaherkhali, Shaherkhali.

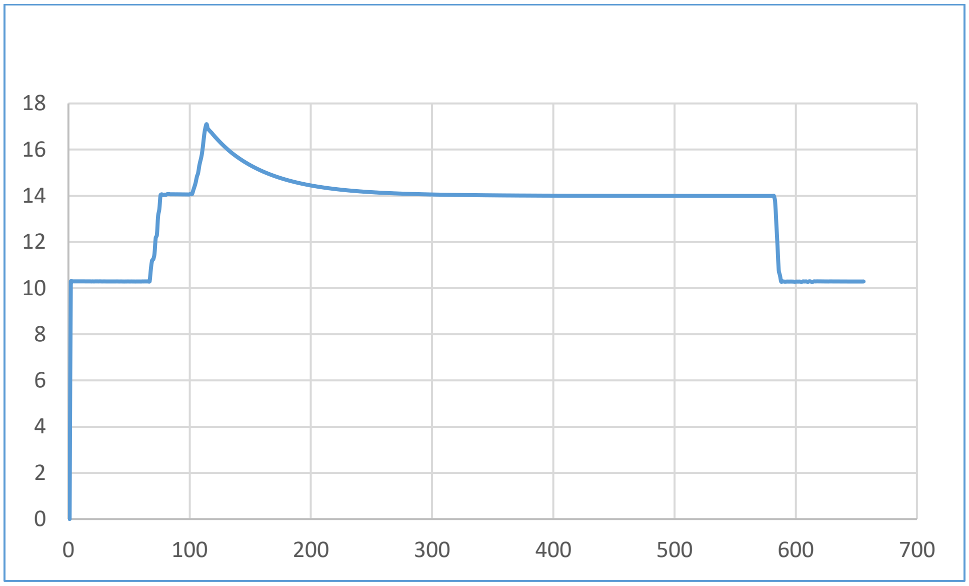

Figure-16: Overdamped Response

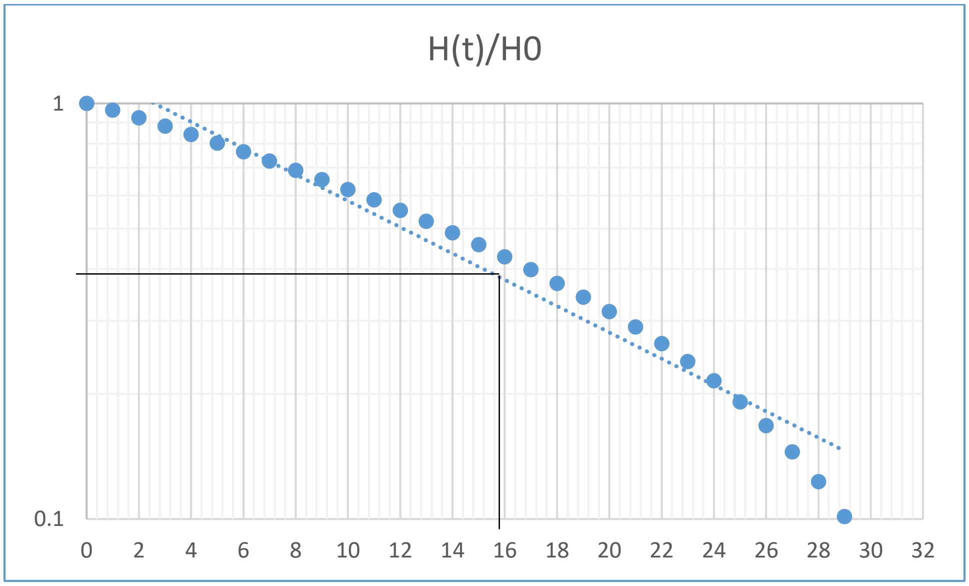

Figure-17: Rising Head curve

Serial_number: *40*

Project ID: SLN40

Location: Paschim Mayani, Mayani

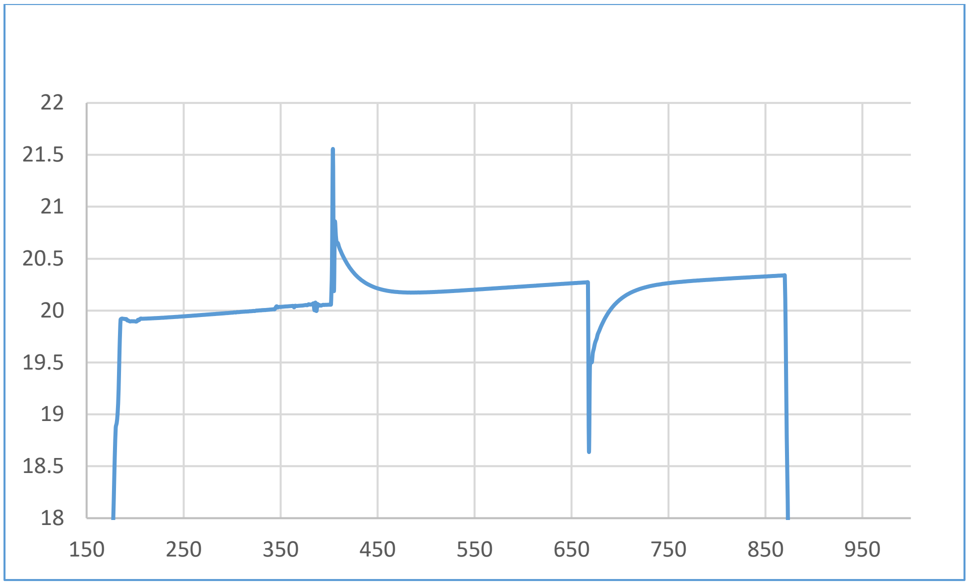

Figure-18: Overdamped Response

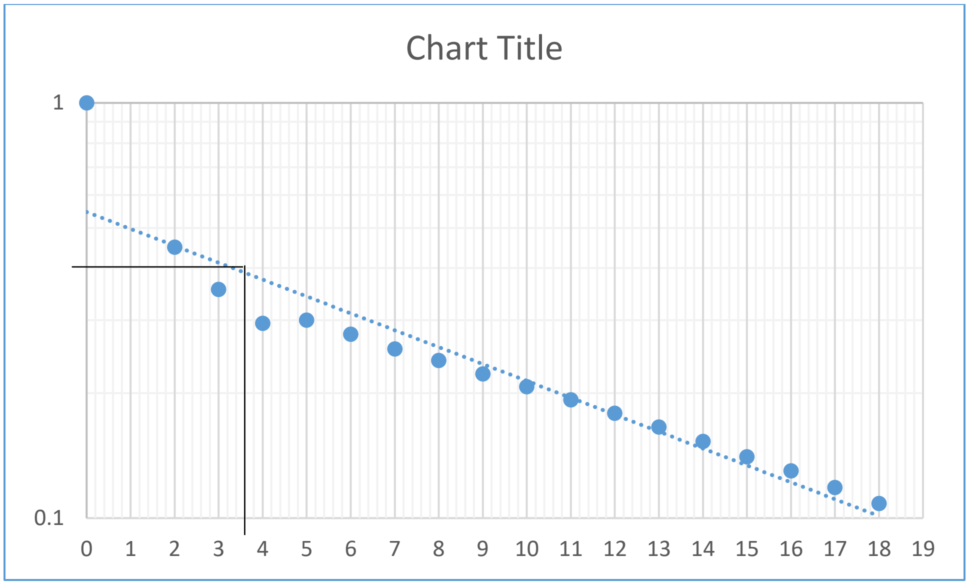

Figure-19: Rising Head curve

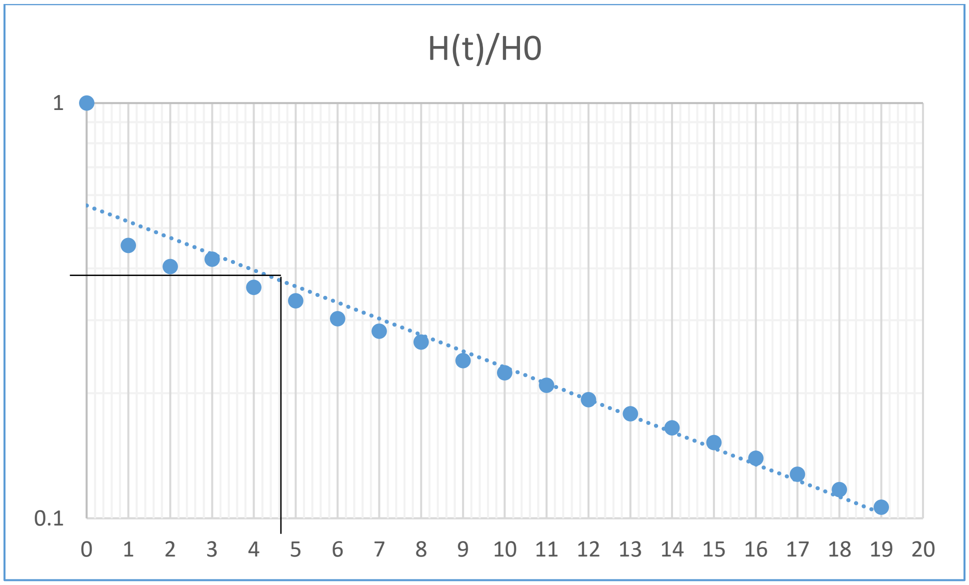

Figure-20: Falling Head curve

Serial_number: 45

Project ID: SLN45

Location: Purba Mayani, Mayani.

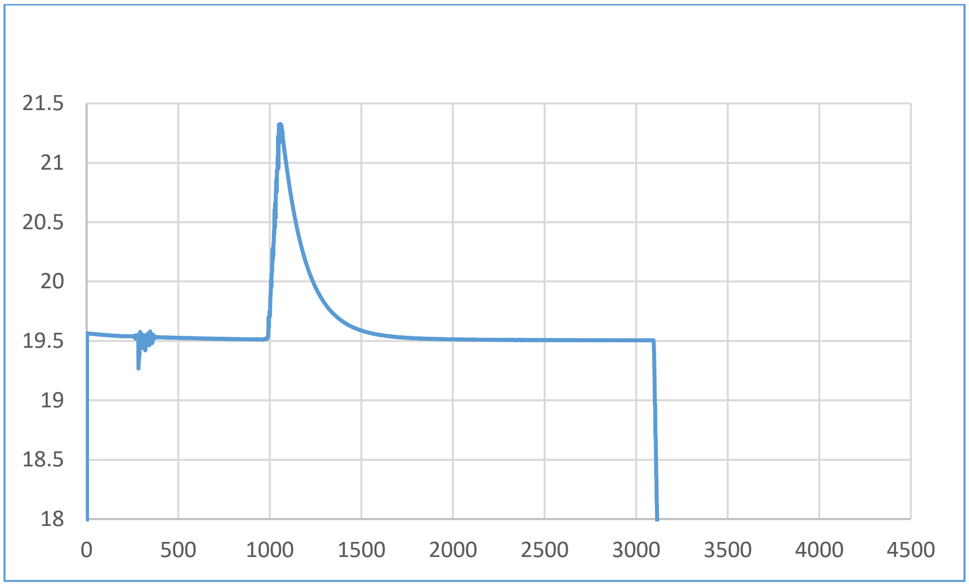

Figure-21: Overdamped Response

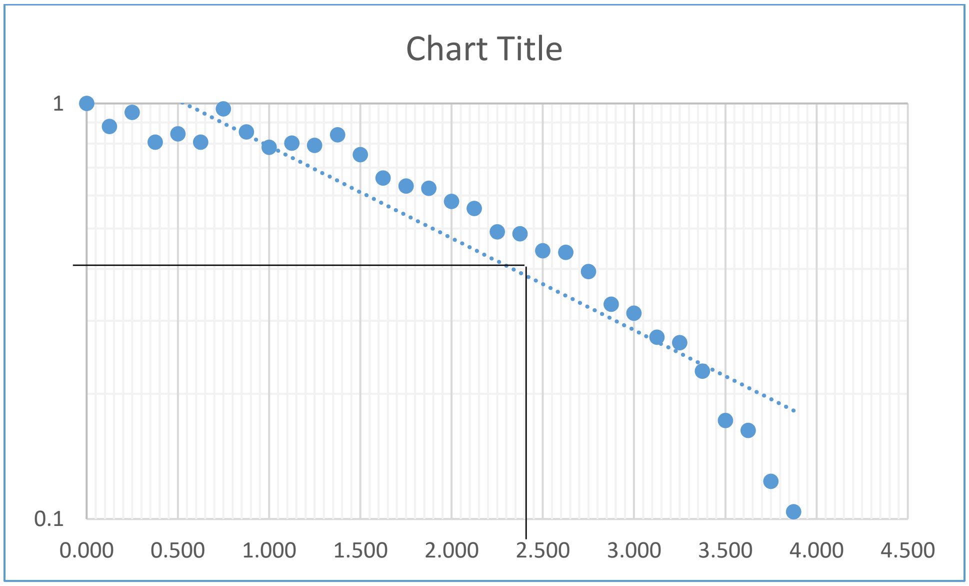

Figure-22: Rising Head curve

Serial_number: *48*

Project ID: SLN48

Location: Podua, Wahedpur

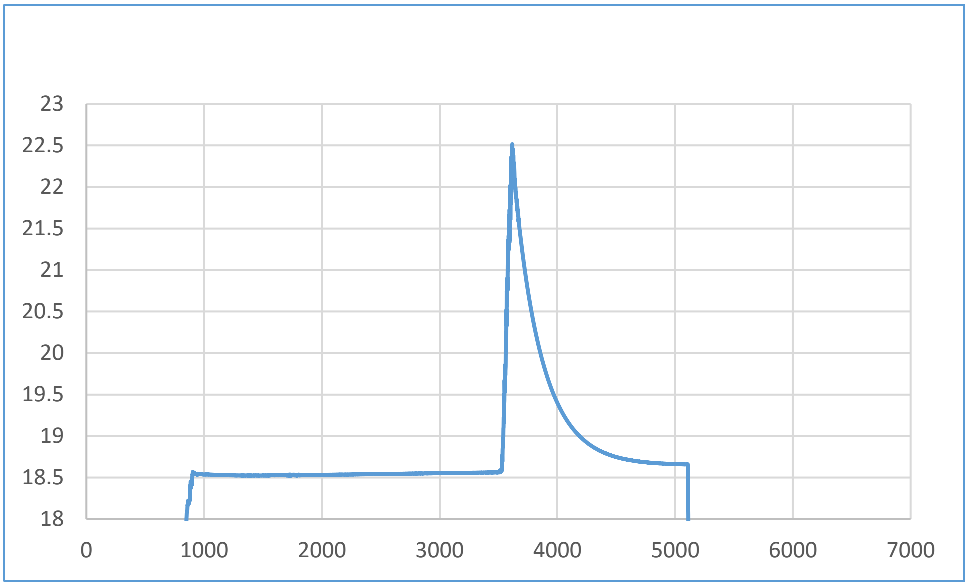

Figure-23: Overdamped Response

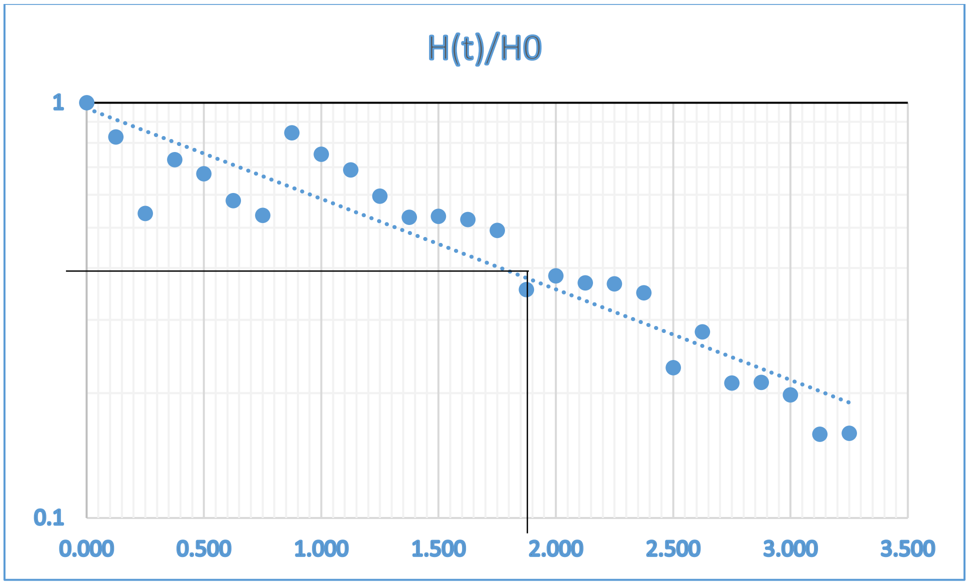

Figure-24: Rising Head curve

Serial_number: *49*

Project ID: SLN49

Location: Podua, Wahedpur.

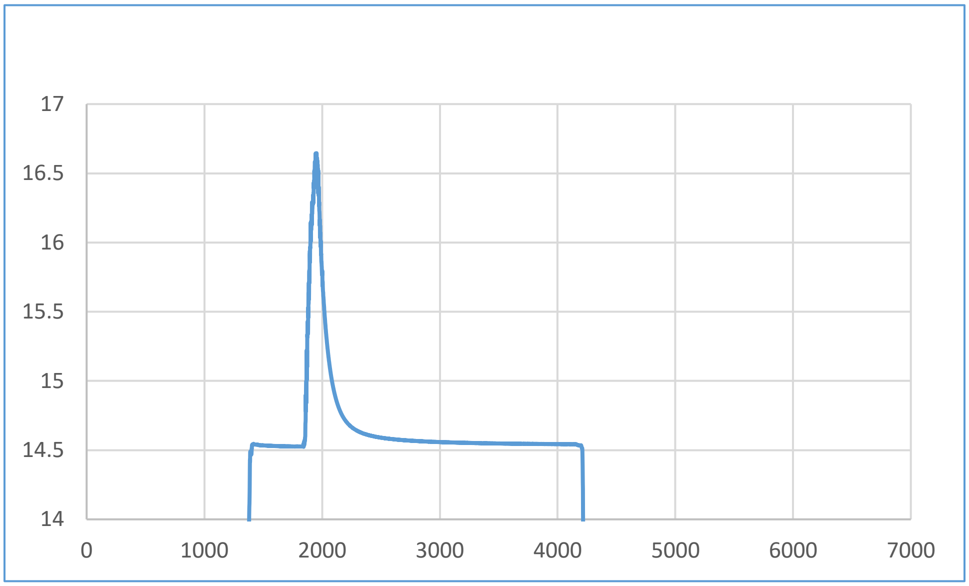

Figure-25: Overdamped Response

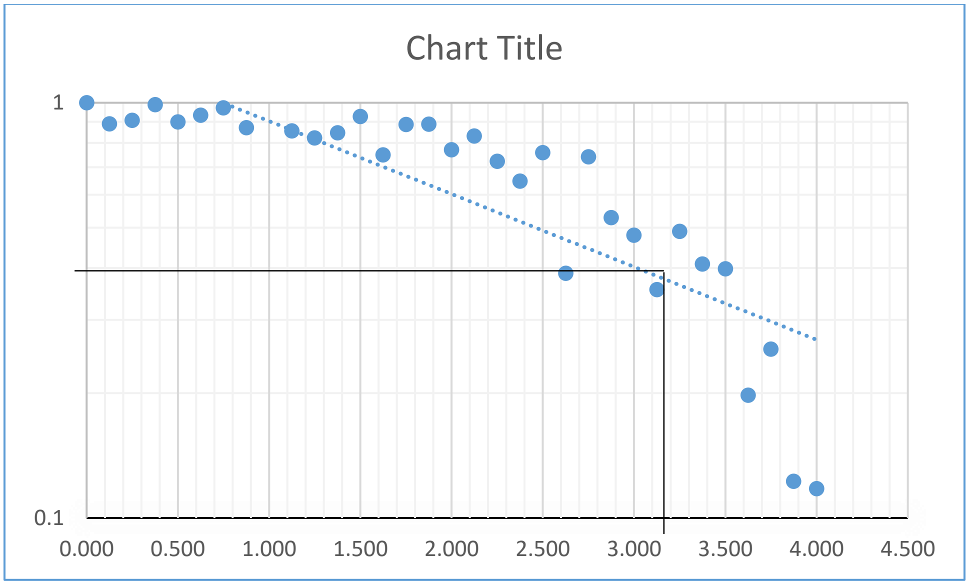

Figure-26: Rising Head curve

APPENDIX-V: HYDRAULIC CONDUCTIVITY BY GRAIN SIZE ANALYSIS

Well	Samle Depth [m]	HC by Grain Size Analysis	Aquifer	Average HC	Depth
MW-1	19-21	3	Aquifer-1	14.18	0-90
	21-24	15			
	24-27	19			
	27-30	17			
	39-42	10			
	51-54	17			
	60-63	17			
	84-87	15.5			
	105-108	17	Aquifer-2	13.63	103-220
	120-123	19.5			
	135-138	19.5			
	141-144	14			
	144-147	17			
	147-150	14			
	150-153	0.4			
	156-159	22			
	150-162	5			
	162-165	6.4			
	165-168	14.4			
	171-174	14.4			
MW-2	21-24	8	Aquifer-1	7.74	5-115
	24-27	10			
	30-33	6.4			
	33-36	17			
	42-45	17			
	54-57	3.6			
	66-69	2.5			
	75-78	1.6			
	90-93	3.6			
	123-126	14.4	Aquifer-2	6.92	123-220
	144-147	8			
	156-159	12			
	162-165	8			
	201-204	14.4			
	204-207	2.5			
	207-210	5			
	210-213	3.6			
	213-216	3.8			
	216-219	0.5			
	219-222	4			

Well	Samle Depth [m]	HC by Grain Size Analysis	Aquifer	Average HC	Depth
MW-3	12-15	2	Aquifer-1	5.24	8-46
	15-18	5			
	18-21	2.5			
	21-24	3.6			
	24-27	10			
	27-30	10			
	36-39	3.6			
	73-76	3.6	Aquifer-2	3	55-105
	79-82	3			
	88-91	2.5			
	159-162	2.5	Aquifer-3	1.8	163-197
	162-165	3			
	165-168	2.5			
	168-171	1			
	177-180	2.5			
	180-183	1			
	183-186	2			
	186-189	1			
	189-192	1			
	192-195	1.6			
	195-198	2			
MW-4	24-27	4	Aquifer-1	3.43	0-40
	30-33	2.5			
	42-45	3.8			
	45-48	2.5	Aquifer-2	1.66	50-120
	48-51	1			
	75-78	1			
	93-96	2			
	108-111	1			
	120-123	2.5			
	135-138	1	Aquifer-3	2.16	138-210
	147-150	4.2			
	153-156	1			
	162-165	2.5			
	177-180	0.5			
	186-189	3			
	189-192	1			
	192-195	3.6			
	195-198	3			
	198-201	0.5			
	201-204	2.5			
	204-207	1			

Well	Samle Depth [m]	HC by Grain Size Analysis	Aquifer	Average HC	Depth
MW-5	18-21	4.2	Aquifer-1	4.28	0-48
	21-24	2.5			
	24-27	6.4			
	27-30	6.4			
	33-36	4.6			
	42-45	1.6			
	54-57	0.5			
	72-75	1			
	84-87	1			
	90-93	3	Aquifer-2	2.3	90-103
	102-105	1.6			
	117-120	1	Aquifer-3	1.65	146-157
	126-129	1			
	132-135	1.6			
	153-138	2.5			
	138-141	1.2			
	141-144	0.5			
	144-147	1.6			
	147-150	2.5			
	150-153	1.6			
	153-156	3			

APPENDIX-VI: WATER QUALITY DATA FROM LABORATORY ANALYSIS

Sample ID	Na$^+$ (ppm)	Na$^+$ (meq/l)	K$^+$ (ppm)	K$^+$ (meq/l)	Ca^{2+} (ppm)	Ca^{2+} (meq/l)	Mg^{2+} (ppm)	Mg^{2+} (meq/l)	Total Cation	HCO$_3^-$ (ppm)
SL08	2.104	0.0915	1.77	0.04527	5.85	0.29177	8.04	0.6617	1.090246	45.75
SL11	77.17	3.3552	3.038	0.0777	30.47	1.5197	30.05	2.4733	7.425867	221.125
SL28	850.56	36.981	3.662	0.09366	26.2	1.30673	85.78	7.0601	45.44134	777.75
SL29	52.951	2.3022	4.862	0.12435	27.89	1.39102	22.58	1.8584	5.676024	244
SL30	444.39	19.321	9.139	0.23373	47.25	2.35661	130.43	10.735	32.64641	709.125
SL32	534.98	23.26	1.808	0.04624	154.7	7.71621	119.15	9.8066	40.82903	129.625
SL33	1204	52.348	5.194	0.13284	171.7	8.56509	239.16	19.684	80.73014	1098
SL34	77.388	3.3647	3.297	0.08432	14.82	0.73915	20.79	1.7111	5.899281	335.5
SL35	102.18	4.4426	3.604	0.09217	16.7	0.83292	21.67	1.7835	7.151196	388.875
SL36	538.36	23.407	10.858	0.2777	55.59	2.77257	123.6	10.173	36.62985	701.5
SL37	117.7	5.1175	2.745	0.0702	12.11	0.60399	20.13	1.6568	7.448463	449.875
SL38	1748.3	76.011	8.25	0.211	139.8	6.97406	280.08	23.052	106.2482	747.25
SL39	156.51	6.8047	2.335	0.05972	11.91	0.59401	17.33	1.4263	8.884767	526.125
SL40	95.967	4.1725	3.074	0.07862	14.41	0.7187	24.63	2.0272	6.996961	419.375
SL41	718.53	31.24	6.019	0.15394	37.1	1.85037	98.16	8.079	41.32354	869.25
SL42	143.88	6.2557	2.486	0.06358	18.34	0.91471	19.78	1.628	8.861973	533.75
SL43	517.77	22.512	8.508	0.2176	65.8	3.2818	148.69	12.238	38.24877	838.75
SL44	148.73	6.4667	2.392	0.06118	14.6	0.72818	21.86	1.7992	9.055229	526.125
SL45	82.522	3.5879	2.558	0.06542	19.78	0.98653	26.19	2.1556	6.795424	404.125
SL46	213.39	9.2776	3.212	0.08215	36.83	1.83691	90.06	7.4123	18.60901	373.625
SL47	89.486	3.8907	3.627	0.09276	26.84	1.33865	31.21	2.5687	7.890835	388.875
SL48	146.24	6.3583	2.2	0.05627	11.57	0.57706	18.92	1.5572	8.548829	480.375
SL49	448.28	19.49	9.621	0.24606	25.05	1.24938	102.37	8.4255	29.41117	472.75
SL51	300.24	13.054	1.355	0.03465	46.64	2.32618	66.12	5.442	20.85673	312.625
SL52	162.88	7.0818	19.51	0.49898	12.75	0.63591	38.26	3.149	11.36564	488
SL53	2.346	0.102	1.444	0.03693	5.44	0.27132	6.67	0.549	0.959224	45.75
SL54	34.666	1.5072	0.638	0.01632	8.35	0.41646	14.08	1.1588	3.098841	114.375
SL55	40.739	1.7713	0.833	0.0213	15.78	0.78703	18.29	1.5053	4.084947	183
SL56	19.487	0.8473	13.639	0.34882	22.51	1.12269	20.01	1.6469	3.965691	183
SL57	7.574	0.3293	0.618	0.01581	7.66	0.38204	13.74	1.1309	1.858019	76.25
SL58	27.591	1.1996	1.383	0.03537	13.51	0.67382	17.51	1.4412	3.349947	167.75
SL60	4.254	0.185	2.44	0.0624	15.7	0.78304	15.15	1.2469	2.277317	106.75
SL61	8.696	0.3781	2.376	0.06077	15.21	0.7586	14.32	1.1786	2.376059	106.75
SL62	6.395	0.278	3.107	0.07946	11.17	0.55711	12.79	1.0527	1.967289	114.375
SL63	45.183	1.9645	3.07	0.07852	17.64	0.8798	19.04	1.5671	4.489874	213.5
SL64	702.35	30.537	4.406	0.11269	17.33	0.86434	61.95	5.0988	36.61275	587.125
SL65	57.314	2.4919	2.477	0.06335	18.41	0.9182	19.47	1.6025	5.075937	297.375
SL66	200.13	8.7011	18.438	0.47156	19.82	0.98853	71.68	5.8996	16.06081	541.375
SL67	47.604	2.0697	1.794	0.04588	17.33	0.86434	23.02	1.8947	4.874611	274.5
SL68	124.34	5.4059	1.935	0.04949	15.53	0.77456	19.37	1.5942	7.82416	465.125
SL69	166.2	7.2259	5.473	0.13997	63.96	3.19002	102.89	8.4683	19.02418	625.25
SL70	123.62	5.3747	2.149	0.05496	16.91	0.84339	21.73	1.7885	8.061526	472.75
SL71	632.4	27.495	7.357	0.18816	45.96	2.29227	111.22	9.1539	39.12977	899.75
SL72	200.83	8.7318	6.987	0.1787	14.42	0.7192	37.52	3.0881	12.71779	571.875
SL73	85.558	3.7199	3.037	0.07767	13.1	0.65337	17.89	1.4724	5.92338	366
SL74	71.459	3.1069	1.936	0.04951	18.46	0.9207	25.97	2.1374	6.214574	327.875
SL75	21.939	0.9539	3.838	0.09816	16.87	0.8414	19.62	1.6148	3.508239	167.75
SL76	39.079	1.6991	20.185	0.51624	37.34	1.86234	19.27	1.586	5.66368	388.875

Sample ID	HCO_3^- (meq/l)	Cl^- (ppm)	Cl^- (meq/l)	SO_4^{2-} (ppm)	SO_4^{2-} (meq/l)	NO_3^- (ppm)	NO_3^- (meq/l)	Total anion
SL08	0.75	5.01	0.141127	0.44	0.009157	0.44	0.007097	0.907381
SL11	3.625	162.26	4.570704	4.31	0.089698	0.48	0.007742	8.293144
SL28	12.75	1467.1	41.32676	98	2.039542	6.2	0.1	56.2163
SL29	4	50.85	1.432394	0.34	0.007076	1.44	0.023226	5.462696
SL30	11.625	977.85	27.54507	52.4	1.090531	8.65	0.139516	40.40012
SL32	2.125	1794.8	50.55775	29.8	0.620187	7.4	0.119355	53.42229
SL33	18	2935.2	82.68169	228.8	4.761707	8.6	0.13871	105.5821
SL34	5.5	6.37	0.179437	0.51	0.010614	0.64	0.010323	5.700373
SL35	6.375	67.64	1.905352	5.38	0.111967	7.61	0.122742	8.515061
SL36	11.5	1217.25	34.28873	217.2	4.520291	2.25	0.03629	50.34531
SL37	7.375	5.94	0.167324	0.67	0.013944	0.83	0.013387	7.569655
SL38	12.25	3719.5	104.7746	443.8	9.236212	4.9	0.079032	126.3399
SL39	8.625	20.91	0.589014	0.35	0.007284	0.8	0.012903	9.234201
SL40	6.875	6.87	0.193521	0.21	0.00437	1.09	0.017581	7.090472
SL41	14.25	1399.5	39.42254	7.45	0.155047	4.5	0.072581	53.90016
SL42	8.75	8.92	0.251268	0.23	0.004787	0.98	0.015806	9.021861
SL43	13.75	1158.25	32.62676	139.65	2.906348	3.6	0.058065	49.34117
SL44	8.625	14.92	0.420282	1.01	0.02102	0.48	0.007742	9.074043
SL45	6.625	5.69	0.160282	0.11	0.002289	0.41	0.006613	6.794184
SL46	6.125	558.1	15.72113	53.65	1.116545	2.15	0.034677	22.99735
SL47	6.375	29.8	0.839437	0.52	0.010822	5.84	0.094194	7.319452
SL48	7.875	32.21	0.907324	0.76	0.015817	0.78	0.012581	8.810721
SL49	7.75	1118.05	31.49437	0.4	0.008325	13.35	0.215323	39.46801
SL51	5.125	782.7	22.04789	0.45	0.009365	2.65	0.042742	27.22499
SL52	8	126.27	3.556901	0.24	0.004995	7.21	0.11629	11.67819
SL53	0.75	1.88	0.052958	0.12	0.002497	0.15	0.002419	0.807874
SL54	1.875	31.18	0.87831	4.58	0.095317	0.4	0.006452	2.855079
SL55	3	32.02	0.901972	2.12	0.044121	0.14	0.002258	3.948351
SL56	3	10.32	0.290704	1.03	0.021436	2.73	0.044032	3.356172
SL57	1.25	2.79	0.078592	0.54	0.011238	0.38	0.006129	1.345959
SL58	2.75	2.91	0.081972	0.11	0.002289	0.3	0.004839	2.8391
SL60	1.75	2.65	0.074648	1.56	0.032466	0.07	0.001129	1.858243
SL61	1.75	1.38	0.038873	1.92	0.039958	0.1	0.001613	1.830445
SL62	1.875	1.62	0.045634	2.01	0.041831	0.24	0.003871	1.966336
SL63	3.5	3.96	0.111549	0.21	0.00437	6.5	0.104839	3.720758
SL64	9.625	812.9	22.89859	0.2	0.004162	6.95	0.112097	32.63985
SL65	4.875	3.3	0.092958	0.15	0.003122	0.37	0.005968	4.977047
SL66	8.875	362.72	10.21746	1.08	0.022477	4.38	0.070645	19.18559
SL67	4.5	3.28	0.092394	0.12	0.002497	0.31	0.005	4.599892
SL68	7.625	5.25	0.147887	0.18	0.003746	0.71	0.011452	7.788085
SL69	10.25	432	12.16901	56.8	1.182102	4.7	0.075806	23.67692
SL70	7.75	7.72	0.217465	0.22	0.004579	0.76	0.012258	7.984301
SL71	14.75	743.8	20.95211	790.94	16.46077	3.6	0.058065	52.22095
SL72	9.375	121.26	3.415775	1.06	0.02206	2.62	0.042258	12.85509
SL73	6	6.6	0.185915	0.38	0.007908	0.84	0.013548	6.207372
SL74	5.375	4.13	0.116338	0.49	0.010198	0.5	0.008065	5.5096
SL75	2.75	3.21	0.090423	1.57	0.032674	0.49	0.007903	2.881
SL76	6.375	12.53	0.352958	0.41	0.008533	0.74	0.011935	6.748426

Sample ID	Balance	EC (μS/cm)	Depth (m)	Comment	Mn^{2+} (ppm)	Fe^{2+} (ppm)	Fl^- (ppm)	Br^- (ppm)
SL08	9.154119	60	237.744	Deep Well	0.005	0.264	0.071	0
SL11	-5.51738	480	207.264	Deep Well	0.476	2.531	0.23	0.46
SL28	-10.5993	5130	18.288	Shallow Well	0.241	1.334	0.4	4.4
SL29	1.915191	520	201.168	Monitoring well	0.116	2.602	0.16	0
SL30	-10.6148	3560	18.288	Shallow Well	0.745	2.005	0.05	4.75
SL32	-13.3614	4570	152.4	Deep Well	0.332	11.024	0.35	4.85
SL33	-13.3389	8540	12.192	Shallow Well	2.449	2.164	0	8
SL34	1.714775	480	217.932	Deep Well	0.044	10.14	0.18	0.04
SL35	-8.70575	600	164.592	Deep Well	0.024	0.497	0.19	0.23
SL36	-15.7694	4090	12.192	Shallow Well	0.707	1.699	0.2	6.3
SL37	-0.80697	650	176.784	Monitoring well	0.019	0.231	0.35	0.05
SL38	-8.63831	9540	15.24	Shallow Well	0.95	4.037	0	17.3
SL39	-1.92856	950	137.16	Shallow Well	0.003	0.201	0.46	0.13
SL40	-0.66379	610	121.92	Shallow Well	0.017	0.962	0.34	0.07
SL41	-13.2074	4780	9.144	Shallow Well	0.156	4.394	0.3	3.9
SL42	-0.89404	730	128.016	Shallow Well	0.019	0.213	0.49	0.08
SL43	-12.664	4160	15.24	Shallow Well	0.587	6.069	0.3	4.85
SL44	-0.10378	740	137.16	Shallow Well	0.003	0.34	0.36	0.11
SL45	0.009127	590	158.496	Deep Well	0.02	1.136	0.25	0.06
SL46	-10.5473	2110	15.24	Shallow Well	0.138	5.511	0.4	1.6
SL47	3.756558		158.496	Monitoring well	0.101	8.824	0.37	0.13
SL48	-1.50863	790	158.496	Deep Well	0.018	0.517	0.16	0.13
SL49	-14.6007	3490	12.192	Shallow Well	0.049	2.542	0.6	6.15
SL51	-13.2447	2420	52.4256	Shallow Well	0.345	9.27	0.4	2.4
SL52	-1.35631	1160	19.812	Shallow Well	0.035	0.981	0.28	0.54
SL53	8.564851	90	167.64	Shallow Well	-0.006	0.386	0.07	0
SL54	4.094148	320	30.48	Shallow Well	0.151	1.217	0.44	0.14
SL55	1.700383	380	21.336	Shallow Well	0.391	2.574	0.25	0.14
SL56	8.324639		155.448	Monitoring well	0.468	2.143	0.37	0.08
SL57	15.98201	150	10.668	Shallow Well	0.596	7.771	0.25	0
SL58	8.254056	260	167.64	Deep Well	0.119	3.069	0.13	0
SL60	10.13342	190	213.36	Artesian Well	0.066	0.369	0.09	0
SL61	12.97073	160	213.36	Artesian Well	0.06	0.047	0.08	0
SL62	0.02421	150	213.36	Artesian Well	0.12	0.166	0.08	0
SL63	9.367307	830	259.08	Deep Well	0.147	1.592	0.21	0.03
SL64	5.736819	2960	19.812	Shallow Well	0.035	2.179	0.65	2.4
SL65	0.983686	460	167.64	Shallow Well	0.183	0.691	0.26	0
SL66	-8.86553	1700	18.288	Shallow Well	0.291	0.99	0.52	0
SL67	2.899562	400	60.96	Shallow Well	0.203	1.471	0.27	0.03
SL68	0.231071	670	182.88	Deep Well	0.021	0.273	0.43	0
SL69	-10.8961	2100	13.716	Shallow Well	0.556	7.384	0.4	0
SL70	0.481276	710	213.36	Deep Well	0.016	0.406	0.34	0
SL71	-14.3307	4310	12.192	Shallow Well	0.424	1.638	0.25	0
SL72	-0.53691	1200	15.24	Shallow Well	0.052	1.926	0.28	0
SL73	-2.34109		193.548	Monitoring well	0.114	0.999	0.51	0
SL74	6.012992	510	213.36	Deep Well	0.154	0.351	0.35	0
SL75	9.817121	270	182.88	Deep Well	0.015	0.418	0.16	0
SL76	-8.73942	570	18.288	Shallow Well	0.402	3.424	0.14	0

Sample ID	PO_4^{-3} (ppm)	$N0_2^{-}$ (ppm)
SL08	0	0
SL11	0	0
SL28	0	0
SL29	0.33	0
SL30	0	0
SL32	0	0
SL33	0	0
SL34	0.47	0.12
SL35	0.44	0
SL36	0	0
SL37	0.37	0.05
SL38	0	0
SL39	0.22	0.05
SL40	3.45	0
SL41	0.9	0
SL42	0.52	0
SL43	2.15	0
SL44	0.59	0.11
SL45	0.62	0
SL46	0	0
SL47	0	0
SL48	1.29	0
SL49	6.45	0
SL51	0	0
SL52	9.8	0
SL53	0	0.3
SL54	0	0.42
SL55	0	0
SL56	2.13	0
SL57	0	0
SL58	0	0
SL60	0.14	0.08
SL61	0	0.11
SL62	0	0
SL63	0	0.23
SL64	4.85	0
SL65	0	0
SL66	1.82	0
SL67	0.68	0
SL68	0.42	0
SL69	0	0
SL70	0.66	0
SL71	0	0
SL72	5.88	0
SL73	0.44	0
SL74	0.78	0
SL75	0	0
SL76	0	0.22